國 立 交 通 大 學

運輸與物流管理學系

博士論文

No.020

駕駛跟車心理物理因素聯合不確定之實驗與分析—量子視覺流觀點

Experiments and Analysis on Joint Uncertainties in Psycho-physical Factors of Car-following Drivers — Quantum Optical Flow Perspective

研 究 生：吳熙仁
指導教授：許鉅秉、陳穆臻

中 華 民 國 一〇六 年 三 月

駕駛跟車心理物理因素聯合不確定之實驗與分析—量子視覺流觀點

Experiments and Analysis on Joint Uncertainties in Psycho-physical Factors of Car-following Drivers— Quantum Optical Flow Perspective

研 究 生：吳熙仁　　Student：Hsi-Jen Wu

指導教授： 許鉅秉 博士　　Advisor：Prof. Jiuh-Biing Sheu

陳穆臻 博士　　Prof. Mu-Chen Chen

國 立 交 通 大 學

運 輸 與 物 流 管 理 學 系

博 士 論 文

A Dissertation

Submitted to Department of Transportation and Logistics Management

College of Management

National Chiao Tung University

in Partial Fulfillment of the Requirements

for the Degree of Doctor of Philosophy

in

Traffic and Transportation

March 2017

Taipei, Taiwan, Republic of China

中華民國一〇六年三月

國 立 交 通 大 學

博碩士論文紙本論文暨全文電子檔著作權授權書

（提供授權人裝訂於紙本論文書名頁之次頁用）

本授權書所授權之學位論文，為本人於國立交通大學運輸與物流管理學系 _____組， 105 學年度第 2 學期取得博士學位之論文。

論文題目：駕駛跟車心理物理因素聯合不確定之實驗與分析—量子視覺流觀點
指導教授：許鉅秉, 陳穆臻

一、紙本論文著作權授權

■同意立即公開

本人依著作權法第15條第2項第3款之規定(採推定原則即預設圖書館得公開上架閱覽)，同意將本著作，以非專屬、無償授權國立交通大學與國家圖書館，基於推動讀者間「資源共享、互惠合作」之理念，與回饋社會與學術研究之目的，國立交通大學圖書館與國家圖書館得以紙本收錄、重製與利用；於著作權法合理使用範圍內，讀者得進行閱覽或列印。

□不同意立即公開

□1. 本論文為本人向經濟部智慧局申請專利的附件之一，請將論文延至____年____月____日公開，申請文號 為： _____。

□2. 本論文已投稿期刊並待審核中，請將論文延至____年____月____日公開。

說明：配合教育部函(100年7月1日臺高(二)字第1000108377號)，紙本不公開期限以5年為限

二、論文全文電子檔著作權授權

本人同意將本著作，以非專屬、無償授權國立交通大學、台灣聯合大學系統圖書館與國家圖書館：基於推動讀者間「資源共享、互惠合作」 之理念，與回饋社會與學術研究之目的，得不限地域、時間與次數，以紙本、光碟或數位化等各種方法收錄、重製與利用；於著作權法合理使用範圍內，讀者得進行線上檢索、閱覽、下載或列印。

論文全文上載網路公開之範圍及時間：	
中英文摘要(不公開以5年為限)	■ 立即公開
本校及台灣聯合大學系統區域網路	■ 立即公開
校外網際網路及國家圖書館	■ 立即公開

研究生：吳聖仁 （親筆簽名）

指導教授：許鉅秉 陳穆臻 （親筆簽名）

中華民國 106 年 6 月 30 日

國立交通大學

研究所博士班

論文口試委員會審定書

本校 運輸與物流管理學系交通運輸 博士班 吳熙仁 君

所提論文 駕駛跟車心理物理因素聯合不確定之實驗與分析—量子視覺流觀點

合於博士資格水準，業經本委員會評審認可。

口試委員：胡守任　　[illegible]

[illegible]　　[illegible]

[illegible]　　[illegible]

[illegible]

指導教授：[illegible]　　[illegible]

系 主 任：[illegible]　　教授

中 華 民 國　一〇六　年　三　月　二十二　日

A DISSERTATION OF *Hsi-Jen Wu*

ENTITLED *Experiments and Analysis on Joint Uncertainties in Psycho-Physical Factors of Car-Following Drivers - Quantum Optical Flow Perspective*

WAS ACCEPTED AS PARTIAL FULFILLMENT
OF THE REQUIREMENTS FOR THE DEGREE OF

DOCTOR OF PHILOSOPHY

Committee

Dissertation Advisor

Department Head
Ph.D. Program for Traffic and Transportation,
Department of Transportation and Logistics Management

National Chiao Tung University

Date : 22.03.2017

駕駛跟車心理物理因素聯合不確定之實驗與分析—量子視覺流觀點

學生：吳熙仁　　指導教授： 許鉅秉教授
陳穆臻教授

國立交通大學運輸與物流管理學系博士班

摘要

道路駕駛者經由眼睛接受外在環境光線刺激，做為同車道內判斷跟車距離的重要參考依據。但目前跟車理論多以前車與目標車之物理距離量做為重要依據，鮮少將視覺的感知納入跟車理論中。故本研究主要目的係由量子視覺流理論之觀點出發，除分析駕駛跟車心理物理因素聯合不確定，例如跟車行為關鍵影響之駕駛者相對速度感知不確定與反應時間不確定外，亦進行環境不確定因素，例如晴天及濃霧天候條件因素之模式構建。

由於真實的跟車現象較為複雜，本研究先行嘗試以刺激-反應理論為基礎，以量子光學流理論觀點提出了一種隨機且具有動態發展潛力之感知模型來研究晴天及濃霧天候條件下相對速度感知的不確定性與駕駛者反應時間不確定性之間的關係。具體來說，該模型推測駕駛者察覺與前車相對速度和反應時間是時變的、不確定的且具有權衡關係，類似於海森堡測不準原理的形式。

本研究先進行定性分析，並以模擬道路駕駛視覺環境的駕駛模擬器，辦理晴朗天候條件下兩階段實驗，分析道路駕駛者對前車相對速度感知標準差與反應時間標準差之關聯性。結果說明了在跟車行為中駕駛者感知的不確定下，存在反應時間的標準差與感知相對速度標準差之間的關係，即由實驗發現說明了當知覺相對速度的標準差相對增加時，同時伴隨著其反應時間的標準差相對減小；反之亦同。再將其模型擴充應用至濃霧之不同天候條件下跟車行為中駕駛者感知的不確定。

本研究成果，例如反應時間部分數據，已應用於事件路段中可供自動駕駛車輛與手動駕駛車輛混合行駛車道之車流模擬。另可有助於描述在駕駛者感知的不確定下的跟車行為現象，促進道路安全之改善，亦可提供當前道路運輸安全中有關駕駛之人因工程與行為之基礎應用，甚至新的車流理論。

關鍵字：跟車、感知相對速度、量子光流、反應時間、感知不確定性

Experiments and Analysis on Joint Uncertainties in Psycho-physical Factors of Car-following Drivers—Quantum Optical Flow Perspective

Student：Hsi-Jen Wu

Advisors：Prof. Jiuh-Biing Sheu
Prof. Mu-Chen Chen

Department of Transportation and Logistics Management
National Chiao Tung University

ABSTRACT

Road drivers receive external light stimuli via eyes as an important judgment to spacing on the same lane. The majority of car-following theories put many emphases on physical spacing between the leading vehicle and the following vehicle. However, an important basis for visual perception rarely was concerned in the car-following theory. The purpose of the research is to analyze uncertainties in car-following behavior and environment, such as the driver's uncertainty of perception of perceived relative speed and uncertainty of reaction time that play a key role on the affect of the car-following behavior, and to construct a model considering those uncertainties from a viewpoint of quantum optical flow theory.

Because the real traffic phenomena are complex, the study grounds on stimulate-response theory and proposes a quantum optical flow theory that presents a stochastic and potential dynamic model on an optical flow point of view. It is a stochastic and potential dynamic driver perception model to investigate the relationship between the uncertainty of perceived relative speed and that of reaction time during car following in clear and foggy weather conditions. Specifically, the proposed model hypothesizes that driver perceived speed and reaction times are time-varying and uncertain, and correlate in a trade-off relationship mimicking the form of Heisenberg Uncertainty Principle.

This study conducts qualitative analysis followed by a two-stage experiment rooted in quantum optical flow theory using data collected from a driver simulator. Then this study tests the relevant between standard deviation of perceived relative speed and that of reaction time of following vehicle driver under a clear weather condition. The results illustrate that under the driver's perception of the uncertainty in the driver’s behavior in the car following there is a trade-off relationship between the standard deviations of perceived relative speed time and the standard deviations of reaction time. That is, if the standard deviation of the perceived relative speed increases, then the standard deviation of reaction time decreases. On the contrary condition, it is similar to the trade-off relationship. Then this model was expanded to analysis those driving uncertainties in a foggy weather condition.

In the application, some of the reaction time data has been applied to an automatic driving vehicle following control logic in a mixed lane where automatic and manual driven vehicles mix near the event area and adjacent to automated highway system. This study could not only help to describe in the driver's perception of uncertainty for car phenomenon, but also contribute to the improvement of road safety. Another can also provide the enhancement of current road safety in the basic application of human factors relating to driving and behavior even as the new development of car following theory.

Keywords: *Car following; perceived relative speed; quantum optical flow; reaction time; perception uncertainty*

誌謝

這是另一個新的開始及成長，而開始成長的養分來自於生命中眾多貴人的指導及協助。

首先感謝指導教授臺灣大學許教授鉅秉及共同指導教授交通大學陳教授穆臻，亦師亦友的許教授引導學生在選擇論文題目、研提計畫書、擴充視學流量子力學模式、實驗設計及論文投稿等過程中充分發展，而陳教授細心叮嚀與提醒，使學生更專注於論文時效。若沒有兩位教授的指引與協助，學生可能還在浩瀚學海中四處漂浮而無法靠岸。另外，在進港靠岸的過程亦要感謝博士論文口試之校外審查委員成功大學胡教授守任及中興工程顧問社鍾主任志成，以及校內審查委員交通大學汪教授進財、盧教授宗成及邱教授裕鈞，對論文提出寶貴審查意見，使論文更加充實。

回想再次進入交大博班時，承蒙開南大學陳院長武正提攜與推薦，學生真心感謝。在博班論文研討時，除前述論文審查委員外，亦要謝謝馮教授正民、黃教授承傳及黃教授台生的訓勉。多年的努力與付出，好比是多年磨一劍，而兩位指導教授與曾經協助的學者，猶如學生背後支撐的動力，督促學生在鍛造這本論文中不斷發出火花。眾多學長學姊的砥礪亦是一大助力，永祥學長、素如學姊、士軒學長、嘉陽學長、聖章學長、佳欣學長、牧民學長等一併感謝。臺北校區辦公室柳小姐美智及何小姐玉鳳的行政幫忙使得論文提送及口試順利進行，在此一併致謝。

更要感謝運輸研究所黃前所長德治、林前所長志明等歷任所長及吳所長玉珍提供在職進修的機會，以及運安組張組長開國與葉副組長祖宏的支持，得以駕駛模擬儀設備進行創新理論的驗證。此時亦需要感謝龍華科技大學董教授基良、許教授俊嘉、莊教授凱翔在駕駛模擬情境程式的協助。

最後要謝謝父母親、岳父母，以及太太的辛勞付出，還有兩位可愛女兒的貼心，讓學生沒有後顧之憂地完成學業。

吳熙仁 謹誌 106.6.30

TABLE OF CONTENTS

LIST OF FIGURES

LIST OF TABLES

CHAPTER 1 INTRODUCTION

1.1 Background and Motivation

Road drivers receive external light stimuli via eyes as an important judgment to spacing on the same lane in car following (Marsh *et al*., 2017). The majority of car-following theories put many emphases on physical spacing between the leading vehicle and the following vehicle. However, an important basis for visual perception rarely was concerned in the car-following theory. Furthermore driver perception uncertainty exists ubiquitously, and plays a key role in characterizing driver car-following behavior and induced other lane traffic phenomena (Sheu, 2013; Sheu and Wu, 2015). Lane traffic phenomena refer to intra-lane and inter-lane traffic phenomena, including car-following, lane-changing, and vehicular queuing. In fact, driving is both visual and psychological complex. Roughly 90% of driving information is input through the eyes (Robinson *et al*., 1972). Unfortunately, no one in driving can perfectly perceive all the driving information with 100% accuracy, according to the quantum optical flow theory (Baker, 1999; Sheu, 2008; Sheu and Wu, 2015). Particularly, perception errors may occur while perceiving moving images in driving due to the wave-image duality during the transfer of visual information (Baker, 1999), thus resulting in the uncertainty of driver perception in car following (Sheu, 2013) which complicates lane traffic phenomena. Furthermore, lane traffic phenomena characterized by the interactions and reactions of drivers of multiple vehicles surrounding are rooted in psychological reactions of the drivers (Papageorgiou and Maimaris, 2012). For example, congestion upstream of a traffic bottleneck or shockwave can vary in propagation length, depending upon the upstream traffic flow and density perceived by drivers (Shiomi *et al*., 2011; Talebpour and Mahmassani, 2016; Qian *et al*., 2017). Therein, shockwaves were also discussed in numerous previous studies (Bose and Ioannou, 2000; Nagai *et al*., 2006; Tanaka *et al*., 2006; Hanaura *et al*., 2007; Chiu *et al*., 2010; Qian *et al*., 2017). From either a theoretical or practical perspective, modeling lane traffic phenomena grounded upon such an unrealistic assumption of traffic parameter determinism may no longer be valid in the context of driver perception uncertainty. Instead, it is arguably agreed that driver perception uncertainty which underlies driver behavioral uncertainty should be taken into account in characterizing lane traffic phenomena.

Car-following is one of lane traffic phenomena. The car-following means that a vehicle follows its leading vehicle (LV) by maintaining appropriate spacing on a

roadway. As to the issue of driver perception uncertainties in car following, relative speed (RS) and reaction time (RT) are two crucial factors. In reality, a new branch of car-following research has been focused on the psycho-physical aspects (Wiedemann, 1974, 1991, 1992; Leutzbach, 1988; Toledo, 2003), particularly with respect to RS (Hoffmann and Mortimer, 1996; Jiang *et al.*, 2002; Shiomi *et al.*, 2011; Durrani *et al.*, 2016; Rößing, 2016; Ngoduy and Jia, 2017) and RT (Mehmood and Easa, 2009; Sheu and Wu, 2011; Wang *et al.*, 2011; Koutsopoulos and Farah, 2012; Wagner, 2012; Sheu, 2013; Markkula *et al.*, 2016; Abbasi-Kesbi *et al.*, 2017). For example, the work of Sheu (2008) which used the quantum-optical-flow-based model to explain driver stimulus and response was one of the pioneering researches in the association of uncertainty in perceived relative speed (PRS) with driver behavior in car following. Specifically, Sheu asserted that as backward PRS increases, the resulting psychophysical momentum (PPM) and psychophysical energy (PPE) increase. Therein, the uncertainty of PRS in car following is defined as the standard deviation of PRS, where PRS refers to as the relative speed between the leading vehicle (LV) and following vehicle (FV) perceived by the FV driver. Using a quantum-mechanics-based approach, Sheu (2013) further developed a dynamic stimulus-response car-following model which consists of the following two recursive phases: (a) transformation of visual stimuli, and (b) approximation of speed adjustment. Nevertheless, the uncertainty in RT and its association with other perception uncertainties remain as critical issues which are not addressed in Sheu's works (2008, 2013). For example, as argued in Sheu (2013) the uncertainty in RT may contribute to irregular start-up delays during a forward shockwave (*e.g.*, when vehicular queuing starts to disperse), thus leading to greater deviations in reproducing vehicular trajectories, compared with normal car-following cases. Moreover, the association of the uncertainty in RT with that in PRS may exist, collectively influencing quantum optical field and driver behavior; and however, remains unclear in characterizing car-following behavior. The mentioned above is the background.

Because the real traffic phenomena are complex, the study grounds on stimulate-response theory and proposes a quantum optical flow theory that presents a stochastic and potential dynamic model on an optical flow point of view. It is a stochastic and potential dynamic driver perception model to investigate the relationship between the uncertainty of PRS and that of RT during car following. Specifically, the proposed model hypothesizes that driver perceived speed and RTs are time-varying and uncertain, and correlate in a trade-off relationship mimicking the form of Heisenberg Uncertainty Principle. Thus, the motivation of this dissertation is to understand the relationship between deviations of speed and RT to the LV in car-following phenomena.

1.2 Research Problems

The most existing car-following models seem to emphasize the space/temporal which are mechanically and physically measured. As we know, the majority of car following models focused on the physical measurements, such as the space and time, which are measured by meter and second. However, some of traffic phenomena can hardly be described by theories of pure physics and mechanics. Furthermore, there are a few drivers who can know the exactly distance between the front car and the objective car. Actually, many drivers keep a safety distance based on the psychological perception, such as very fast or very slow. Baker (1999) and Sheu (2008, 2013) indicated that the car following models based on quantum mechanics of optic flow can consider driver perception uncertainties. One of the most important reasons is that human beings would take a response for a stimulus based on the optical flow. The car following models based on quantum mechanics of optic flow can consider driver perception uncertainties.

According to the properties of quantum optical flow theory mentioned in the background, this study inferred that both PRS and RT have dynamic and stochastic characteristics which collectively dominate driver perception uncertainty, thus influencing the dynamics of driver car-following behavior under uncertainty. Accordingly, this study aims to answer the following questions regarding driver perception uncertainty revealed in driver car-following behavior and in clear and foggy weather conditions.

1. Does a trade-off relationship between the uncertainty in PRS and that in RT exist in car following in a clear condition?

2. Does a trade-off relationship between the uncertainty of psychophysical energy and that of RT exist in car following in a clear condition?

3. Does a trade-off relationship between the uncertainty of PRS and that of RT given that the mean values of PRS and driving mental workload are known in a clear condition?

4. Do these trade-off relationships mentioned above also exist in a foggy weather condition?

1.3 Research Objectives

In order to answer the study problems mentioned above, the main objectives of this study can be shown as followed points:

(1) According to quantum optical flow theory in car following, expand a model containing PRS and RT that dominate driver perception uncertainty. The proposed model is not limited to driver psychology, but to characterize the antecedents of driver car-following behavior under perception uncertainty. The entire methodology is new against existing models, and may stimulate more research for the development of stochastic and potential dynamic traffic behavior modeling and stochastic traffic flow theories by taking different ways (*e.g.*, experimental physics and applied quantum mechanics).

(2) Design a two-stage experiment to test two relationships: (a) a trade-off relationship between the uncertainty of psychophysical energy and that of RT exist in car following; (b) a trade-off relationship between the uncertainty in PRS and that in RT exist in car following.

(3) Improve the simulation capability of the car-following models based on trade-off principle for RT and PRS from the LV in clear and foggy weather conditions.

This research focused on participants' homogeneity of rather than their heterogeneity, thus their age and gender were not discussed.

1.4 Research Flow Chart

Aiming to answer the problem and reach the goal of this study, this study was organized as Figure 1-1 and was divided into seven chapters. In Chapter 2, the literatures regarding the car following theories and quantum mechanics in optical flow were reviewed. In Chapter 3, quantum mechanics-based car-following model and two hypotheses were provided. In Chapter 4, a two-stage experiment rooted in quantum optical flow theory using data collected from a driver simulator and in a clear weather condition. Then, in Chapter 5, the applications contains three parts, (1) uncertainties of PRS and RT in foggy and emergency braking conditions; (2) the processes to a upgraded simulation design; (3) some of the RT data has been applied to an automatic driving vehicle following control logic in a mixed lane where automatic and manual driven vehicles mix near the event area and adjacent to an automated highway system. In Chapter 6, this study provided discussions from the some perspectives. Finally, the conclusions and recommendations were made in Chapter 7.

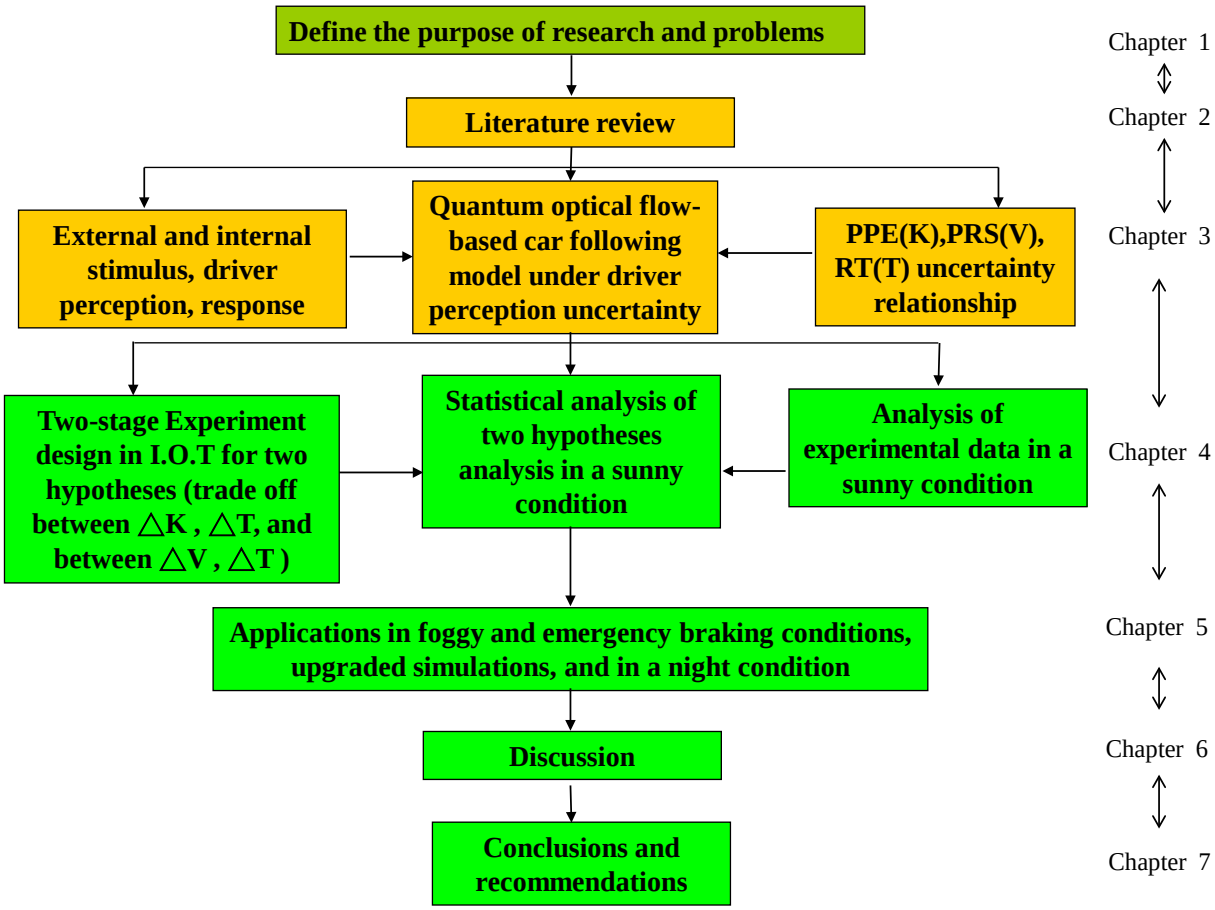

Figure 1-1 Research flow chart

CHAPTER 2 LITERATURE REVIEW

Based on the proposed research framework, issues of psychological and psychophysical factors, car following models, psychological quantum mechanics, quantum theory of vision, visual perception, and a foggy weather condition would be discussed. This section reviews some of the relevant literature in these areas.

2.1 Psychological and Psychophysical Factors

Trade-off between safety and other goals and motives of driving is a fundamental feature of the road user and the traffic system (Summala, 2005). In aspect of psychology, the psychological pacing factors in car driving are including emotional tension, subjective risk monitor, excitatory motives (target speed level), safety zone in driver's task control, time margin, attentional resource capacity, and work load shown in Figure 2-1 (Summala, 2005). At sight on the individual differences, Rothengatter (2002) indicated that optimism bias and illusion of control in relation to driver behavior to be correlated, but self enhancement and self justification to be separate constructs. Furthermore Lewis-Evans *et al*. (2010) not only reported that subjective impressions of task difficulty, risk, effort, and comfort are key variables of several theories of driver behavior, but also showed the result that a threshold awareness of task difficulty, risk, effort, and comfort are related to time headway.

Vehicle control is extensively based on time margins. Time safety margins have an important feature. Available time determines brake reaction latencies and time sharing, among other things. The detection of an obstacle often triggers nothing more than gas pedal response (lifting a foot off the pedal) and steeling response. Braking takes place at the threshold determined by time-to-collision (Summala, 2005). The audio-visual display resulted in improved traffic efficiency while not compromising safety (Houtenbos *et al*., 2017).

Waard (2010) observed hand positions (high ,medium, and low) of participants in a driving simulator during the performance of a demanding task to measure driver's perception of risk and then concluded that changes in hand positions do seem to be associated with changes in workload demand and hand position can give some information about driving mental workload. Dijksterhuis (2011) used a driving simulator to determine changes in mental effort in response to manipulations of steering demand while speed was fixed in all conditions to prevent a compensatory

reaction.

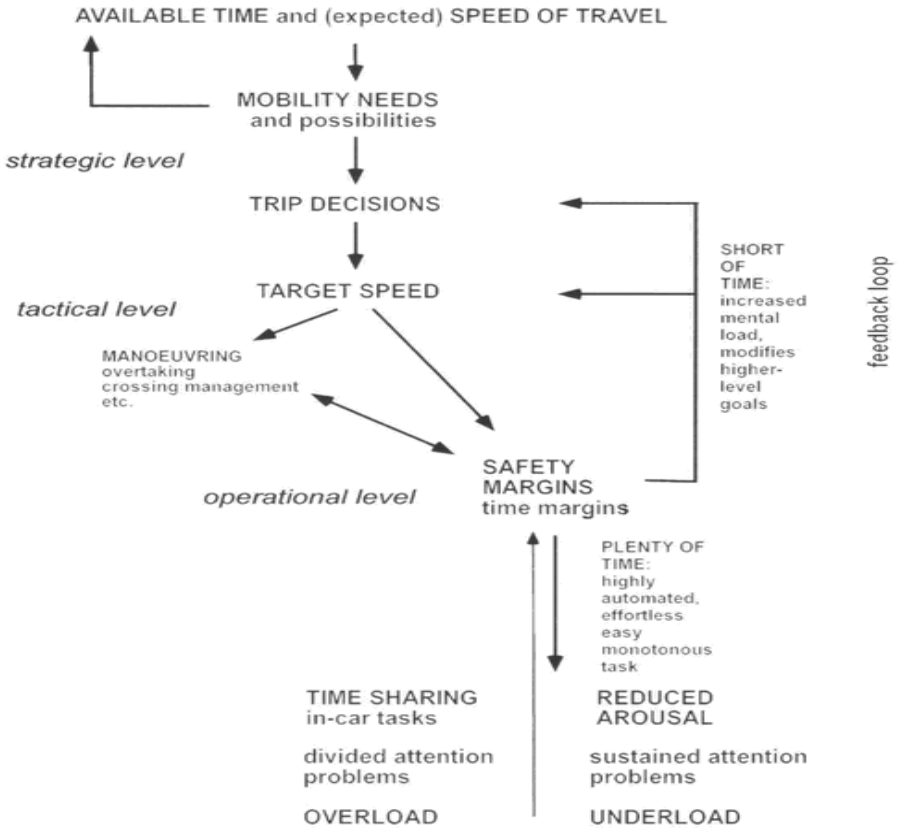

Figure 2-1 Time margins and available time for action, through mental load, mediate between different level of driving.

Resource: Summala (2005)

In aspect of perceived stimulus' psychophysical factors, Baker (1999) discussed the quantum mechanics of optic flow and its application to driving in uncertain environments. Some forms of the Heisenberg Uncertainty Principle (trade-off) was considered when the uncertainty in the position of the focal point, Δx, and psychophysical momentum, $\Delta \gamma$, are at best equal to a time-based action constant h'. $\Delta x \cdot \Delta \gamma \geqq h'$. Furthermore, to consider psychological values of psychophysics, Sheu (2008) took a deep insight in the variations of psychological factors under anomalous traffic environments, *e.g.*, lane-blocking incidents, and their influences in driver behavior may contribute to the existing car-following models falling short in deducing the resulting lane traffic phenomena. Sheu also extended a study about a quantum optical flow-based driver's stimulus-response model to characterize car-following behavior (Sheu, 2013).

Typically, driver, vehicle, roadway, and environment characteristics influence collision occurrence and injury severity. Driver characteristics (or human factors)

include age, gender, driving experience, and mental/physical health. Research has shown that two principal factors involved in the majority of rear-end collisions are driver's inability to perceive and/or react to a lead vehicle's actions and following a lead vehicle too closely (Knipling *et al*., 1993). Studies have revealed that driver perception and reaction to the lead vehicle's action is the prime contributing factor in rear-end collisions (Dingus *et al*., 2006; Xiang *et al*., 2016). Environmental factors such as ice and poor road surface contribute to relatively few rear-end collisions since they predominately occur during daylight hours, on straight roads, and under clear weather conditions (Baldock *et al*., 2005). Whenever the uncertainty about when the light is going to come on increases, the RT increases (Fitts and Posner, 1967).

RT can be deemed as a psychophysical factor. That is, RT is the time between the moment sensory stimulus appears and the consequent behavioral response. Mehmood and Easa (2009) asserted that RT exists when the front vehicle brakes and its brake light is on, and deceleration RT starts when the FV driver reacts and changes his/her speed. They also obtained experimental results indicating that RT differed significantly in normal, urgent, and stationary scenarios. Both urgency and expectancy significantly affect RT. Some empirical studies (Lee, 1976; Wang *et al*., 2011) indicated that braking RT is roughly 1s for an alert driver.

The RT is introduced with the aim of delaying the perception and processing of information about the neighboring vehicles. A delay is assumed to exist between the driver's acquisition of information and the effective use of that information. In a car-following context, the RT seems to be an essential parameter that defines a physiological delay. (Tordeux *et al*., 2010) A RT was incorporated in a version of optimal speed model. (Davis, 2003)

There are some important results of RT from researchers. Davis *et al*. (2006) found that (a) short following headways by the colliding drivers were probable causal factors for the collisions, (b) for each collision, at least one driver ahead of the colliding vehicles probably had a RT that was longer than his or her following headway, and (c) that driver's RT had been equal to his or her following headway, the rear-end collision probably would not have happened. Treiber *et al*. (2006) considered four factors, (a) finite RTs, (b) estimation errors, (c) spatial anticipation, and (d) temporal anticipation, to basic physics-oriented traffic models incorporating into the human driver model. Summala *et al*. (1998) showed the result that RT was a function of the lead-car eccentricity (forced by different in-car display positions) for each experience group and distance–speed combination.

Others researchers considered the RT as an important influence in their research

(Young and Stanton, 2002; Tseng, 2005; Wang, 2004; Liu, 2010). The variables affecting car-following behavior include (a) distance between a LV and the FV, (b) speed differential between a LV and the FV, (c) the FV's speed, and (d) traffic conditions (Tseng, 2005). Liu (2010) presented that there was apparent influence in response time in the stimulus intensity and the intensity of stimulus was stronger, the shorter of the response time was.

Figure 2-2 presents how the RT increases with the quantity of information that needs to be processed (World Road Association, 2003). It can be seen that RTs widely used in traffic engineering practices (1 second in urban areas, 2.0-2.5 seconds in rural areas correspond to very simple situations. The unit of information is bit that a bit is one decision (*e.g.*, turning left/right, fast/slow, etc.). According to Lunenfeld and Alexander (1990), factors to be judged when computing the information load include land use, access control, traffic volumes, speed, task/maneuver, hazard (quantity and visibility), hazard visibility, sight distance, expectancy violations, and complexity.

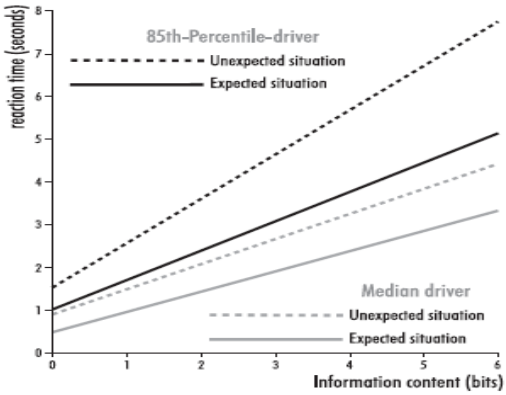

Figure 2-2 Reaction Time

Resource: World Road Association (2003)

In most experiments upon RT, a preparatory signal is given before the presentation of the stimulus. It is found that the RT varies with the length of the interval between the preparatory signal and reaction signal. Constant intervals are between 2 and 4 sec.

The use of psycho-physiological measures to determine human responses to workload, particularly driving mental workload, has been extremely limited in the human factors test and evaluation (HFTE) realm. The U.S. Army has used physiological measures extensively to determine individual soldier responses to physical workload under battlefield conditions by collecting heart rate, ventilation rate,

skin temperatures, and core temperature. At least one attempt at integrating psycho-physiological measurement into HFTE procedures has been suggested (Miller, 1988).

To sum up, the variables effecting car-following behavior include (a) distance between LV and FV, (b) speed differential between LV and FV, (c) FV's speed, (d) uncertain environment. Furthermore, few researches analyze the relationship for the deviation of RT Δt with Δv (deviation of relative speed).

Uncertainty is a parameter that means the dispersion of values. If a value of a mass is set as (1 ± 0.5) kg, the actual value is stated as likely to be somewhere between 0.5 kg and 1.5 kg. The uncertainty is 0.5 kg as a standard deviation and a positive quantity. By contrast, an error may be positive or negative. Random and systematic errors have contrasting natures. Random errors can be exposed when we replicate the measurement as attempting to keep the conditions constant. On the other hand, systematic errors can be exposed when we change the conditions, whether consciously or unintentionally (Kirkup and Frenkel, 2006).

An uncertainty index (UI) is constructed as the value of deviation of observation (x) over the distribution interval (from a left endpoint to a right endpoint of an interval) of observation (x).

$$UI = \frac{\delta(x)}{\left|\underline{x} - \overline{x}\right|} \tag{2.1}$$

The Eq. (2.1) above is where $\delta(x)$ is the value of deviation of observation (x), $\underline{x}$ a left endpoint on interval, and $\overline{x}$ a right endpoint on interval.

2.2 Car Following Models

There are some major groups of the published car following models including (a) Gazis-Herman-Rothery (GHR) model, (b) psychophysical or action point (AP) models, and (c) safety distance or collision avoidance were discussed (Brackstone *et al*. 1999). A Car following situation is shown in Figure 2-3 (Toledo, 2003). The two kind of car-following models, such as GM model and Psycho-physical model, and car-following logic are reviewed as follows.

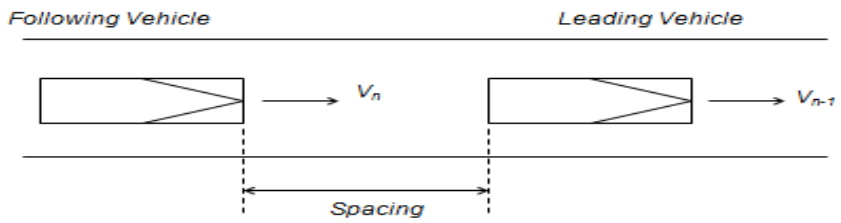

Figure 2-3 A Car following situation

Resource: Toledo (2003)

2.2.1 GM model

Researchers at the GM Research Laboratories presented the sensitivity-stimulus framework that is the basis for most car following models to date. According to this framework a driver reacts to stimuli from the environment. The response (acceleration) the driver applies is lagged to account for RT and is given by Eq. (2.2),

$$response_n(t) = sensitivity_n(t) \times stimulus_n(t - \tau_n) \qquad (2.2)$$

where, t is the time of observation and τ_n is the RT for driver n. The RT includes perception time (time from the presentation of the stimulus until the foot starts to move) and foot movement time. The GM models assume that the stimulus is the leader relative speed (the speed of the leader less the speed of the subject vehicle).

The main advantage of the linear GM model is its simplicity. However, the assumption that the response to the relative leader speed is independent of the spacing between the vehicles is unrealistic. Moreover, steady state equations derived from this model yield a linear flow-density relationship, in which capacity is obtained at zero density. To overcome this problem Gazis *et al*.(1961) proposed a nonlinear model, in which the response is inversely proportional to the spacing.

2.2.2 Psycho-physical model

Weidmann (1974, 1991, 1992) and Leutzbach (1988) showed two unrealistic behavioral inferences of the GM models. The model presumes that drivers follow

their leader even when the spacing between them is large, and it presumes perfect perception and reaction even to small changes in the stimulus. They introduced the term perceptual threshold to define the minimum value of the stimulus that the driver will react to. The perceptual threshold value increases with the space headways. This captures both the increased alertness of drivers at small headways and the lack of car following behavior at large headways. Perceptual thresholds were found to be different for acceleration and deceleration decisions.

Figure 2-4 demonstrates how car following proceeds under these assumptions. A vehicle traveling faster than its leader will get closer to it until the deceleration perceptual threshold is crossed (a). The driver will decelerate in an attempt to match the leader speed. However, the driver is unable to do this accurately and the headway will increase until the acceleration threshold is reached (b). The driver will again accelerate and so on. This model is able to explain the oscillating phenomenon observed in car following experiments. However, no rigorous framework for calibration of this model was proposed.

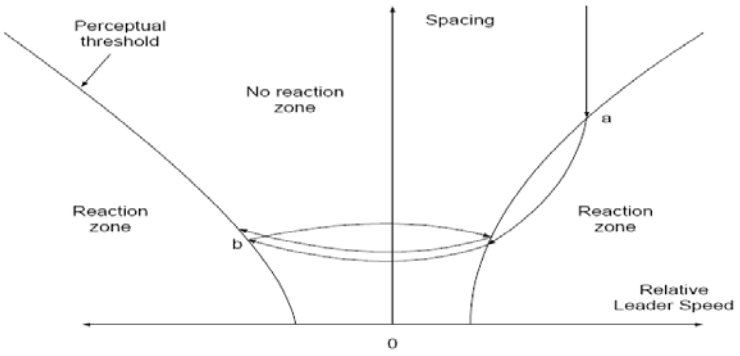

Figure 2-4 Behavior of the Psycho-physical model

Resource: Weidmann (1974, 1991, 1992) and Leutzbach (1988)

2.2.3 Car Following Logic

There are numerous literatures about car following logic. According to the types of vehicle on a lane (manual driven vehicles (MDVs), automatic driving vehicles (ADVs), and a mixed lane where automatic and manual driven vehicles mix (mixed vehicles)) and the event status, there are six categories as follows.

1. MDVs and no event status (Brackstone *et al.*, 1999; Pipes, 1953; Forbes *et al.*, 1959; Gazis *et al.*, 1961; Chandler *et al.*, 1958). Some researchers focused on the traffic consisting of manually driven vehicles and no event status and explored the car following logic, such as GM Model mentioned above. GM model took distance between a LV and the FV, acceleration and deceleration, the RT, the sensitivity

coefficient, the front distance factor (l) and the speed factor (m). Based on the quantum mechanical point of view, researchers considered important variables, such as psychological momentum, energy psychology, RT and the relative speed of a LV and the FV to describe the car following logic of external eyesight stimuli (Sheu, 2008; Sheu and Wu, 2011; Sheu, 2013; Sheu and Wu, 2015).

2. MDVs and an event status (Sheu and Dan, 2001). Acceleration, deceleration, and position of FV when the incident happened with the LV, relative speed between the LV and the FV, the RT and other important variables, were considered to build the logic of manual vehicle to predict events in advance.

3. ADVs and no event status (Ohtsuka and Vlacic, 2002). Acceleration, vehicle speed, relative speed from the front vehicle, road gradient, vehicle weight and other important variables were considered to construct the car following judgment logical formula for the speed and braking system judgment.

4. ADVs and an event status (Sheu, 2007; Sheu, 2004; Dong, 2006). Some researchers studied the acceleration change, event detection time point, distances from the front vehicles to the event point of occurrence, a spacing between ADVs, and other variables, constituted the dynamic proportion of combination and formulated an acceleration mode logic for ADV.

5. Mixed vehicles and no event status (Huang *et al.*, 1999). Some researchers thought about the relative speed, relative distance, vehicle distance, a safe distance, and RTs, and used situational judgment and decision tree to find the formula of judging the car following logic.

6. Mixed vehicles and an event status (Sheu, 2007; Tsai, 2005). Some researchers considered an event detection point in time, a distance from the front vehicle to the point of occurrence of the event, vehicle speed regulation rate, the time to complete the lane change, buffer time, instant speed and other important variables to explore how to avoid the incident with the car control logic from a microscopic point of view.

2.3 Quantum Mechanics in optical flow

Some pioneering researches (Gibson and Crooks, 1938; Gibson, 1950, 1966; Lee, 1980; Baker, 1999; Sheu, 2008, 2013) have investigated quantum mechanics in optical flow. These researches are to deal with the procedure of transmitting the driver’s perceived motion-related phenomena and the induced driving responses by computational judgment theories or the ecological optic theories. The researchers

Contel *et al*. (2009) stated that mental states, during perception and cognition of ambiguous figures, show to follow quantum mechanics.

Sheu (2008) recommended the stimulus-response driver behavior model including two chronological phases: (a) visual stimulus, and (b) approximation of speed adjustment to reproduce the intra-lane individual driver's decision process under the effects of perceived changes in external traffic environments. The formulation of the model is described in brief as follows.

The states of linear momentum that satisfy the equality in the Heisenberg uncertainty principle for position and momentum, that is the intelligent states, are also the states that minimize the uncertainty product for position and momentum (Pegg *et al*.,2005). Briggs and Rost (2001) stated that energy-time uncertainty principle in quantum mechanics that Heisenberg himself assumed the subsistence of an analogous relationship for energy and time rooted in their classical conjugate relationship. Some rearchers (Shapiro, *et al*., 2005) developed the minimum uncertainty-product property from the perspective of wave functions and called the zero-mean squeezed state, a squeezed vacuum state.

2.3.1 Visual stimulus

A stimulus is such a change of energy in the environment as affects a sense organ. Light becomes a stimulus when it enters the eye and falls upon a sensitive retina. The quantum mechanics-based optical flow model is considered as an extension of a cognitive approach (MacLeod *et al*., 1983; Cavallo and Laurent, 1988; Baker, 1999). Herein, the optical flow-induced stimulus process is conceptualized in the quantum optical field, followed by a psychophysical momentum function to infer the driver's post-stimulus response. The uncertainties in a quantum optical field change as a vehicle speed changes shown as Figure 2-5.

Figure 2-5 The uncertainties in a quantum optical field change as a vehicle speed changes.

Resource: https://www.skybrary.aero/index.php/Vision_(OGHFA_BN)

The conclusions of Baker (1999) were borrowed, and quantum mechanics to develop the incident-induced optical flow model was applied. The process is shown as follows. First, a peripheral visual field ($D[\Delta x(t), \Delta y(t)]$) is defined and shown in Figure 2-6. Here, the scope of the peripheral visual field may change with the instantaneous speed ($v_i(t)$). A driver driving in higher speeds need the concentration of processing resources and "tunnel vision"' must be considered as a demonstration of focused forward motion. Thus, Δx (the uncertainty in the forward field) and Δy (the uncertainty in the peripheral field), must be dealt with separately, due to experimentally recorded asymmetry from the interaction of the two field elements, namely. As claimed in Baker (1999), a higher vehicular speed may require the concentration of processing resources, thus forming the driver's "tunnel version", which is a manifestation of focused forward motion. Therefore, a trade-off relationship between $\Delta y(t)$ and $v_i(t)$ may exist (Sheu, 2008).

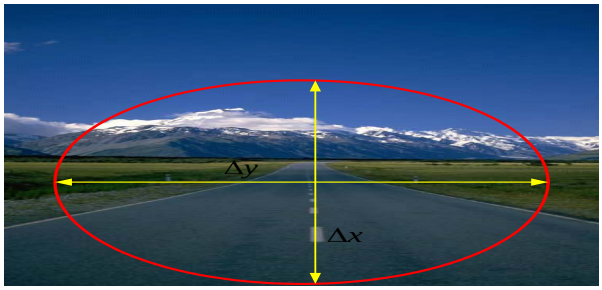

Figure 2-6 Definition of a peripheral visual field

Resource: Sheu (2008)

Reaction times (RTs) are usually reduced when temporal uncertainty about stimulus occurrence is minimized. Rolke and Hormann (2007) concluded that temporal uncertainty influences stimulus processing at a perceptual level.

In a study using computer simulations of car-following scenes, De Lucia and Tharanathan (2005) measured the time it took participants to respond to the deceleration of a LV. Mean response time was significantly shorter when headway was relatively near (0.5 s vs. 1.0 s). Furthermore, optic flow information became less effective (*e.g.*, farther headways and slower rates of deceleration, which had smaller optical expansion rates).

2.3.2 Approximation of speed adjustment

Based on the quantum optical flow theory, the stimulus-response of the target driver can be treated as the outcome of the target vehicle's speed adjustment

($\dot{v}_i(t+\Delta t_i)$) at time $t+\Delta t_i$ for continuously responding to the aggregate quantum optical flow resulting from the perceived vehicles dispersing ahead. The mathematical form of $\dot{v}_i(t+\Delta t_i)$ is given by Eq. (2.3),

$$\begin{aligned}\dot{v}_i(t+\Delta t_i) &= \alpha_1 \times \mathbf{M}_{J_F}(t) \\ &= \alpha_1 \times \sum_{\forall j_F \in J_F} w_{i,j_F}(t) \times M_{j_F}(t) \\ &= \alpha_1 \times U_i(t) \times \sum_{\forall j_F \in J_F} w_{i,j_F}(t) \times \left\{ m_{j_F} \times \left[\Delta v_{j_F \to i}(t) \right] \right\}\end{aligned} \tag{2.3}$$

where α_1 represents a positive parameter; the aggregate psychological momentum ($\mathbf{M}_{J_F}(t)$); the instantaneous psychophysical momentum ($M_{j_F}(t)$); a time-varying weight ($w_{i,j_F}(t)$); the driver's workload ($U_i(t)$), and Δt_i is the RT of the target driver i.

There are some reasons to accept the proposed model mentioned above. First, the proposed model shows applicable particularly under the effects of lane-blocking incidents (Sheu *et al*., 2001a; Sheu, 2003). Second, from a psychophysical point of view, it seems agreeable that the magnitude of speed adjustment by the target vehicle relies also on the driver's workload ($U_i(t)$). Third, if two different types of front vehicles, *e.g.*, truck and private vehicle, were perceived in the above example, then the resulting amount of speed adjustment can be different in these two cases. Psychologically, the target driver can be more sensitive to the perceived front truck's behavior, relative to the case of perceiving a private vehicle.

2.4 Quantum Theory of Vision

According to present vision theory (*e.g.*, Geldard, 1972), the stimulus for the sensory modality of vision/sight is electromagnetic radiation (light) between approximately 380 and 740 nanometers (billionth of a meter), and where the initial processing of visual information is the receptor system consisting of photosensitive cells (rods and cones) in the retina of the eye. Vision is the process of transforming physical light energy into biological neural impulses that can then be interpreted by the brain. The electromagnetic radiation can vary in intensity (which is perceived as a difference in brightness level) and wavelength (which is perceived as a difference in color). The quantum theory of vision (*e.g.*, Harris and Levey, 1975) sustains that light energy travels to the eye in the form of discrete or discontinuous changes in energy where wavelength frequencies correspond to definite energies of the light quanta called photons (Roeckelein, 1998). Furthermore Kilpeläinen and Summala (2007) indicated that daylight should assist drivers' perceptions of road conditions and compose condition estimates more valid.

2.5 Visual Perception

The wholly empirical approach to perception, created by Purves and Lotto (2003), grasps that percepts depend on evolutionary and individual experience with sensory impressions and the objects from which they derive. Much evidence advises that the perception of color, contrast, distance, size, length, and motion, may be verified by empirically associations between the sensory patterns and the relative success of behavior in response to those patterns (Wikipedia, 2013).

Perception of motion is bewildered by a problem: movement in three dimensional spaces does not map absolutely onto movement on the retinal plane. A far object moving at a certain speed will interpret more slowly on the retina than a nearby object moving at the same speed. As stated above size, distance and orientation are given only the retinal image. As with other aspects of perception, empirical theorists propose that this problem is solved by trial-and-error experience with moving stimuli, their associated retinal images and the consequences of behavior.

The same ambiguity pertains to the positional origin of light rays. Since size, distance and orientation are also conflated in the retinal projection (Purves and Lotto, 2003). Fukushima (2008) recommended a method of extracting local speed from retinal images. X- and Y-cells of the retina extract spatial-temporal contrast of brightness from visual stimuli.

Motion is a perceptual attribute. The visual system deduces motion from the changing pattern of light in the retinal image. Often the inference is correct.

The optic flow then provides information about the observer's heading and the relative distance to each surface in the world. Gibson hypothesized that there's sufficient information in the visual stimulus to specify a unique, unambiguous interpretation of 3D motion and depth. Recently, mathematicians have proven that this hypothesis is basically correct. There is a caveat, however: distance and speed are ambiguous (*e.g.*, they trade off). That is, a small, close object when you are moving slowly creates the identical retinal images over time as a large, distant object when you are moving quickly. That's why a driver needs a speedometer in a car. A driver is awful at making absolute speed and distance judgments. But, a driver is very good at relative speed/direction and relative distance.

2.6 Foggy Weather Condition

A Foggy weather condition affects driver perceptual judgments of speed and distance (Ni *et al.*, 2012; Anwar and Khosla, 2015). Some researchers (Yan *et al.*, 2014) presented that the drivers reduced their speeds to decrease the driving risk

under foggy conditions. For safety reason drivers might slow the FV speed (Pretto *et al.*, 2012) and enlarge the spacing between the LV.

2.7 Sub-Summary

Most car-following models emphasize vehicular spatial/temporal characteristics, *e.g.*, relative speed, spacing, and headway, which are assumed to follow the laws of pure physics and mechanical engineering, where the uncertainties in human psychological factors and their interactions jointly influencing drivers can be ignored. This study emphasizes the importance of the driver perception uncertainty characterized in PRS and RT when analyzing or predicting driver response during car following in clear and foggy weather conditions.

Theoretically, human psychological factors, such as driver perception of moving environments and stimulated responses should be embedded in a driver behavior model to characterize "real" driver behavior (Paz and Peeta, 2009; Chen *et al*., 2014). Particularly, this work aims at the effect of joint uncertainty of PRS and RT on car-following behavior in clear and foggy weather conditions.

Previous research has shown that the two principal factors accounting for the majority of rear-end collisions are a driver's inability to perceive and/or react to the actions of the LV and following an LV too closely (Knipling *et al.*, 1993). Whenever uncertainty about when the LV's brake lights will come on increases, RT increases (Fitts and Posner, 1967). Additionally Wang *et al*. (2011) developed a safety-based behavioral approaching model with different driving characteristics.

Understanding the relationship of uncertainty in PRS with that in RT can provide additional insights regarding the correlation between driver perception and behavior under uncertainties, such that one can rationalize the dynamics of driver behavior in car-following scenarios. Notably, this work defines RT as the elapsed time ($T \equiv t_2 - t_1$) from the time when the LV driver takes action to change speed (*e.g*., the brake light of the LV is on) at time t_1 to the time when the FV driver takes action (*e.g.*, puts a foot on the brake pedal) in response to the speed change of the LV at time t_2. Thus, RT relies on mental processes, including perception, comparison, and decision-making (Salvia *et al.*, 2012). Using quantum optical flow theories, such effects can be characterized in the form of quantum-based PPM, thereby stimulating a driver's intuitive adjustment in speed (Sheu, 2008). Additionally, a PRS (scale) is described as an FV driver perceiving physical relative speeds measured from records in driving simulator software during RT. Hoffmann and Mortimer (1996) developed a method to scale the relative speed between an FV and an LV, indicating that a power law relationship existed between subjective and physical quantities of the form (Stevens,

1957). This study took the operator, the natural logarithm (ln), on both sides of the form to obtain the linear relationship that relates subjective relative speeds to physical relative speeds.

CHAPTER 3 MODEL

In this section, first this study introduced several key elements which underlie the fundamentals of existing quantum optical flow-based driver behavior models (Baker, 1999; Sheu, 2008; 2013) in subsection 3.1. Then, this study presented the proposed quantum-theoretic analytical models, including proposed hypotheses, in subsequent subsections to characterize driver perception uncertainty in the car-following scenario using the properties of quantum uncertainty in optics.

3.1 Stimulus, Driver Perception, and Response

In this work, stimulus, driver perception, and response are regarded as three key functional components determining the outcome of driver car-following behavior. The relationships among stimulus, driver perception, and response are indicated as follows. As such, stimuli can be classified into external and internal stimuli. External stimuli include visual stimuli (*e.g.*, PRS and perceived rear brake lights) and driving environmental conditions (*e.g.*, roadway and weather conditions). According to stimuli-response human behavior models (Jacoby, 2002; Tan *et al*., 2007), visual stimuli induce perceptual processing in brains when they are perceived. From the quantum optical flow perspective, the external stimuli can then be transformed into internal stimuli, *e.g.*, PPE and PPM determined by driver characteristics such as driving mental workload which refers to the size of driving mental workload allocated for driving behavior. Using Sheu's model (2008, 2013), such internal stimuli can then be associated with driver response, *e.g.*, acceleration and deceleration, in car following. Figure 3-1 showed the relevant relations of external stimuli, internal mental process, and response behavior.

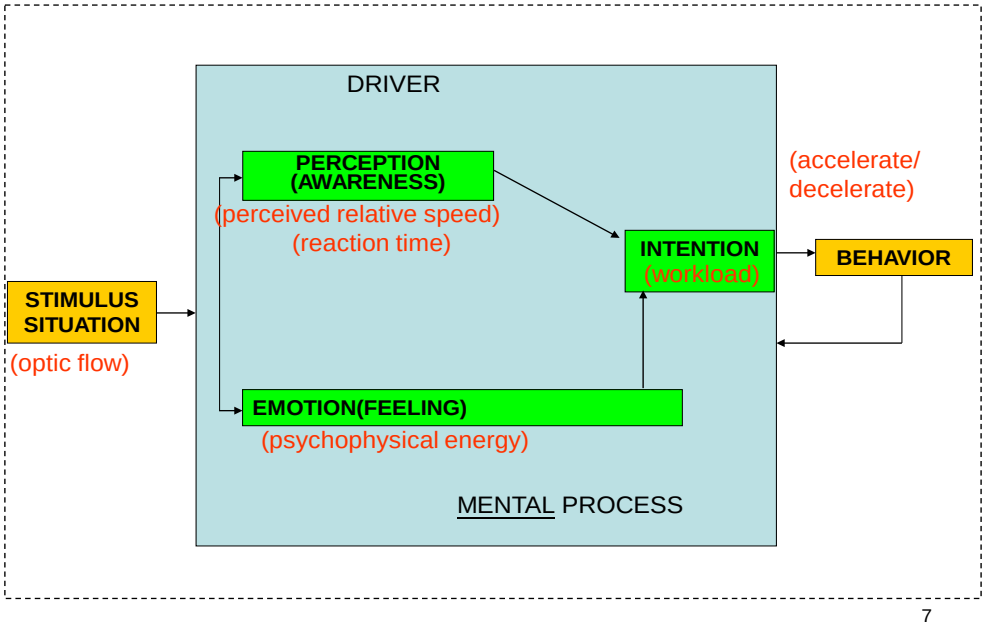

Figure 3-1 The Relations of Stimulus, Driver Perception, and Behavior in Research

Resource: Jacoby (2002); Tan *et al*. (2007)

3.2 External and Internal Stimuli under Driver Perception Uncertainty

According to quantum optical flow theories (Miura, 1987; Bartmann *et al.*, 1991; Baker, 1999), one can define a quantum optical field ($D[\Delta x(t), \Delta y(t)]$) associated with any driver (*e.g.*, the FV driver), to characterize the time-varying probability-based range (*i.e.*, $\Delta x(t)$ and $\Delta y(t)$) of the driver attention allocated across the longitudinal (X) and lateral (Y) dimensions of $D[\Delta x(t), \Delta y(t)]$ shown in Appendix A. Therein, $\Delta x(t)$ and $\Delta y(t)$ vary with time, and have stochastic features, mimicking Guassian processes, indicating that driver attention is not allocated evenly in $\Delta x(t)$ and $\Delta y(t)$. Instead, driver attention is likely to spread in both the longitudinal (X) and lateral (Y) dimensions of $D[\Delta x(t), \Delta y(t)]$, where the highest intensity of a driver's attention can be allocated at the center of the optical field $D[\Delta x(t), \Delta y(t)]$ with the highest probability, thus forming a two-dimensional Gaussian wave packet (Morrison, 1990; Sheu, 2008).

Now consider an FV (termed FV-vehicle i moves in a given lane l at time t. The FV driver observes surrounding traffic flows composed of a certain number of vehicles ahead (denoted by J_D) within the corresponding quantum optical field ($D[\Delta x(t), \Delta y(t)]$) at time t. Notably, $\Delta x(t)$ also represents the instantaneous visual scope in the longitudinal dimension of the quantum optical field at time t. Let each perceived vehicle (*i.e.*, the vehicle perceived by the driver of FV vehicle i) be denoted by j_D ($\forall j_D \in J_D$). Then, vehicle j_D contributes to the external stimulus

(*i.e.*, PRS) to the driver of FV i (denoted by $V_{j_D \to i}(t)$) at time t. Therein, $V_{j_D \to i}(t)$ is given by Eq. (3.1) under driver perception uncertainty.

$$V_{j_D \to i}(t) = v_{j_D}(t) - v_i(t) + \varepsilon_{j_D \to i}(t) \quad (\forall i, t; \ \forall j_D \in J_D) \tag{3.1}$$

where $v_i(t)$ and $v_{j_D}(t)$ are the instantaneous speeds of FV-vehicle i and j_D at time t; and $\varepsilon_{j_D \to i}(t)$ represents the time-varying error term of PRS associated with the driver of FV-vehicle i under perception uncertainty with the standard deviation $\Delta V_{j_D \to i}(t)$ ($\forall i, j_D, t$). It is noted that $\Delta V_{j_D \to i}(t)$ can also be regarded as the magnitude of the uncertainty of PRS changing with time.

As mentioned earlier (subsection 3.1), such an external stimulus attributed to PRS (*i.e.*, $V_{j_D \to i}(t)$) then contributes to internal stimuli, including PPM (denoted by $\mathrm{P}_{j_D \to i}(t)$) and PPE (denoted by $\mathrm{K}_{j_D \to i}(t)$) associated with the driver of FV vehicle i via the effect of the optical flow. Using the computational judgment modeling approach to optical flow characterization in the quantum optic field (Baker 1999, Sheu, 2008, 2013), we have $\mathrm{P}_{j_D \to i}(t)$ and $\mathrm{K}_{j_D \to i}(t)$ given by Eq.s (3.2) and (3.3), respectively.

$$\mathrm{P}_{j_D \to i}(t) = m_{j_D \to i}(t) \cdot V_{j_D \to i}(t) \cdot W_i(t) \qquad (\forall i, t; \forall j_D \in J_D) \tag{3.2}$$

$$\mathrm{K}_{j_D \to i}(t) = \frac{m_{j_D \to i}(t) \cdot \left[V_{j_D \to i}(t)\right]^2 \cdot W_i(t)}{2} \qquad (\forall i, t; \forall j_D \in J_D) \tag{3.3}$$

where $m_{j_D \to i}(t)$ is light mass of j_D perceived by the driver of FV vehicle i at time t; and $W_i(t)$ is the instantaneous driving mental workload of the driver of FV vehicle i at time *t*, based on physiological measures (Brookhuisa and de Waard, 2010). According to Eq.s (3.1) and (3.2), a negative PPM ($\mathrm{P}_{j_D \to i}(t) < 0$) may occur when $V_{j_D \to i}(t) < 0$, meaning that the driver of FV vehicle i perceives vehicle j_D

moving backward (*e.g.*, moving toward FV vehicle i). In this work, such a negative psychophysical momentum ($\mathrm{P}_{j_D \to i}(t) < 0$) is regarded as a negative internal stimulus to the driver of FV vehicle i, thus contributing to a negative effect on the speed adjustment (*e.g.*, deceleration) of the driver.

Using the quantum solution for stability we can further define PPE and PPM as functions of the optic flow, as suggested in Baker (1999). The induced image-wave duality relationship can then be utilized to derive that the uncertainty ($\Delta \mathrm{P}_{j_D \to i}(t)$) of PPM revealed in the quantum optical field $D[\Delta x(t), \Delta y(t)]$ has the trade-off relationship with $\Delta x(t)$, which can be expressed in the form of Heisenberg Uncertainty Principle as Eq. (3.4):

$$\Delta x(t) \Delta \mathrm{P}_{j_D \to i}(t) \geq h' \qquad (\forall i, t\,; \forall j_D \in J_D) \tag{3.4}$$

where h' is an action constant, as defined in Baker (1999). For example, given that the driver of FV vehicle i perceives a leading vehicle j_D located ahead (*e.g.*, $x_{j_D \to i}(t)$) within the quantum optical field $D[\Delta x(t), \Delta y(t)]$ of the driver, where $x_{j_D \to i}(t)$ ($x_{j_D \to i}(t) \leq \Delta x(t), \forall t$) represents the relative distance between vehicle j_D and FV vehicle i perceived by the driver of FV vehicle i at time t. Equation (3.4) indicates that the magnitude ($\Delta \mathrm{P}_{j_D \to i}(t)$) of uncertainty in PPM increases (decrease) as the range ($\Delta x(t)$) of the driver's quantum optical field $D[\Delta x(t), \Delta y(t)]$ decreases (increases) in the longitudinal dimension under driver perception uncertainty.

In the following, we further discuss the reasoning underlying the PPE function (Eq. (3.3)) in several aspects.

First, we reasonably assume that it is possible to model the relationship between PPE and PRS using an analogy to a kinetic energy equation.

Second, from a psychophysical viewpoint, that the magnitude of PPE associated with the FV driver also relies on the driver's driving mental workload ($W_i(t)$) seems reasonable. Theoretically, a driver with high driving mental workload may have a better awareness of surrounding traffic situations than a driver with a small driving mental workload (Recarte and Nunes, 2002). This may generate greater deceleration after perceiving an LV braking in the surrounding traffic situations. Therefore, PPE

($\mathrm{K}_{j_D \to i}(t)$) is proportional to driving mental workload ($W_i(t)$), as indicated in Eq. (3.3).

Third, given two different LVs, such as a truck and a sedan, perceived in the above example, the resulting magnitude of PPE can differ. Psychophysically, the FV driver can be more sensitive to the perceived leading truck's behavior than to the perceived sedan's behavior, thereby contributing to different magnitudes of PPE in these two cases. Such a type-of-vehicle effect on car-following behavior can also be differentiated by using psychophysical momentum and energy in the proposed model and may not be addressed in existing car-following models.

In addition, some properties derived from PPM and PPE (*e.g.*, Eq.s (3.2) and (3.3)) are provided in the following to characterize the correlation between the external and internal stimuli during car following from the FV driver perspective.

Corollary 1. Let $X_{j_D \to i}(t)$ be the relative distance between the FV i and LV j_D at time t. The change in $V_{j_D \to i}(t)$ has a time-varying effect (*i.e.*, $\mathrm{K}'_{V_{j_D \to i}}(t)$, $\mathrm{K}'_{j_D \to i}(t) \equiv \frac{\partial \mathrm{K}_{j_D \to i}(t)}{\partial V_{j_D \to i}(t)}$) on $\mathrm{K}_{j_D \to i}(t)$, which can be characterized by either Eq. (6a) or (6b).

$$\mathrm{K}'_{j_D \to i}(t) = \left[\frac{2X_{j_D \to i}(t) \cdot V_{j_D \to i}(t) \cdot \partial t + \left(V_{j_D \to i}(t) \cdot \partial t\right)^2}{\left(X_{j_D \to i}(t)\right)^2 \partial V_{j_D \to i}(t)} \right] \cdot \mathrm{K}_{j_D \to i}(t) + \mathrm{P}_{j_D \to i}(t) \quad (\forall i, t \; ; \forall j_D \in J_D) \quad (3.6a)$$

or

$$\mathrm{K}'_{j_D \to i}(t) = \left[\frac{2X_{j_D \to i}(t) \cdot \partial X_{j_D \to i}(t) + \left(\partial X_{j_D \to i}(t)\right)^2}{\left(X_{j_D \to i}(t)\right)^2 \partial V_{j_D \to i}(t)} \right] \cdot \mathrm{K}_{j_D \to i}(t) + \mathrm{P}_{j_D \to i}(t) \quad (\forall i, t \; ; \forall j_D \in J_D) \quad (3.6b)$$

Corollary 1 indicates that given the driver of the FV i perceives the change in $V_{j_D \to i}(t)$ (termed external stimulus change, *i.e.*, $\partial V_{j_D \to i}(t) \neq 0$), the resulting change in PPE (termed internal stimulus change, *i.e.*, $\mathrm{K}'_{V_{j_D \to i}}(t)$) has something to do with the perceived instantaneous inter-vehicle relationship such as relative distance ($X_{j_D \to i}(t)$) and PRS ($V_{j_D \to i}(t)$), as well as the instantaneous internal stimulus itself, *i.e.*, PPE

($\mathrm{K}_{j_D \to i}(t)$) and PPM ($\mathrm{P}_{j_D \to i}(t)$). Specifically, the magnitude of such a time-varying effect on PPE ($\mathrm{K}'_{V_{j_D \to i}}(t)$) is positively associated with PRS ($V_{j_D \to i}(t)$) and the perceived change of relative distance (*i.e.*, $\partial X_{j_D \to i}(t)$); and however, negatively associated with $X_{j_D \to i}(t)$. The proof of Corollary is provided in Appendix A.

In addition, motivated by the work of Briggs and Rost (2001) on the derivation of the time-dependent Schrödinger equation (TDSE), we further postulate that the uncertainty in PPE (denoted by $\Delta\mathrm{K}_{j_D \to i}(t)$) has the trade-off relationship with the uncertainty in driver RT (denoted by $\Delta T_{j_D \to i}(t)$). In reality, numerous researchers of quantum mechanics attempted to introduce the time construct into the quantum system to characterize the association of a particle's quantum state of movement with time. Therein, TDSE is a well-known fundamental equation of quantum mechanics which was proposed by Schrödinger (Schrödinger, 1926) to generalize the time-dependent Hamiltonians from conservative time-independent Hamiltonians. Nevertheless, TDSE had gave rise to quite a few challenges (*e.g.*, Born *et al.*, 1926; Briggs and Rost, 2001) and resolutions (*e.g.*, Dirac, 1927) on its mathematical plausibility and validity in precisely determining a particle's position given its energy at time t, which may violate the properties of a quantum system. Furthermore, Heisenberg also reasoned that a trade-off analogous relationship between the uncertainty in energy and time (denoted by $\Delta E \Delta t \geq h$) may exist in a conjugate form similar to Heisenberg Uncertainty Principle (Eq. (3.4)). Accordingly, we infer that an analogy may exist between the PPE－RT uncertainty principle revealed in car following and the energy–time uncertainty principle in quantum mechanics, and thus, postulate the hollowing hypothesis (Hypothesis 1).

Hypothesis 1. For a given driver of FV i who perceives LV j_D in car following at time t, the uncertainty in psychophysical energy ($\Delta\mathrm{K}_{j_D \to i}(t)$) and that in RT ($\Delta T_{j_D \to i}(t)$) are two complementary variables which also exhibit the properties of quantum uncertainty in a conjugate form given by Eq. 3.7).

$$\Delta\mathrm{K}_{j_D \to i}(t) \cdot \Delta T_{j_D \to i}(t) \geq h' \qquad (\forall i, t\,; \forall j_D \in J_D) \tag{3.7}$$

According to Hypothesis 1 regarding the PPE–RT uncertainty principle, we illustrate two extreme cases that may occur in the imaginary traffic car-following scenario. The first case is that the uncertainty of PPE is infinitesimal, mimicking the situation in which a space-control device connected between the LV and FV, linking LV and FV like articulated cars. This can make the FV driver feels so comfortable in car following without any change of PPE, leading to the phenomenon that the uncertainty in the FV driver's RTs goes infinite as no chance exists for the FV to collide with the LV. The other case is that uncertainty of PPE is infinite, sort of like the situation when both the LV and FV move fast in a small spacing and free-cruising state while the LV changes speed frequently and irregularly. Under such a condition, the FV driver may pay fully attention on the movement of FV for any quick response in car following, thus leading to the phenomenon that the uncertainty in FV driver's RT goes infinitesimal (*e.g.*, a constant RT), as indicated in Hypothesis 1.

Furthermore, it is worth mentioning that statistically defining $\Delta T_{j_D \to i}(t)$ as the standard deviation of RT is advantageous, as is defining $\Delta \mathrm{K}_{j_D \to i}(t)$ statistically as the standard deviation of PPE for the perception of an FV driver during RT in the car-following scenario. Thus, one can easily see that a trade-off might exist between $\Delta \mathrm{K}_{j_D \to i}(t)$ and $\Delta T_{j_D \to i}(t)$ $(\forall i, t\,; \forall j_D \in J_D)$.

As the properties of the squeezed state of light have been verified in the area of quantum optics (Iida *et al*., 2012; Mitra and Mukhopadhyay, 2013), we further posit that the squeezed state of quantum uncertainty attributed to the quadrature components $\Delta \mathrm{K}_{j_D \to i}(t)$ and $\Delta T_{j_D \to i}(t)$ may exist under driver perception uncertainty such that minimizing the uncertainty product of Eq. (3.7) yields an approximate expression equivalent to an action constant h'. Therein, the squeezed state is regarded as a minimum quantum uncertainty state in which the quantum uncertainty associated with a quadrature component is squeezed at the expense of the other, *e.g.*, two quadrature components of quantum uncertainty are squeezed unequally; however, the quantum uncertainty represented by the product of the quadrature components can reach to its minimum value. Therefore, the conjugate form which characterizes the trade-off relationship between $\Delta \mathrm{K}_{j_D \to i}(t)$ and $\Delta T_{j_D \to i}(t)$ in Hypothesis 1 can be transformed into a linear relationship, as presented

in Eq. (3.8).

$$\begin{aligned}
&\Delta \mathrm{K}_{j_D \to i}(t) \cdot \Delta T_{j_D \to i}(t) = h' \\
&\Rightarrow \ln(\Delta \mathrm{K}_{j_D \to i}(t)) + \ln(\Delta T_{j_D \to i}(t)) = \ln(h') \qquad (\forall i, t\,; \forall j_D \in J_D) \\
&\Rightarrow \ln(\Delta T_{j_D \to i}(t)) = \ln(h') - \alpha_1 \ln(\Delta \mathrm{K}_{j_D \to i}(t))
\end{aligned} \tag{3.8}$$

where α_1 represents a dummy parameter to facilitate conducting the hypothesis tests for Hypothesis 1 using the one-tailed t-test. Specifically, one can propose the null hypothesis (H_{null}) given by $H_{null} : \alpha_1 \le 0$ to infer that $\ln(\Delta T_{j_D \to i}(t))$ and $\ln(\Delta \mathrm{K}_{j_D \to i}(t))$ are not related. The alternative hypothesis (H_{1A}) is $H_{1A} : \alpha_1 > 0$ indicating that $\ln(\Delta T_{j_D \to i}(t))$ and $\ln(\Delta \mathrm{K}_{j_D \to i}(t))$ are negatively related.

3.3 Relationship of Uncertainty between $\Delta V_{j_D \to i}(t)$ and $\Delta T_{j_D \to i}(t)$

Grounded on the principles derived above, this subsection presents the extended model which permits characterizing the relationship between the uncertainty of PRS and that of RT under driver perception uncertainty in car following.

First, employing the method proposed by Ferson *et al.* (2007) we approximate $\Delta \mathrm{K}_{j_D \to i}(t)$ in the form of the weighted quadrature sum with respect to the standard deviation of PRS ($\Delta V_{j_D \to i}(t), \forall i, j_D, t$) and that of driving mental workload ($\Delta W_i(t)$, $\forall i, t$), as expressed in Eq. (3.9).

$$\begin{aligned}
\Delta \mathrm{K}_{j_D \to i}(t) &\cong \sqrt{\left(\frac{\partial \mathrm{K}_{j_D \to i}(t)}{\partial V_{j_D \to i}(t)}\right)^2 \cdot \left(\Delta V_{j_D \to i}(t)\right)^2 + \left(\frac{\partial \mathrm{K}_{j_D \to i}(t)}{\partial W_i(t)}\right)^2 \cdot \left(\Delta W_i(t)\right)^2} \\
&= \sqrt{\left(\mathrm{K}'_{j_D \to i}(t)\right)^2 \cdot \left(\Delta V_{j_D \to i}(t)\right)^2 + \left(\frac{m_{j_D \to i}(t) \cdot \left[V_{j_D \to i}(t)\right]^2}{2}\right)^2 \cdot \left(\Delta W_i(t)\right)^2}
\end{aligned} \qquad (\forall i, t\,; \forall j_D \in J_D) \tag{3.9}$$

Using Eq. (3.9), we can easily derive Corollary 2 presented as follows.

Corollary 2. *Given driving mental workload is fixed at time* t *(i.e.,* $\Delta W_i(t) = 0$, $\forall t$ *), we then have*

$$\Delta \mathrm{K}_{j_D \to i}(t) = \mathrm{K}'_{j_D \to i}(t) \cdot \Delta V_{j_D \to i}(t) \Leftrightarrow \frac{\partial \mathrm{K}_{j_D \to i}(t)}{\partial V_{j_D \to i}(t)} = \frac{\Delta \mathrm{K}_{j_D \to i}(t)}{\Delta V_{j_D \to i}(t)} \quad (\forall i,t;\forall j_D \in J_D) \quad (3.10)$$

Corollary 2 indicates that the change of PRS ($\partial V_{j_D \to i}(t)$) causes the change of PPE ($\partial \mathrm{K}_{j_D \to i}(t)$) which can be statistically approximated by the standard deviation of PPE ($\Delta \mathrm{K}_{j_D \to i}(t)$) divided by the standard deviation of PRS ($\Delta V_{j_D \to i}(t)$). Furthermore, Corollary 2 can be regarded as a generalization complementary to Corollary 1 to characterize the association of the external stimulus ($\partial V_{j_D \to i}(t)$) with the internal stimulus ($\partial \mathrm{K}_{j_D \to i}(t)$).

By applying Corollary 2 to Hypothesis 1, then we can rewrite Eq. (3.7) as

$$\begin{aligned} &\Delta \mathrm{K}_{j_D \to i}(t) \cdot \Delta T_{j_D \to i}(t) \geq h' \\ &\Rightarrow \mathrm{K}'_{j_D \to i}(t) \cdot \Delta V_{j_D \to i}(t) \cdot \Delta T_{j_D \to i}(t) \geq h' \qquad (\forall i,t;\forall j_D \in J_D) \\ &\Rightarrow \Delta V_{j_D \to i}(t) \cdot \Delta T_{j_D \to i}(t) \geq \frac{h'}{\mathrm{K}'_{j_D \to i}(t)} \geq \frac{h'}{\overline{\mathrm{K}'}} \end{aligned} \quad (3.11)$$

where $\overline{\mathrm{K}'}$ represents the upper bound of $\mathrm{K}'_{j_D \to i}(t)$ ($\forall i,t$; $\forall j_D \in J_D$). Accordingly, we postulate Hypothesis 2 as follows.

Hypothesis 2. *For a given driver of FV* i *who perceives LV* j_D *in car following at time* t*, the uncertainty in PRS* ($\Delta V_i(t)$) *and that in RT* ($\Delta T_{j_D \to i}(t)$) *are two complementary variables which also exhibit the properties of quantum uncertainty in a conjugate form given by* $\Delta V_{j_D \to i}(t) \cdot \Delta T_{j_D \to i}(t) \geq \frac{h'}{\overline{\mathrm{K}'}}$ ($\forall i,t$; $\forall j_D \in J_D$).

In contrast with Hypothesis 1, Hypothesis 2 provides two implications. First, Eq. (3.11) infers that the trade-off relationship exists between the uncertainty of PRS ($\Delta V_i(t)$) and uncertainty of RT ($\Delta T_{j_D \to i}(t)$), similar to the trade-off relationship of uncertainty between $\Delta \mathrm{K}_{j_D \to i}(t)$ and $\Delta T_{j_D \to i}(t)$ revealed in Hypothesis 1. Such an information uncertainty relationship enhances our reasoning about the association of

external stimulus (*e.g.*, $\Delta V_{j_D \to i}(t)$) with internal stimulus (*e.g.*, $\Delta T_{j_D \to i}(t)$) in car following under driver perception uncertainty. Second, by comparing the lower bounds of Eq.s (3.7) and (3.11) we infer that the magnitude of the trade-off of uncertainty between $\Delta V_{j_D \to i}(t)$ and $\Delta T_{j_D \to i}(t)$ (Hypothesis 2) is greater than that between $\Delta \mathrm{K}_{j_D \to i}(t)$ and $\Delta T_{j_D \to i}(t)$ (Hypothesis 1). Such a reasoning infers the natural existence of a human mental buffer mechanism, sort of like the decoupling function of logistics—inventory, to decouple the effect of uncertainty in external stimulus on human psychology and behavior.

Similar to Eq. (3.8), using the properties of the squeezed state of quantum uncertainty we further transform the conjugate form (Eq. (3.11)) presented in Hypothesis 2 into a linear relationship to characterize the trade-off relationship between $\Delta V_{j_D \to i}(t)$ and $\Delta T_{j_D \to i}(t)$ bounded with a minimum lower bound. Thus, we have

$$\begin{aligned} &\Delta V_{j_D \to i}(t) \cdot \Delta T_{j_D \to i}(t) \geq \frac{h'}{\overline{\mathrm{K}'}} \\ &\Rightarrow \ln(\Delta V_{j_D \to i}(t)) + \ln(\Delta T_{j_D \to i}(t)) = \ln(\tilde{h}') \quad (let\ \tilde{h}' = \frac{h'}{\overline{\mathrm{K}'}})\ (\forall i,t\,;\forall j_D \in J_D) \\ &\Rightarrow \ln(\Delta T_{j_D \to i}(t)) = \ln(\tilde{h}') - \beta_1 \ln(\Delta V_{j_D \to i}(t)) \end{aligned} \tag{3.12}$$

Thus, the conjugate form presented in Hypothesis 2 can be represented by the other form given by Eq. (3.12) to facilitate conducting the hypothesis test. Therein, we have the null hypothesis $H_{null}: \beta_1 \leq 0$ such that $\ln(\Delta T_{j_D \to i}(t))$ and $\ln(\Delta V_{j_D \to i}(t))$ are not related. The alternative hypothesis (H_{2A}) is $H_{2A}: \beta_1 > 0$ indicating that $\ln(\Delta T_{j_D \to i}(t))$ and $\ln(\Delta V_{j_D \to i}(t))$ are negatively related.

Figure 3-2 shows the quantum optical flow-based research roadmap for linking the relationship of uncertainties $\Delta V_{j_D \to i}(t)$ and $\Delta T_{j_D \to i}(t)$. The research roadmap indicates that the trade-off between $\Delta V_{j_D \to i}(t)$ and $\Delta T_{j_D \to i}(t)$ $(\forall i,t\,;\forall j_D \in J_D)$ in the car-following scenario under driver perception uncertainty. By defining the

uncertainties as the standard deviations of probability distributions, the aforementioned uncertainties, *e.g.*, $\Delta V_{j_D \to i}(t)$ and $\Delta T_{j_D \to i}(t)$, can then be approximated for hypothesis tests using the driving simulator.

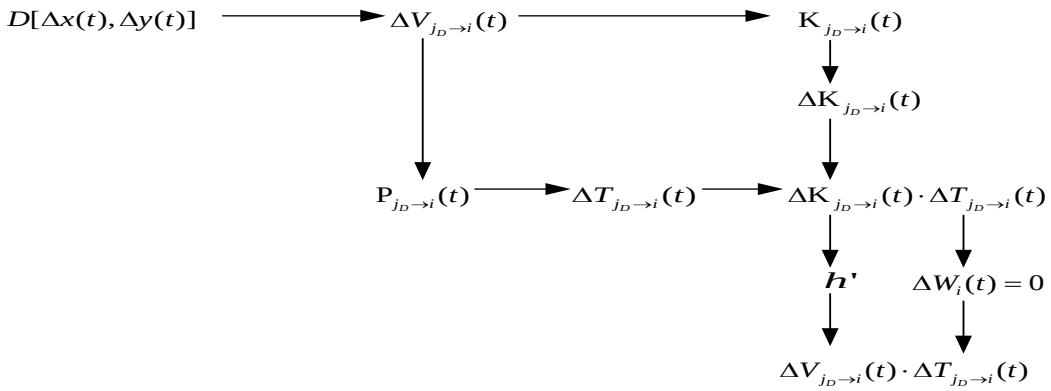

Figure 3-2 The quantum optical flow-based research roadmap linking the relationship between uncertainties $\Delta V_{j_D \to i}(t)$ and $\Delta T_{j_D \to i}(t)$

CHAPTER 4 EXPERIMENTS AND RESULTS

Following the procedure of the experiment adopted in Sheu and Wu (2011, 2015), this work designs a two-stage experiment, which is detailed in the next section to facilitate conducting the corresponding hypothesis tests. The two-stage experiment contains two separate experiments executed one after the other (Figure 4-1), where the first stage experiment explores psychophysical energy-time uncertainty and tests Hypothesis 1; and the second stage experiment discovers the revised trade-off between ΔPRS and ΔRT, and tests Hypothesis 2. The two-stage experiment was conducted using a driving simulator. The following details the experimental procedures in the upgraded simulation software.

Based on Figure 4-1, we further specified the primary procedures required to conduct the first stage and second stage experiments which contained eight and seven steps, respectively, as presented in Figure 4-2 and Figure 4-3. Furthermore, we adopted the measure suggested in Bar-Anan *et al*. (2009) to reveal the detailed information about the purpose of and procedures in the two-stage experiment to each participant to avoid uncertainty caused by a lack of information.

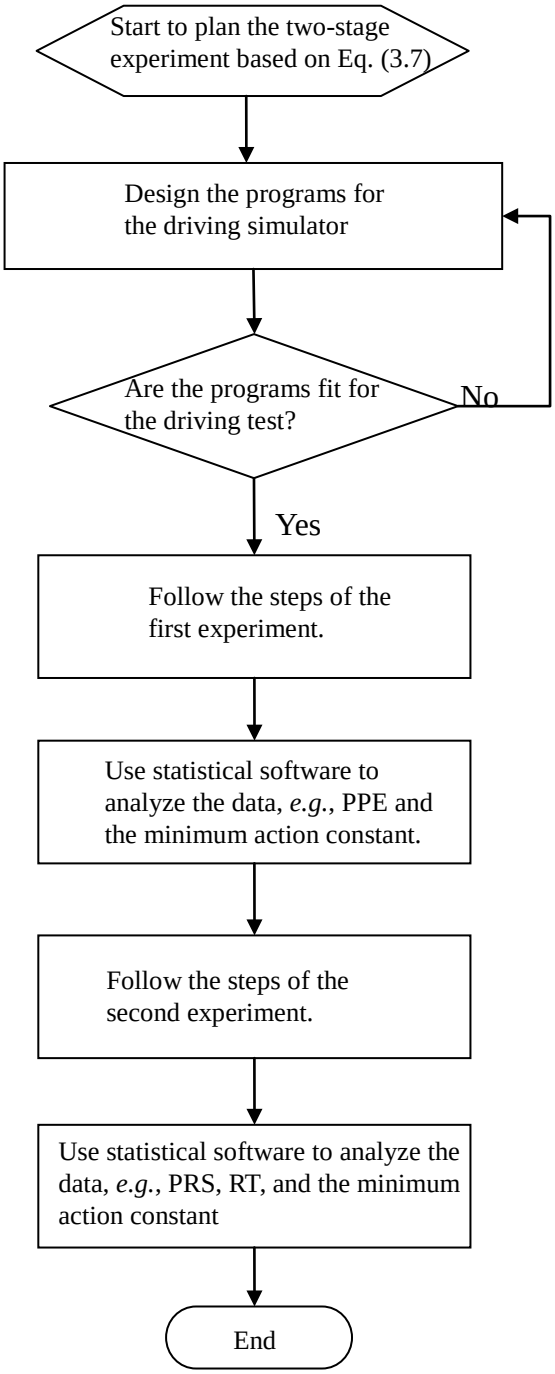

Figure 4-1 The two-stage experimental flowchart

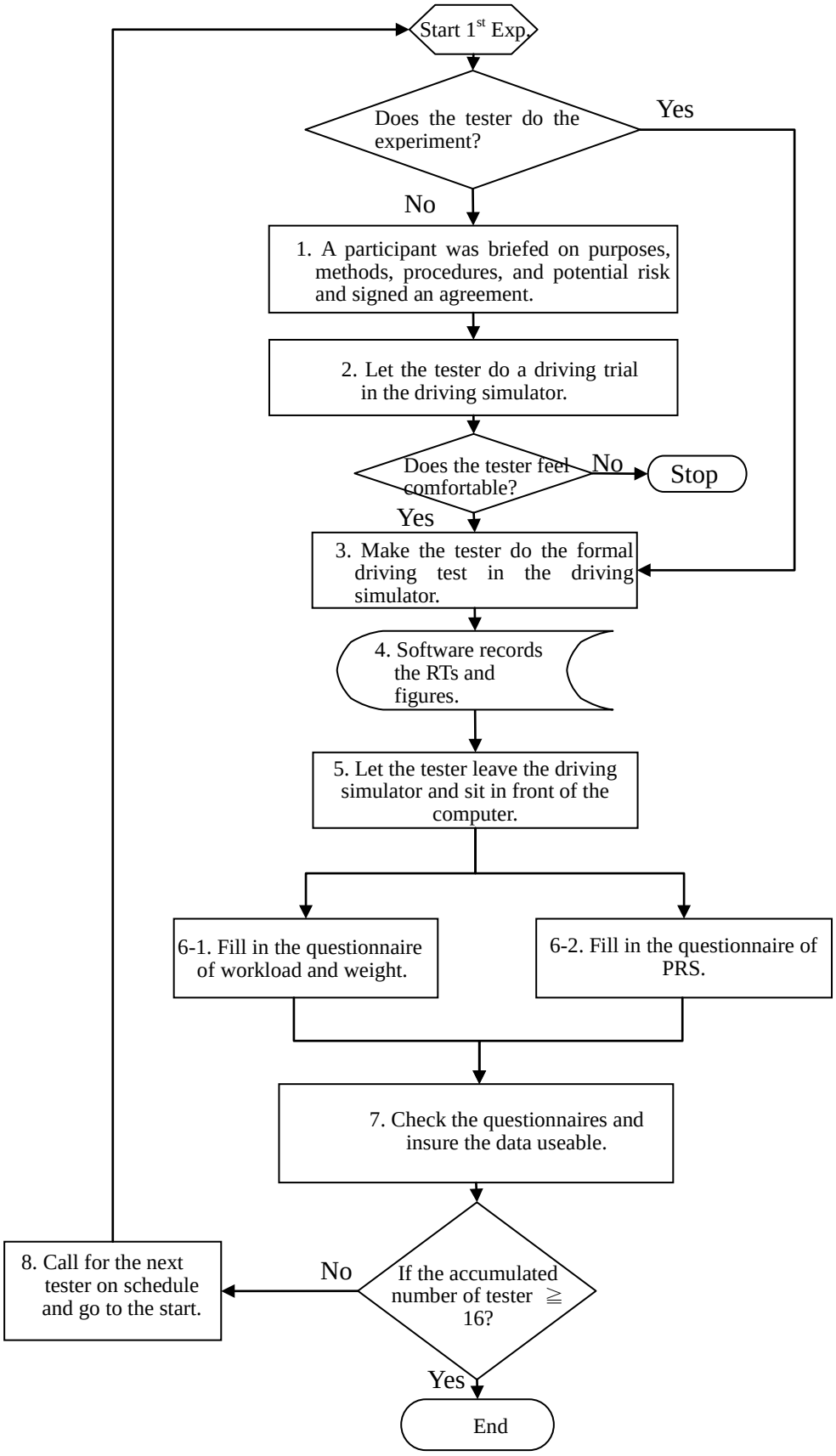

Figure 4-2 The first stage experimental procedure

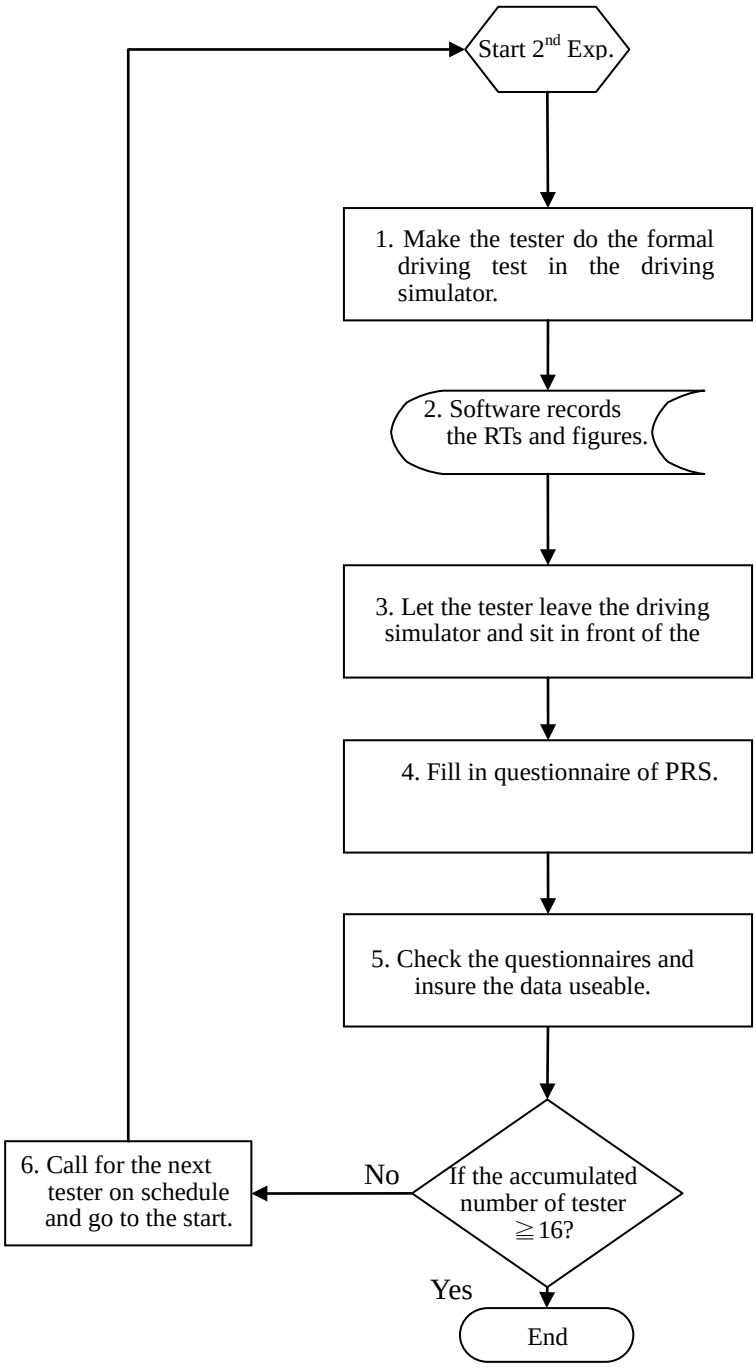

Figure 4-3 The second stage experimental flowchart

4.1 Participants

The original number of participants was 20. Due to some participants were

distracting, or not feel well, the finally number of participants was 16. Sixteen volunteers, 8 males and 8 females who had an average age of 37.9 years, (range 20–60 years), were selected to join in the experiments. Criteria for enrollment were normal or corrected vision, no medication use, no alcohol consumption in the previous 24 hours, and aged 18 or older. Each participant was aware of test requirements and provided written consent.

4.2 Independent and Dependent Variables

The quantum optical flow-based driver's stimulus-response model (Sheu, 2008) was applied to characterize car-following behavior. The quantum optical flow from the rear brake light blinking on/off and the different environmental situations was affected by speed and spacing (space headway) determined intuitively. Thus, different levels of speed and spacing were the input stimuli and independent variables in the experiments. The PRS and RT were outputs and dependent variables.

The specifications of independent variables are provided as follows. This work defines three independent variables: speed, spacing and perceived light mass of LV. The variable of speed refers to as the speed of the FV. In the work, we consider three levels of speed, 30 kph, 60 kph and 90 kph, preset for experiments using the driver simulator. In each experiment, the speed level was chosen randomly by the program. Participants who acted as the FV drivers were, then, given an audio suggest via the system to maintain comparable speed during the tests. The spacing between the simulated LV and FV had three levels: 20 m, 40 m, and 60 m. The three levels of spacing in virtual environments were also simulated using EON Studio 4.0 in the lab. The perceived light mass of LV (*i.e.*, $m_{j_D \to i}(t)$) refers to the magnitude of $m_{j_D \to i}(t)$ perceived by the FV driver (*i.e.*, the participant). The magnitude of $m_{j_D \to i}(t)$ at different relative speeds was transformed into input types using the Lucas–Kanade optical flow algorithm (Doğan *et al*., 2010) in OpenCV software in the experiment.

In addition to independent variables, this work specifies four dependent variables, including RT, PRS, driving mental workload, and PPE. The following presents the definitions of dependent variables.

Reaction time (RT)—The RT is defined as the elapsed time $t_2 - t_1$, and recorded by the driving simulator software, where t_1 is the time at which the brake light of the LV turns on/off, and t_2 is the time at which the driver of the FV car takes action and

places a foot on the brake/accelerate pedal.

Perceived relative speed (PRS)－The PRS reported by the FV driver was recorded. Furthermore, the brake/accelerate pedal of the FV vehicle was used to trace the RT to changes in FV driver's visual perception. Participants' PRSs were obtained after each task using a method adopted from Hoffmann and Mortimer (1996). Hoffmann and Mortimer (1996) scaled the relative speed between vehicles by setting the same spacing and different decelerations/accelerations of the LV. By contrast, our experiments designed additional scenarios with same deceleration/acceleration values and different spacings (Tian *et al*., 2015) and initial speeds to enhance the reality of driver perception in experiments. To reduce the measurement bias of PRS, this study conducted a scaling-PRS experiment that had also been conducted in Hoffmann and Mortimer (1996). A seven-point Likert scale (1–7) was used to assess PRS with 20 m, 40 m, and 60 m spacings. The seven subjective perceptual points and their physical relative speeds were as follows: 1, no relative speed (0 m/s); 2, quite slow (1 m/s); 3, slightly slow (2.2 m/s); 4, moderate (3.4 m/s); 5, slightly fast (4.5 m/s); 6, quite fast (5.6 m/s); and 7, extremely fast (6.7 m/s). The physical relative speed was shown in Figure 4-4. Comparing with the physical relative speed and the PRS, the consistence exists in both of them (Hoffmann and Mortimer, 1996).

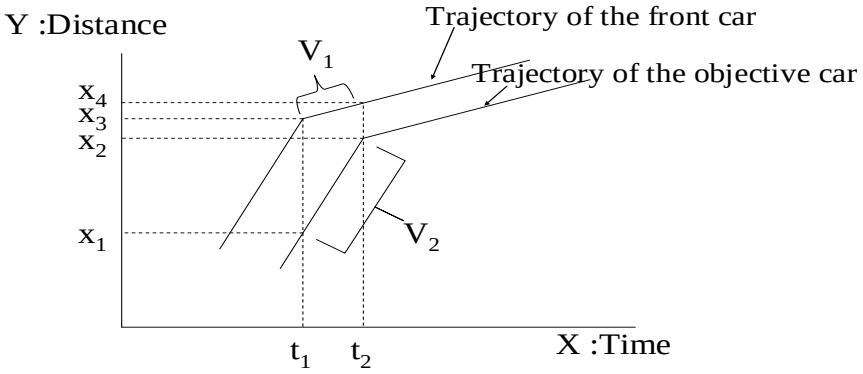

physical relative velocity=V_1-V_2= (x_4-x_3)/(t_2-t_1)- (x_2-x_1)/(t_2-t_1)

Figure 4-4 Physical relative speed.

Driving mental workload－Driving mental workload scores were subjective as they were reported by the participants on a Likert seven-point scale in the experiment,

ranging from 1 for no time pressure to 7 for extreme time pressure, in the nine scenarios. Compared with the six factors of the National Aeronautics and Space Administration-Task Load Index (NASA-TLX) (Hart, 2006)—mental demand, physical demand, time pressure, performance, effort and frustration level—time pressure in different driving scenarios in the first stage experiment is the most important factor and the others factors are the same in different scenarios.

Perceived psychological energy (PPE)—The PPE defined in Eq. (3.3) mentioned above is half of the product of perceived light mass, square of PRS, and driving mental workload. The variable PPE is not one that we can measure directly. However, according to the definition that PPE is a function of PRS originated in the quantum mechanics of optic flow aspect (Baker, 1999) we can measure PPE indirectly by means of PRS. Until now this may be the only way to measure PPE due to the limitations in the driver simulator. So this indirect measurement can be regarded as a preliminary experiment to identify the correlation between RT and PPE.

We collected experimental data associated with RTs and PRSs which were same variables in the first stage and the second stage experiments. Then we divided the collected data into two sub-data-sets. The first sub-data-set were used in the first stage experiment for investigating the psychological energy-time uncertainty, $\Delta \mathrm{K}_{j_D \to i}(t) \cdot \Delta T_{j_D \to i}(t) \geq h'$. The $\mathbf{K}$ consists of the factors of PRS and W. The RT is affected by the speed perception and optical information produced by driving on a straight open road. The second sub-data-set were used in the second stage experiment to identify the revised trade-off relationship between the value of $\ln(\Delta T_{j_D \to i}(t))$ and that of $\ln(\Delta V_{j_D \to i}(t))$ under driver perception uncertainties. To decrease the propagation of uncertainty, we assumed that the uncertainty of the driving mental workload is zero. Then the simplified relationship between the uncertainty of PRS and the uncertainty of RT was tested in the second stage experiment.

4.3 First Stage Experiment

The purpose of first stage experiment was to test Hypothesis 1, where the corresponding null hypothesis is $H_{null}: \alpha_1 \leq 0$; and alternative hypothesis (H_{1A}) is $H_{1A}: \alpha_1 > 0$ such that the relationship between $\Delta T_{j_D \to i}(t)$ and $\Delta \mathrm{K}_{j_D \to i}(t)$ (*i.e.*,

$\Delta K_{j_D \to i}(t) \cdot \Delta T_{j_D \to i}(t) \geq h'$) presented in Hypothesis 1 can be verified.

According to hypothesis test for regression slope, we focused on the slope of the regression line, $\ln(\Delta T_{j_D \to i}(t)) = \ln(h') - \alpha_1 \ln(\Delta K_{j_D \to i}(t))$, where $\ln(h')$ is a constant, α_1 is the slope (also called the regression coefficient). If we found that the slope, α_1, of the regression line is significantly different from zero, then we concluded that there is a significant relationship between $\ln(\Delta T_{j_D \to i}(t))$ and $\ln(\Delta K_{j_D \to i}(t))$, and we rejected the null hypothesis. This involved comparing the P-value to the significance level and rejecting the null hypothesis when the P-value is less than the significance level (α).

A driving simulator provided by Institute of Transportation (IOT), Taiwan was used in the following experiments. This simulator has a physical driving cabin, virtual reality–based visual and audio systems, a computer program for vehicle motion simulation, and an FV computer system that simulates a lifelike driving environment. Figure 4-5 (a) shows a screen view of the driving environment. The driving cabin is a real car body. The virtual environments are generated using EON Studio 4.0 (EON Reality, Inc., USA), a program for developing 3D interactive applications (Sheu and Wu, 2015).

(a) (b)

Figure 4-5 The IOT driving simulator：(a) a lifelike screen view; (b) a personal computer screen view.

Furthermore, a powerful software Unity that can be applied in a personal computer shown in Figure 4-5 (b) was also used in this study shown in Appendix B.

The simulated driving scenario is described as follows. The roadway was 4,500 m long with three 3.65 m wide straight lanes and took rough nine minutes to complete. The nearby virtual environment was a rural road. Participants were told to drive as naturally as possible. The 4,500 m roadway was divided into nine sections, each 500 m long, and randomly assigned one scenario to one of the nine sections. Figure 4-6

illustrates a simulated LV appeared in one road section. According to literature for relative speed perception (Hoffmann and Mortimer, 1996), participant drivers were requested to drive the simulated FVs at a constant speed chosen randomly from the designed three speed levels (*i.e.*, 30 kph, 60 kph and 90 kph). The spacing between the LV and FV was controlled by a computer program for vehicle motion simulation at three spacing levels (*i.e.*, 20 m, 40 m, and 60 m). Then the LV was controlled such that the LV－FV spacing remained at one of the three designed spacing levels 20 m, 40 m, and 60 m in a given test. Therefore, there were nine combined test scenarios. Figure 4-7 shows the concepts of the nine test scenarios. The red dotted-line ovals represent visual scope and the arrows show the optical flow in the rear window of the LV.

In an initial condition, the LV started with a 40 m space between the FV without any surrounding traffic in any road section. Then, the audio system gave an audio suggestion of speed to the FV driver to facilitate the driver's adjusting vehicular speed when reaching to the 200 m LV－FV spacing range in a simulated road section. Then the brake light of the LV was randomly turned on for rest of the road section and the LV decelerated at 3.4 m/s^2 for 2 seconds. The driver of the FV then activated the brakes to avoid a collision. In the next road section, the FV driver heard another speed, saw the event and took action. For instance, in the first road section, the driver of the FV heard 60 kph and drove the FV at that speed with the 40 m spacing. The program assigned one scenario randomly to one road section. The driving simulator does not provide the function to simulate the distance fluctuating when the LV moves with constant speed. However, in the experiments the participants were instructed to follow the LV in the same way as they would on a simulated highway during maneuvers. The RT was recorded. In each section, the optical flow was recorded when the LV was braking at a constant deceleration rate and duration.

We wrote a sub-program in the driving simulation program to record the nine scenarios throughout the driving simulation for each participant. Then each participant could replay the result of each scenario on the screen in the driving simulation lab to measure the relative speeds, and complete the questionnaire. So the measurement of PRS is considerable reliant. The measurement of PRS in our study was taken according to the literature of Hoffmann and Mortimer (1996). So, there is considerable credible.

Figure 4-6 A personal computer screen simulated LV in one road section

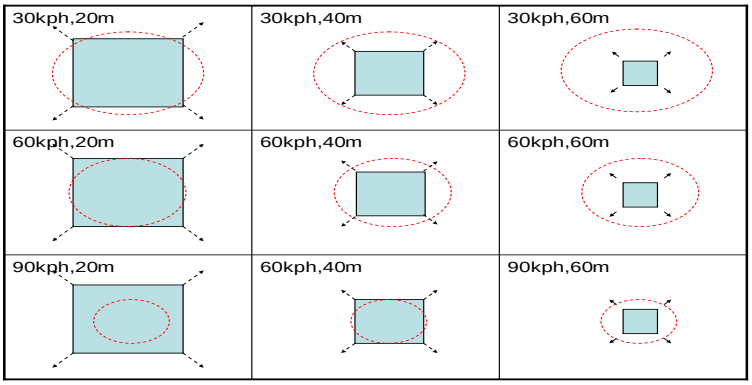

Figure 4-7 Concepts of nine test scenarios when the LV decelerated

The participants were briefed on study purposes, methods, procedures, and potential risk, and then, tested individually. Each participant was seated at comfortable viewing distance from the display. After reading the instructions, they took a driving test using the driving simulator. Each experimental session began with a five-min. practice trial designed to allow participants to become comfortable with driving in this virtual environment. They were instructed to stay in the middle lane and to drive at any speed that was comfortable. They were further instructed to keep focused on road in front of their car. After successfully completing a practice drive, each participant finished the following sequence five times: (a) complete an experimental drive; (b) exit the vehicle and report the PRS in nine scenarios in the experimental drive; and (c) complete the Likert seven-point scale (1 for no time pressure to 7 for extreme time pressure) for the comparative driving mental workload in the nine scenarios. The individual scores were averaged to provide a total workload

score. To prevent fatigue and boredom due to sitting for long periods and focusing on images in the simulator, participants exited the car and completed a non-driving test between experimental drives.

Then, the repeated measures analysis of variance (repeated measures ANOVA) was applied to calculate differences in PPE, RT, PRS, and driving mental workload. Two-factor ANOVA (speed vs. spacing) was applied to the nine simulated scenarios to investigate main effects and interactions. Experimental data were analyzed using mathematical transformation, the natural logarithmic function (ln), and a model of Curve Fitting with Analyze/Regression/Curve-Estimation in SPSS Software. In the first stage experiment, we generated 720 records (16 participants× 5 tests× 9 scenarios). Table 4-1 and Figure 4-8 present the measurements of the key dependent variables, PPE and RT, obtained in different speed－spacing scenarios of the first stage experiment. Moreover, Table 4-2 indicates that speed and spacing are two repeated-measure factors which have significant effects on the dependent variables PPE and RT, according to the test results of the repeated measures ANOVA (Sheu and Wu, 2015).

Table 4-1 Experimental results of the first stage experiment

Spacing scenario / Speed scenario	$\overline{K}$ (scale)	ΔK (scale)	$\overline{T}$ (msec)	ΔT (msec)	h' *(note)	$\overline{W}$ (scale)
Spacing= 20 m						
Speed= 30 kph	13.6	7.6	1485.9	342.7	2.6	3.4
Speed= 60 kph	26.2	12.6	1314.7	317.1	4.0	4.6
Speed= 90 kph	48.4	22.6	1250.7	258.8	5.8	5.4
Spacing= 40 m						
Speed= 30 kph	6.5	3.7	1827.2	416.3	1.5	2.6
Speed= 60 kph	13.3	6.8	1782.9	416.9	2.8	3.7
Speed= 90 kph	24.8	10.7	1585.7	273.7	2.9	4.4
Spacing= 60 m						
Speed= 30 kph	2.4	2.4	1770.1	426.4	1.0	2.2
Speed= 60 kph	6.0	4.2	1655.2	386.3	1.6	3.1
Speed= 90 kph	11.5	6.9	1703.7	356.6	2.5	3.6

$\overline{K}$: mean value of PPE; ΔK: standard deviation of k ; $\overline{T}$: mean value of RT; ΔT: standard deviation of RT; h': action constant; $\overline{W}$: mean value of driving mental workload. Note: the Unit of h' =sec* scale* scale.

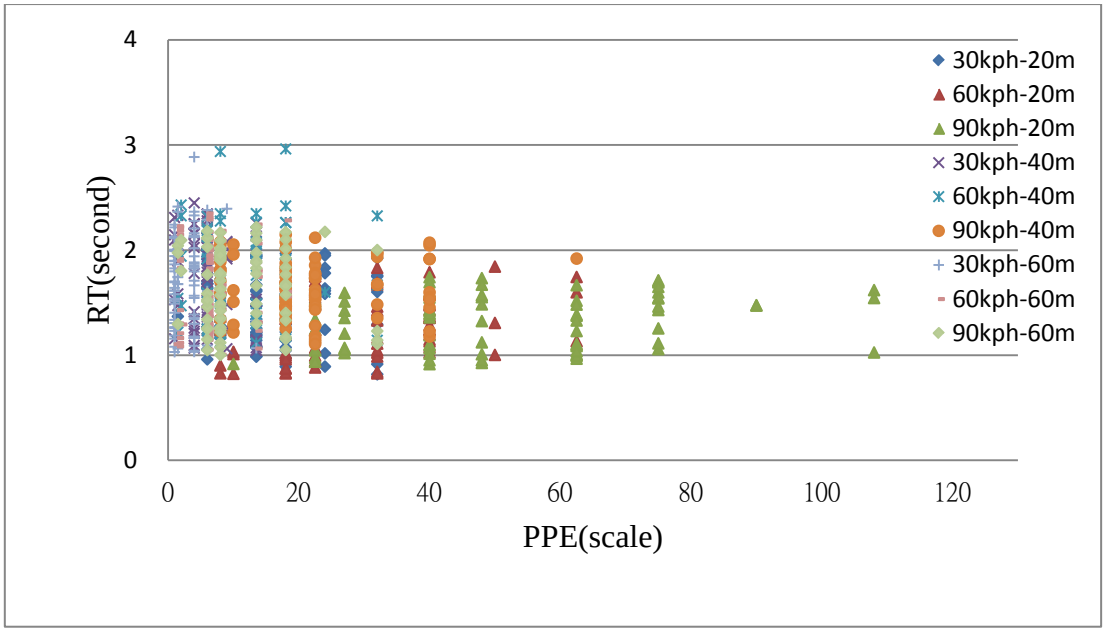

Figure 4-8 Plots of PPE and RT (first stage experiment)

Table 4-2 ANOVA statistics for PPEs and RTs

Variable	F	p
PPE (df=2, 98)		
Speed	19.1	<.0005
Spacing	113.5	<.0005
Speed·Spacing	3.8	<.01
RT (df=2, 98)		
Speed	5.8	<.01
Spacing	32.6	<.01
Speed·Spacing	1.0	.13

Resource: Sheu and Wu (2015)

Then, we fitted $\ln(\Delta K)$ versus $\ln(\Delta T)$, where the corresponding test results are presented in Table 4-3. As can be seen from the R-squared statistics of Table 4-3, the empirical equation postulated in Hypothesis 1 (Eq. (3.8)), overall, fits data well. For example, the R-squared value of the linear function yielded in the scenario of PRS<0 was 0.705, significant at 0.005 <0.05, indicating that 88% of the first stage experiment result is explained by independent explanatory variables for the case when PRS<0. The result of the curve fit was shown in Figure 4-9. Furthermore, we calculated the t-statistics for $\ln(\Delta K_{j_D \to i}(t))$ by the ratio $(\hat{\alpha}_1 - 0)/S_{\hat{\alpha}_1}$, where $\hat{\alpha}_1$ is the estimator of coefficient α_1; and $S_{\hat{\alpha}_1}$ is the standard deviation of $\hat{\alpha}_1$. The

corresponding test results of Table 3 indicate that the null hypothesis ($H_{null}:\alpha_1 \le 0$) of Hypothesis 1 is rejected at a 0.05 level of significance. Accordingly, the negative relationship between $\ln(\Delta K_{j_D \to i}(t))$ and $\ln(\Delta T_{j_D \to i}(t))$ postulated in Hypothesis 1 is verified.

Table 4-3 Test results for Hypothesis 1

PRS	R-square	Adjusted R-square	Unstandardized Coefficients $\hat{\alpha}_1$ (Std. Error)	t-value	Significant	Test result
<0	0.705	0.663	0.197 (0.048)	4.089	0.005	Reject H_{null}
=0	0.454	0.376	0.289 (0.120)	2.411	0.047	Reject H_{null}
>0	0.452	0.374	0.279 (0.116)	2.405	0.046	Reject H_{null}

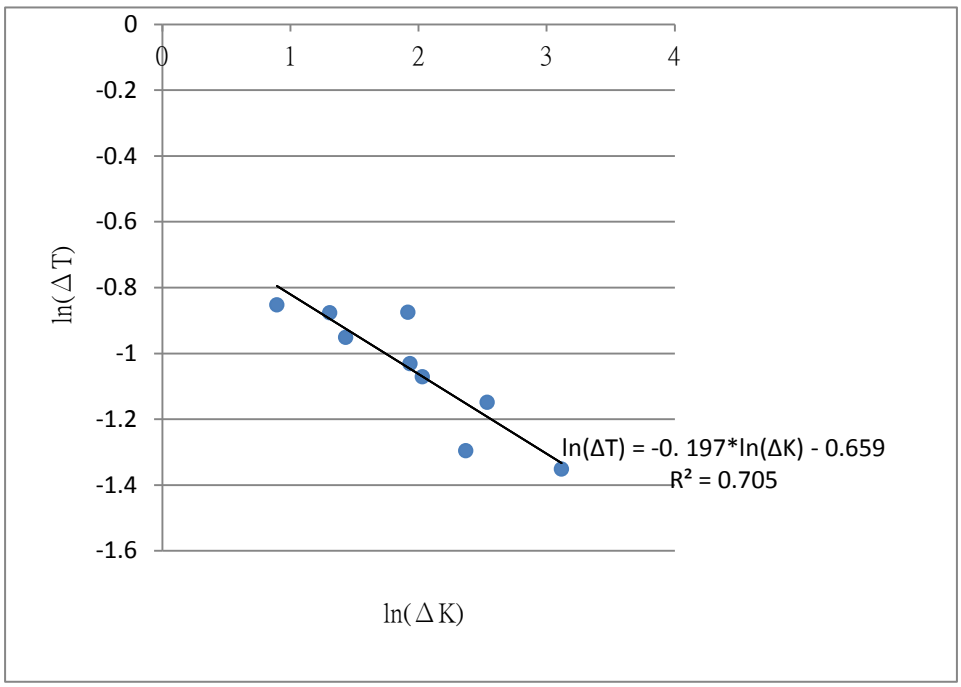

Figure 4-9 The integral relationship between $\ln(\Delta K)$ and $\ln(\Delta T)$.

The individual test results showed that the slopes of the sixteen participants were positive, shown in Figure 4-10. So the each null hypothesis ($H_{null}:\alpha_1 \le 0$) of the each participant was rejected at level of significance, 0.05.

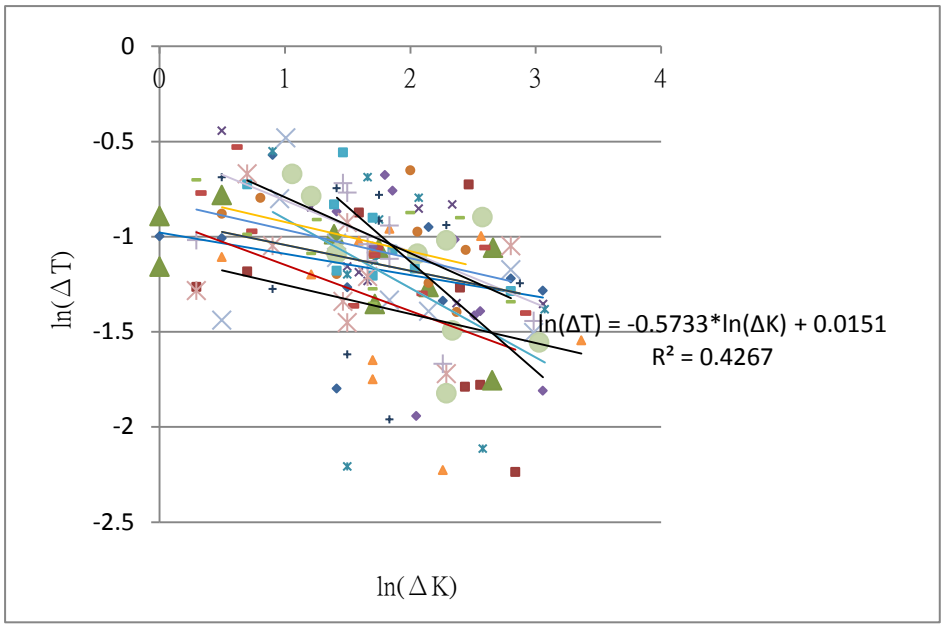

Figure 4-10 The individual relationship between ln(ΔK) and ln(ΔT).

4.4 Second Stage Experiment

The purpose of the second stage experiment is to test Hypothesis 2 so as to ensure that the corresponding null hypothesis ($H_{null}: \beta_1 \leq 0$) which postulates that $\ln(\Delta T_{j_D \to i}(t))$ and $\ln(\Delta V_{j_D \to i}(t))$ are negatively related. The driving simulator is the same as in the first stage experiment. The procedures in the second stage experiment were similar to those in the first stage experiment. As is the first stage experiment, the second stage experiment designed nine driving scenarios by combining three speed levels (speed= 30 kph, 60 kph, and 90 kph) with three spacing levels (FV－LV spacing= 20 m, 40 m, and 60 m). A different number of participants and testing times, including one participant doing 30 tests and ten participants who did three tests each, were used.

Table 4-4 and Figure 4-11 present the measurements of the key dependent variables, PRS and RT, obtained in different speed－spacing scenarios of the second stage experiment. Moreover, the test results (Sheu and Wu, 2015) of repeated measures ANOVA indicate that both speed and spacing are two factors significantly influencing the measurements of dependent variables PRS and RT, as presented in Table 4-5.

Table 4-4 Experimental results of the second stage experiment

	$\overline{V}_{j_D \to i}$ (scale)	$\Delta V_{j_D \to i}$ (scale)	$\overline{T}_{j_D \to i}$ (msec)	$\Delta T_{j_D \to i}$ (msec)	$\tilde{h}'$ (sec*scale)
	Spacing= 20 m				
Speed= 30 kph	2.85	0.71	1,486	342.7	0.17
Speed= 60 kph	3.35	0.76	1,315	317.1	0.10
Speed= 90 kph	4.15	0.94	1,251	258.8	0.07
	Spacing= 40 m				
Speed= 30 kph	2.15	0.64	1,827	416.3	0.27
Speed= 60 kph	2.55	0.71	1,783	416.9	0.16
Speed= 90 kph	3.15	0.69	1,586	273.7	0.10
	Spacing= 60 m				
Speed= 30 kph	1.425	0.57	1,770	426.4	0.51
Speed= 60 kph	1.85	0.63	1,655	386.3	0.27
Speed= 90 kph	2.375	0.70	1,704	356.6	0.17

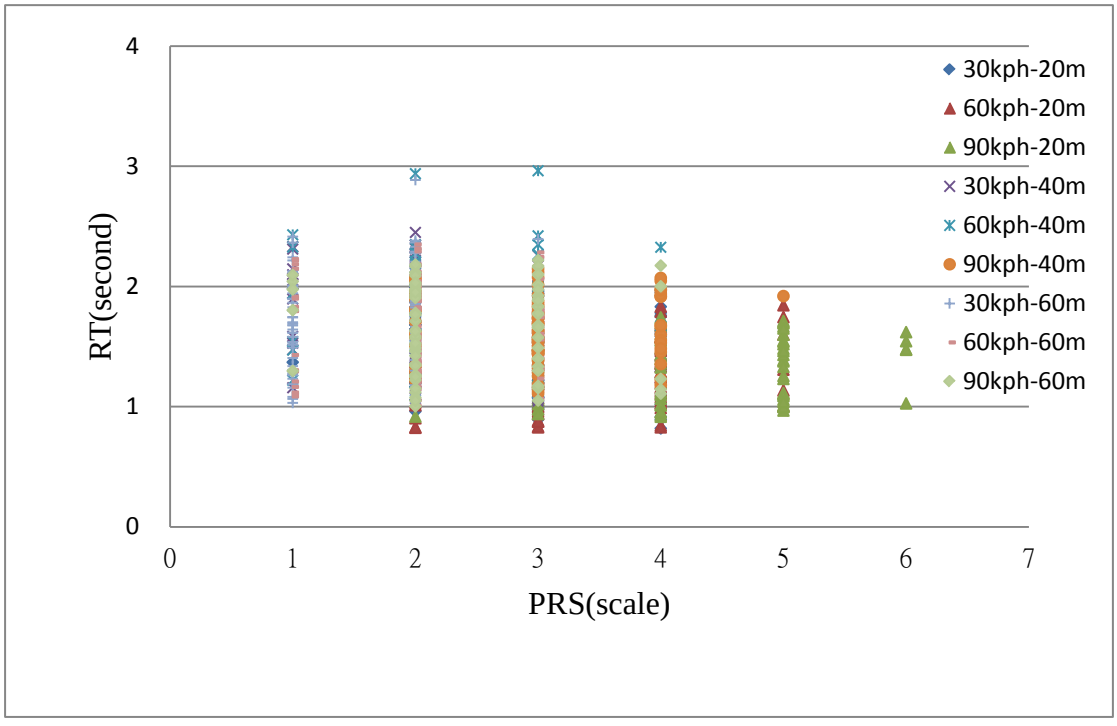

Figure 4-11 Plots of PRS and RT (second stage experiment)

Table 4-5 ANOVA statistics for PRSs and RTs

Variable	F	p
PRS (df= 2, 98)		
Speed	24.8	<.0005
Spacing	113.5	<.0005
Speed·Spacing	0.6	.08
RT (df= 2, 98)		
Speed	3.1	<.05
Spacing	43.9	<.0005
Speed·Spacing	0.4	.15

Resource: Sheu and Wu (2015)

Similarly, the linear curve-fitting function in SPSS was applied to identify the transformed relationship between ln(ΔT) and ln(ΔV). The corresponding test results are presented in Table 4-6. Overall, the empirical equation fits the data well. In total, 77% of experiment results are explained by the independent explanatory variables in the equation, as indicated by the R-squared values of Table 4-6. Furthermore, the t-statistics for ln ($\Delta V_{j_D \to i}(t)$) were calculated using the ratio $(\hat{\beta}_1 - 0)/S_{\hat{\beta}_1}$, where $\hat{\beta}_1$ is an estimator of coefficient β_1; and $S_{\hat{\beta}_1}$ is the standard error of the estimator $\hat{\beta}_1$. The estimated t-statistics indicate that the null hypothesis ($H_{null}: \beta_1 \le 0$) of Hypothesis 2 is rejected at a 0.05 level of significance. Therefore, the negative relationship between ln($\Delta V_{j_D \to i}(t)$) and ln($\Delta T_{j_D \to i}(t)$) postulated in Hypothesis 2 is verified. The result of the curve fit was shown in Figure 4-12.

Table 4-6 Test results of Hypothesis 2

PRS	R-square	Adjusted R-square	Unstandardized Coefficients $\hat{\beta}_1$ (Std. Error)	t-value	Significant	Test result
<0	0.590	0.532	1.022(0.322)	3.177	0.016	Reject H_{null}
=0	0.632	0.580	1.009(0.291)	3.470	0.010	Reject H_{null}
>0	0.636	0.585	1.281(0.366)	3.501	0.010	Reject H_{null}

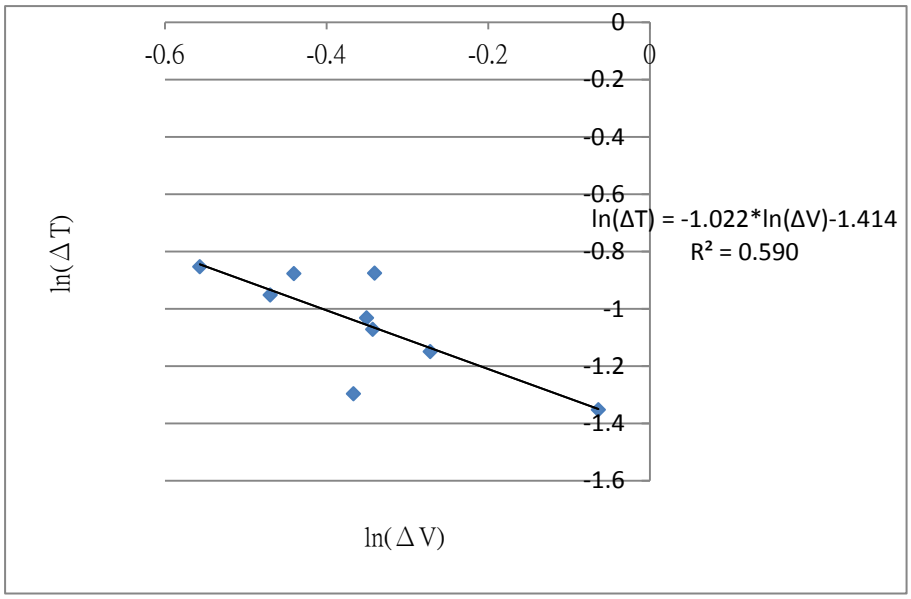

Figure 4-12 The integral relationship between ln(Δ T) and ln(Δ V)

The individual test results showed that the individual slopes ($\hat{\beta}_1$) of the sixteen participants were positive and the P-values of the participants were less than 0.05, shown in Figure 4-13. The sixteen individual null hypotheses ($H_{null}: \beta_1 \leq 0$) of the sixteen participants were rejected at level of significance, 0.05. The others were rejected at level of significance, 0.1.

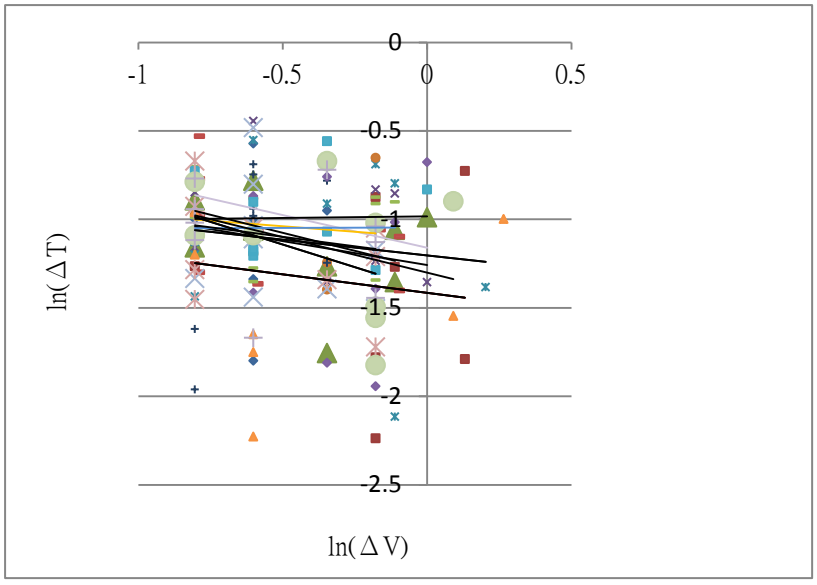

Figure 4-13 The individual relationship between ln(Δ T) and ln(Δ V)

4.5 Findings

Drawn from the above experimental results, the following provides some interesting findings.

The experimental results yielded from the first stage experiment reveal some important findings. First, given the FV and LV move at high speed in fixed spacing scenarios on a straight highway segment. From the FV driver perspective, any sudden braking behavior of the LV may occur, leading to the increase in the uncertainty of PPE as both the light mass of LV perceived and negative (backward) PRS may change unexpectedly. Furthermore, the workload of the FV driver may increase, shifting attention from distraction to concentration, according to Tenenbaum and Connolly (2008) to avoid a vehicle collision. Meanwhile, the FV driver may spend less RT to react to the LV braking at high speed, thus contributing to the decrease in the uncertainty of RT. This is what exactly reasoned by Hypothesis 1. Second, consistent with car-following and RT literature we observe that the average of RT decreases as spacing decreases and speed increases. Third, we observe that the average of PPE increases as spacing decreases, and vehicle speed increases. Although PPE is treated as a kind of internal stimulus, to a certain extent it can also contribute to negative affective responses, *e.g.*, nervousness, stress, and strain (Öz *et al.*, 2010), as PPE remains in a highly unstable and uncertain status (*i.e.*, the uncertainty of PPE increases). Extensive literature supports the claim that individual affective states may influence evaluative judgments, ranging from those concerned with the purchase of consumer goods, the evaluation of people, and driving behavior (Matthews, 2001; Malhotra, 2005). Such a finding may provide some directions for improving safe and comfortable driving environments from a psychological perspective.

Experimental results gained from the second stage experiment to verify the trade-off relationship between the uncertainties of PRS and RT yield similar findings. First, on a straight highway segment and in fixed spacing scenarios, the FV driver's RT decreases, when recognizing that the uncertainty related to PRS increases as the perceived light mass and backward speed of LV increases, and thus, the FV driver's RT uncertainty decreases. The likely reason is similar to that aforementioned when a LV brakes at high speed, the workload of the FV driver increases to quickly respond to the sudden change of PRS to avoid a vehicle collision. Second, the standard deviation of RT($^{\Delta T_{j_D \to i}(t)}$) decreases as the standard deviation of PRS($^{\Delta V_{j_D \to i}(t)}$) increases, and vice versa. Specifically, the associated R-squared value yielded in each PRS scenario of the second stage experiment is sufficiently large to be statistically useful in linking the trade-off relationship between uncertainties $^{\Delta V_{j_D \to i}(t)}$ and $^{\Delta T_{j_D \to i}(t)}$, although driving mental workload in each scenario differs. The implication

is that the trade-off between $\Delta V_{j_D \to i}(t)$ and $\Delta T_{j_D \to i}(t)$ can be statistically verified by transforming them into $\ln(\Delta V_{j_D \to i}(t))$ and $\ln(\Delta T_{j_D \to i}(t))$ through curve-fitting analysis. Such a generalization may help us in elaborately characterizing and rationalizing how and when an FV driver responds to the change of perceived LV speed in car-following behavior under driver perception uncertainty conditions.

Furthermore, this study confirms some experimental observations consistent with generalizations/implications of published psychophysical models in related literature (Gibson, 1966; Wiedemann, 1974, 1991, 1992; Lee, 1980; Leutzbach, 1988; Baker, 1999; Toledo, 2003; Oron-Gilad *et al*., 2008; Mehmood and Easa, 2009; Sheu, 2011). For instance, the association of driver alertness with driver behavior (Oron-Gilad *et al*., 2008) can be easily reasoned by either Hypothesis 1 or 2. Specifically, driver alertness increases with small spacing as $\Delta \mathrm{K}_{j_D \to i}(t) \uparrow$ and $\Delta T_{j_D \to i}(t) \downarrow$ (by Hypothesis 1) in the case of small spacing. By contrast, a driver lacks alertness in car following when spacing is large as $\Delta \mathrm{K}_{j_D \to i}(t) \downarrow$ and $\Delta T_{j_D \to i}(t) \uparrow$ (by Hypothesis 1), leading to $\Delta V_{j_D \to i}(t) \downarrow$, *i.e.*, PRS indifference (by Hypothesis 2). Moreover, PPE is redefined, and empirically confirmed in this study, thus providing supporting evidence for those previous studies in quantum optical flows to characterize the effect of PPE on driver psychology and behavior (Gibson, 1966; Lee, 1980; Baker, 1999). Additionally, the definition of RT in this study differs from that in Mehmood and Easa (2009). Specifically, this study measures RT using the term $t_2 - t_1$ which can be easily recorded during simulation. As analytical results show, this definition is fit for developing and improving quantum optical flow-based car-following models. For instance, according to experimental results the standard deviation of RT($\Delta T_{j_D \to i}(t)$) can be applied to the quantum optical flow-based car-following model created by Sheu (2013), where the simulation capability of the quantum mechanics–based car-following model in an uncertain traffic environment can be significantly improved.

Overall, the above experimental results have indicated that the proposed quantum mechanics-based driver perception model permits characterizing the stochastic and potential dynamic features of driver perception which may improve the robustness and reality of existing car-following models applied in the context of driver behavioral uncertainty. In reality, parts of the fundamentals and analytical results of quantum optical flow theory have been applied to modeling car-following

behavior under driver perception uncertainty in Sheu (2013). Compared to the 2D ID model created by Jiang *et al*. (2014), our experimental results support the 2D ID model that allows the traffic states to be spanned in a two-dimensional region, *i.e.*, the speed-spacing plane. For example, our experimental results support the arguments "Only when the spacing is large (small) enough, will they accelerate (decelerate) to decrease (increase) the spacing." and "At a given speed, drivers do not have a fixed preferred spacing." which were mentioned by Jiang *et al*. (2014). Compared to the parsimonious model proposed by Laval *et al*. (2014), our experimental results are consistent with evidence that human errors alone may be responsible for traffic instabilities shown by Laval *et al* (2014).

CHAPTER 5 APPLICATIONS

There are three applications, (1) uncertainties of PRS and RT in foggy and emergency braking conditions, (2) the same processes transferred to a upgraded simulation design, (3) uncertainties of PRS and RT at night, (4) some of the RT data has been applied to an automatic driving vehicle following control logic in a mixed lane where automatic and manual driven vehicles mix near the event area and adjacent to an automated highway system as follows.

5.1 Uncertainties of PRS and RT in foggy and emergency braking conditions

Foggy weather conditions affect uncertainties of driver perceptual judgments of speed and distance. However, in a heavy foggy condition and a leading vehicle braking condition uncertainties of PRS and RT are complicated and need to be identified (Chen and Wu, 2017). If those uncertainties in a foggy weather condition exist in a perspective imitating Heisenberg Uncertainty Principle, then some phenomena for the following driver behaviors can be explained. The purpose of the subsection 5.1 aimed to test the first hypothesis that explained a trade-off relationship between uncertainties of perceived psychological energy and uncertainties of RT of following vehicle drivers, and the second hypothesis that stated a trade-off relation between uncertainties of RT and uncertainties of PRS in regard to averages of PRS and driving mental workload. The experiment have conducted in Chapter 4, giving comparisons with those uncertainties exist in a clear weather condition having been tested in this two-stage experiment based on a quantum optical flow-based model. The findings of this study not only show that those uncertainties also exist in foggy and braking conditions but also indicate the statistical significant no-difference between the two action constants in foggy and clear weather conditions when the LV is in emergency braking conditions.

5.1.1 Experimental data in emergency braking conditions

Experimental data were analyzed using mathematical transformation, the natural logarithmic function (ln), and a model of Curve Fitting with Analyze/Regression/Curve-Estimation in SPSS Software. In the first stage experiment, we generated 720 records (16 participants × 5 tests × 9 scenarios in a foggy condition). The speed and spacing are two repeated-measure factors which have statistical significant effects on the dependent variables PPE and RT (Sheu and Wu, 2015).

The negative relationship between $\ln(\Delta K^{f}{}_{j_D \to i}(t))$ and $\ln(\Delta T^{f}{}_{j_D \to i}(t))$ postulated in Hypothesis 1 in a foggy condition is verified. The corresponding test results were

presented in Table 5-1. As can be seen from the R-squared statistics of Table 5-2, the empirical equation postulated in Hypothesis 1 (Eq. (3.7)), overall, fits data well. For example, the R-squared value of the linear function yielded in the scenario of foggy condition was 0.81, significant at 0.002 <0.05, indicating that 90% of the first stage experiment result is explained by independent explanatory variables for the case when PRS<0. The result of the curve fit was shown in Figure 5-1. Furthermore, we calculated the t-statistics for $\ln(\Delta K^{f}{}_{j_D \to i}(t))$ by the ratio $(\hat{\alpha}_1^{f} - 0)/V_{\hat{\alpha}_1{}^{f}}$, where $\hat{\alpha}_1{}^{f}$ is the estimator of coefficient $\alpha_1{}^{f}$; and $V_{\hat{\alpha}_1{}^{f}}$ is the standard deviation of $\hat{\alpha}_1{}^{f}$. The corresponding test results of Table 5-2 indicate that the null hypothesis ($H_{null}: \alpha_1{}^{f} \le 0$) of Hypothesis 1 is rejected at a 0.05 level of significance.

Table 5-1 Experimental results of the first stage experiment in a foggy weather condition

Spacing scenario / Speed scenario	$\overline{K}$ (scale^3)	ΔK (scale^3)	$\overline{T}$ (msec)	ΔT (msec)	h'^{*} (note)	$\overline{w}$ (scale)
Spacing = 20 m, in foggy						
S= 30 kph	28.1	17.2	1703.4	385.7	6.6	5.3
S= 60 kph	39.5	25.1	1464.9	337.3	8.5	6.0
S= 90 kph	58.3	37.8	1340.6	340.9	12.9	6.7
Spacing = 40 m, in foggy						
S= 30 kph	10.0	8.6	2208.5	593.5	5.1	4.0
S= 60 kph	13.5	13.0	2008.5	559.1	7.2	4.7
S= 90 kph	24.2	14.4	1891.4	441.3	6.3	5.5
Spacing = 60 m, in foggy						
S= 30 kph	4.1	3.7	2620.4	1048.5	3.9	3.3
S= 60 kph	7.0	5.7	2111.0	545.9	3.1	3.4
S= 90 kph	10.2	10.3	2012.0	451.9	4.7	4.2

Note: the Unit of h' =sec*Workload-scale*PPE-scale^2

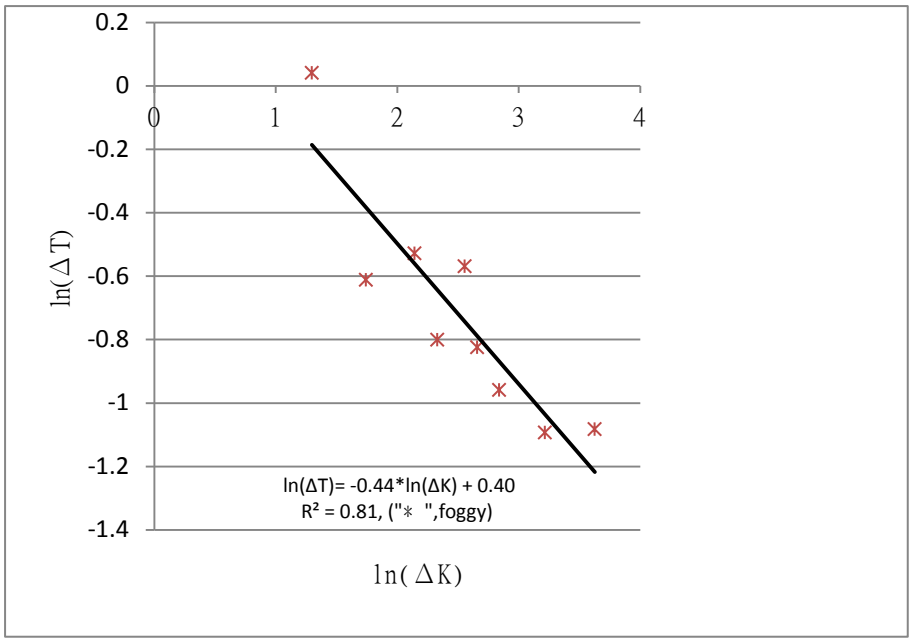

Figure 5-1 Relationship between ln(ΔT) and ln(ΔK) in foggy

Those results in foggy were presented in Table 5-2.

Table 5-2 Test results for Hypothesis 1: relationship between Ln(ΔT) and Ln(ΔK)in a foggy condition at a 0.05 level of significant

	in foggy
R^2	0.81
Adjusted R^2	0.77
Unstandardized Coefficients (Std. Error)	$\hat{\alpha}^f{}_1$=-0.44 (0.09)
t-value	-4.97
Significant	0.002
Accept or Reject H_{null}	Reject H_{null}

5.1.2 The second-stage experiment

The purpose of the second stage experiment is to test Hypothesis 2 in a foggy condition so as to ensure that the corresponding null hypothesis ($H_{null}: \beta_1{}^f \leq 0$) which postulates that $\ln(\Delta T_{j_D \to i}(t))$ and $\ln(\Delta V_{j_D \to i}(t))$ are negatively related. The procedures in the second stage experiment were similar to those in the first stage

experiment.

Then, we compared the action constant in a foggy condition with one in a clear condition. The statistical significant no-difference between two action constants in foggy and clear weather conditions was confirmed by a two-sided .05 α level Wilcoxon signed-rank test (n= 9, *P*= 0.46). The speed and spacing are two factors statistical significantly influencing the measurements of dependent variables PRS and RT in foggy and clear weather conditions (Sheu and Wu, 2015).

The negative relationship between $\ln(\Delta V^{f}{}_{j_D \to i}(t))$ and $\ln(\Delta T^{f}{}_{j_D \to i}(t))$ postulated in Hypothesis 2 in a foggy condition is verified. The linear curve-fitting function in SPSS was applied to identify the transformed relationship between $\ln(\Delta V^{f}{}_{j_F \to i}(t))$ and $\ln(\Delta T^{f}{}_{j_D \to i}(t))$ in a foggy condition. The corresponding test results are presented in Table 5-3. Overall, the empirical equation fits the data well. In total, 80% of experiment results are explained by the independent explanatory variables in the equation, as indicated by the R-squared values of Table 5-3. Furthermore, the t-statistics for $\ln(\Delta V^{f}{}_{j_D \to i}(t))$ were calculated using the ratio $(\hat{\beta}_1{}^{f} - 0)/V_{\hat{\beta}_1{}^{f}}$, where $\hat{\beta}_1{}^{f}$ is an estimator of coefficient $\beta_1{}^{f}$; and $V_{\hat{\beta}_1{}^{f}}$ is the standard error of the estimator $\hat{\beta}_1$. The estimated t-statistics indicate that the null hypothesis ($H_{null}: \beta_1{}^{f} \le 0$) of Hypothesis 2 is rejected at a 0.05 level of significance. The results of curves fit were shown in Figure 5-2.

Table 5-3 Experimental results of the second stage experiment in a foggy weather condition

	$\overline{V}$ (scale)	ΔV (scale)	$\overline{T}$ (msec)	ΔT (msec)	$\tilde{h}'$ (sec*scale)
	Spacing =20m, in foggy				
S= 30 kph	3.0	1.0	1703.4	385.7	0.30
S= 60 kph	3.5	1.1	1464.9	337.3	0.25
S= 90 kph	4.0	1.3	1340.6	340.9	0.19
	Spacing= 40 m, in foggy				
S= 30 kph	2.1	1.	2208.5	593.5	0.61
S= 60 kph	2.1	1.2	2008.5	559.1	0.51
S= 90 kph	2.9	1.4	1891.4	441.3	0.34
	Spacing= 60 m, in foggy				
S= 30 kph	1.5	0.6	2620.4	1048.5	1.08
S= 60 kph	1.9	0.8	2111.0	545.9	0.82
S= 90 kph	2.0	0.9	2012.0	451.9	0.63

Resource: Chen and Wu (2017)

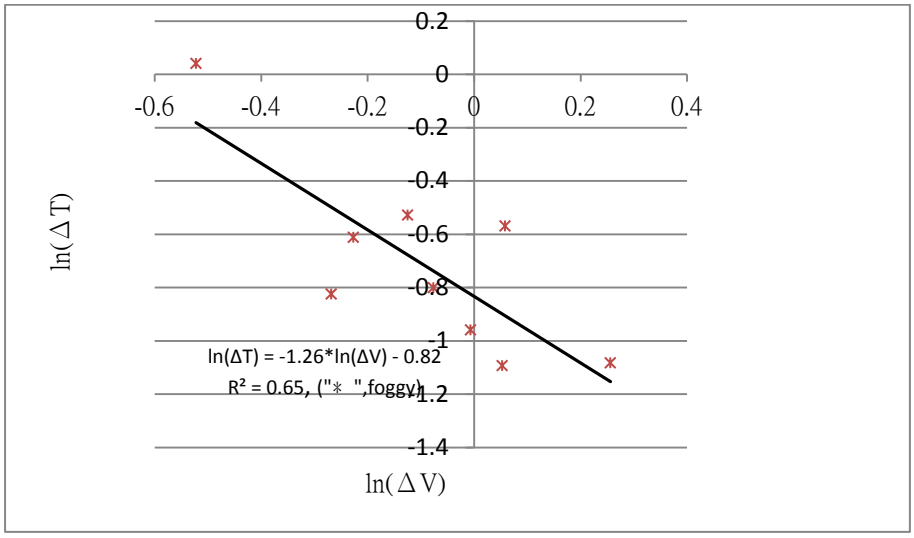

Resource: Chen and Wu (2017)

Figure 5-2 Relationship between $\ln(\Delta V)$ and $\ln(\Delta T)$ in foggy.

Those results in a foggy condition were indicated in Table 5-4.

Table 5-4 Test results for Hypothesis 2: relationship between Ln(ΔT) and Ln(ΔV)in a foggy weather condition at a 0.05 level of significant

	in foggy
R^2	0.65
Adjusted R^2	0.54
Unstandardized Coefficients(Std. Error)	$\hat{\beta}_1^{\,f}$ =-1.26(0.35)
t-value	-3.22
Significant	0.02
Accept or Reject H_{null}	Reject H_{null}

Resource: Chen and Wu (2017)

5.1.3 Findings

The first stage experiment results disclosed some important findings. First, a trade-off relationship between uncertainties of PPE and RT might exist in a foggy condition based on a perspective imitating Heisenberg Uncertainty Principle and be similar to the trade-off relationship in clear condition (Sheu and Wu, 2015). Second, the workloads, the RT alterations, and the averages of PPE of the FV driver in foggy and clear conditions are alike. For example, two workloads of the FV driver in two conditions may both enlarge, changing attention from distraction to concentration (Tenenbaum and Connolly, 2008) to avoid a vehicle collision. The FV driver may spend less RT to react to the LV braking at high speed, thus contributing to the decrease in the uncertainty of RT in two conditions. The averages of PPE in two conditions both increase as spacings decrease, and vehicle speeds increase. These are what exactly caused by Hypothesis 1. Third, each PPE in two conditions is treated as a kind of internal stimulus, to a certain extent it can also contribute to negative affective responses, *e.g.*, nervousness, stress, and strain (Öz *et al.*, 2010), as PPE remains in a highly unstable and uncertain status (*i.e.*, the uncertainty of PPE increases). Extensive literature sustains the claim that individual affective states may influence evaluative judgments, ranging from those concerned with the purchase of consumer goods, the evaluation of people, and driving behavior (Matthews, 2001; Malhotra, 2005). Fourth, the two action constants imitating Heisenberg Uncertainty Principle in two conditions were compared and confirmed statistical significant no-difference between them. If the uncertainty of PPE ($\Delta K^{f}{}_{j_D \to i}(t)$) in a foggy condition is less than one of PPE ($\Delta K^{c}{}_{j_D \to i}(t)$) ($\Delta T_{j_D \to i}(t)$) in clear condition, then

the uncertainty of RT ($\Delta T^{f}{}_{j_D \to i}(t)$) in a foggy condition is bigger than one of PT ($\Delta T^{c}{}_{j_D \to i}(t)$) in a clear condition. Additionally, the average of RT ($\Delta T^{f}{}_{j_D \to i}(t)$) in a foggy condition increasing as the uncertainty of RT is increasing may lead to higher risk driving (Cavallo, 2002; Yan *et al.*, 2014) than doing in clear condition. Such a finding may provide some directions for improving safe and comfortable driving environments from a psychological perspective.

Experimental results obtained from the second stage experiment to validate the trade-off relationship between the uncertainties of PRS and RT in foggy and clear conditions produced interesting findings. First, a trade-off relationship between uncertainties of PRS and RT subsists in regard to the averages of PRS and driving mental workload in a foggy condition as a trade-off one in a clear condition. The likely reason is similar to that aforementioned when a LV brakes at high speed, the workload of the FV driver increases to quickly respond to the sudden change of PRS to avoid a vehicle collision regardless in a foggy or a clear condition. Second, in a foggy condition the associated R-squared value produced in each PRS scenario of the second stage experiment is not only sufficiently large to be statistically useful in linking the trade-off relationship between uncertainties $\Delta V^{f}{}_{j_D \to i}(t)$ and $\Delta T^{f}{}_{j_D \to i}(t)$ but also similar to one in a clear condition, although driving mental workload in each scenario differs. The implication is that the trade-off between $\Delta V^{f}{}_{j_D \to i}(t)$ and $\Delta T^{f}{}_{j_D \to i}(t)$ in a foggy condition can be statistically validated by transforming them into $\ln(\Delta V^{f}{}_{j_D \to i}(t))$ and $\ln(\Delta T^{f}{}_{j_D \to i}(t))$ through curve-fitting analysis, and is like a implication in a clear condition. Such a generalization may help us in elaborately characterizing and rationalizing how and when an FV driver responds to the change of perceived LV speed in driving behavior under driver perception uncertainty conditions, such as in a foggy weather condition and in a clear one.

Furthermore, according to experimental results the standard deviations of RTs ($\Delta T^{f}{}_{j_D \to i}(t)$ and $\Delta T^{c}{}_{j_D \to i}(t)$) can be both applied to the quantum optical flow-based car-following model created by Sheu (2013), where the simulation capability of the quantum mechanics–based car-following model in an uncertain traffic environment (*e.g.*, foggy or clear weather conditions) can be significantly improved.

5.2 Upgraded Simulation Design

For the purpose of catching up with technical development, such as virtual reality (VR), the powerful software, Unity, was applied in this subsection shown in Figure 5-3 and Figure 5-4. The upgraded simulation software aims at a foggy condition and contains the expansion of experiments in clear and night weather conditions. Each weather condition includes three LV driving situations. First, a LV decelerates and is backward to the FV. The PRS is negative. Second, a LV accelerates and is forward to the FV. The PRS is positive. Third, a LV keeps a same speed with the FV. The PRS is zero.

Figure 5-3 The upgraded IOT driving simulator.

(a) (b) (c)

Figure 5-4 Simulated LVs in one road section in three conditions; (a) clear; (b) night; (c) foggy.

The results in a foggy condition were shown in Table 5-5 and Table 5-6 as follows.

First, we fitted $\ln(\Delta K)$ versus $\ln(\Delta T)$, where the corresponding test results are presented in Table 5-5. As can be seen from the R-squared statistics of Table 5-5, the

empirical equation postulated in Hypothesis 1 (Eq. (3.8)), overall, fits data well. For example, the R-squared value of the linear function yielded in the scenario of PRS>0 was 0.662, significant at 0.008 <0.05, indicating that 81% of the first stage experiment result is explained by independent explanatory variables for the case when PRS>0. The corresponding test results of Table 5-5 indicate that the null hypothesis of Hypothesis 1 is rejected at a 0.05 level of significance. Accordingly, the positive and zero relationships between $\ln(\Delta K^{f}{}_{j_D \to i}(t))$ and $\ln(\Delta T^{f}{}_{j_D \to i}(t))$ postulated in Hypothesis 1 are verified.

Table 5-5 Test results for Hypothesis 1 in foggy.

PRS	R-square	Adjusted R-square	Unstandardized Coefficients $\hat{\alpha}_1$ (Std. Error)	t-value	Significant	Test result
<0	0.835	0.811	0.437 (0.074)	5.95	0.001	Reject H_{null}
=0	0.446	0.367	0.137 (0.058)	2.37	0.049	Reject H_{null}
>0	0.662	0.614	0.336 (0.091)	3.70	0.008	Reject H_{null}

Second, the corresponding test results are presented in Table 5-6. Overall, the empirical equation fits the data well. For example, the R-squared value of the linear function yielded in the scenario of PRS>0 was 0.609, significant at 0.013 <0.05. In total, 78% of experiment results are explained by the independent explanatory variables in the equation. The estimated t-statistics indicate that the null hypothesis ($H_{null}: \beta_1 \le 0$) of Hypothesis 2 is rejected at a 0.05 level of significance. Therefore, the positive and zero relationships between $\ln(\Delta V^{f}{}_{j_D \to i}(t))$ and $\ln(\Delta T^{f}{}_{j_D \to i}(t))$ postulated in Hypothesis 2 are verified.

Table 5-6 Test results of Hypothesis 2 in foggy

PRS	R-square	Adjusted R-square	Unstandardized Coefficients $\hat{\beta}_1$ (Std. Error)	t-value	Significant	Test result
<0	0.598	0.541	1.229 (0.381)	3.228	0.014	Reject H_{null}
=0	0.679	0.633	0.706 (0.183)	3.851	0.006	Reject H_{null}
>0	0.609	0.553	1.643 (0.498)	3.299	0.013	Reject H_{null}

Finally, the results of hypothesis one and hypothesis two are similar to the original experiment in Chapter 4. This application shows that processes of the original experiment can be transferred to the upgraded software and have a potential in virtual reality.

5.3 Uncertainties of PRS and RT at night

The results in a night condition were shown in Table 5-7 and Table 5-8 as follows.

First, we fitted ln(ΔK) versus ln(ΔT), where the corresponding test results are presented in Table 5-7. As can be seen from the R-squared statistics of Table 5-7, the empirical equation postulated in Hypothesis 1 (Eq. (3.8)), overall, fits data well. For example, the R-squared value of the linear function yielded in the scenario of PRS<0 was 0.781, significant at 0.002 <0.05, indicating that 88% of the first stage experiment result is explained by independent explanatory variables for the case when PRS<0. The corresponding test results of Table 5-7 indicate that the null hypothesis of Hypothesis 1 is rejected at a 0.05 level of significance. Accordingly, the positive and zero relationships between ln($\Delta K^n{}_{j_D \to i}(t)$) and ln($\Delta T^n{}_{j_D \to i}(t)$) postulated in Hypothesis 1 are verified.

Table 5-7 Test results of Hypothesis 1 at night

PRS	R-square	Adjusted R-square	Unstandardized Coefficients $\hat{\alpha}_1$ (Std. Error)	t-value	Significant	Test result
<0	0.781	0.749	0.344 (0.069)	4.992	0.002	Reject H_{null}
=0	0.464	0.387	0.287 (0.116)	2.461	0.043	Reject H_{null}
>0	0.635	0.583	0.336 (0.091)	3.490	0.010	Reject H_{null}

Second, the corresponding test results are presented in Table 5-8. Overall, the empirical equation fits the data well. For example, the R-squared value of the linear function yielded in the scenario of PRS<0 was 0.543, significant at 0.024 <0.05, in total, 69% of experiment results are explained by the independent explanatory variables in the equation. The estimated t-statistics indicate that the null hypothesis ($H_{null}: \beta_1 \le 0$) of Hypothesis 2 is rejected at a 0.05 level of significance. Therefore, the positive and zero relationships between ln($\Delta V^n{}_{j_D \to i}(t)$) and ln($\Delta T^n{}_{j_D \to i}(t)$) postulated in Hypothesis 2 are verified.

Table 5-8 Test results of Hypothesis 2 at night.

PRS	R-square	Adjusted R-square	Unstandardized Coefficients $\hat{\beta}_1$ (Std. Error)	t-value	Significant	Test result
<0	0.543	0.477	1.318 (0.457)	2.881	0.024	Reject H_{null}
=0	0.527	0.459	0.858 (0.307)	2.790	0.027	Reject H_{null}
>0	0.635	0.583	0.943 (0.270)	3.490	0.010	Reject H_{null}

Finally, the results of hypothesis one and hypothesis two are similar to the original experiment in Chapter 4. This application at night shows that processes of the original experiment can be transferred to the upgraded software and have a potential in virtual reality.

5.4 Application in MDV and ADV Logic

According to the literature review about car following logic, this study introduced the domestic driver RTs collected from the two-stage experiment (Sheu and Wu, 2015), and other important variables, such as the following distance, relative speeds, to the control logic of ADV on a mixed lance where automatic and manual driven vehicles mix near the event area and adjacent to an automated highway system (Sheu *et al.*, 2016).

The verification and validation of MDV and ADV Logic (Sheu *et al.*, 2016) are as follows. First, it is necessary to verify and validate the MDV simulation program with driving traffic characteristics that are similar to those of the general traffic flow simulation software, such as PARAMICS. This section proposed car-testing standards, and the use of traffic simulation software to adjust MDV control logic. Then, simulations within acceptable error range were tested. Furthermore, domestic driver RT at different speeds and the relative distance from survey data were used to improve the probability of fitness for local traffic.

Second, under the premise of safe and comfortable with the ADV passengers, in order to ensure that the AVD control logic model, four-quadrant mode , of usability and the feasibility, the present study used a programming simulation language and not only veritied but also validated that the four quadrants can be in the most appropriate distance, with the use of parabolic acceleration and decceleration, to confirm the feasibility of the model. After detection the four situation results confirmed feasible.

Furthermore, some traffic indicators, such as sensitivity, distance gap, shock wave speed, mean length of platoon, were introduced to judge the suitability of the

ADV models, as well as the impact of ADV judged on the amount of traffic generated by the state. For example, a stability index ($C = \alpha$ (Δt), multiplied by the sensitivity and the RT) was used to avoid ADV facing the LV deceleration and making following vehicles have brakes.

Third, to make those simulation programs of ADV and MDV applicable, it is necessary not only to judge the application of AVD car following, but also to determine the suitability of the MDV being close to the general humankind judgment. So the initial flow rate and density of the simulation program were set. The results of this study were compared to those of manually microscopic traffic simulation software PARAMICS. The control logic of ADV was similar to the traffic behavior of the simulation program PARAMICS. The results presented the verification and validation of the simulation program on acceleration and deceleration of the vehicle, as well as mixed traffic lane overall smoothness.

Finally, the specific contributions of this application are as follows. Parameters of the PRS and RT for domestic drivers were considered as driving subjective factors and were introduced into ADV logic models not only to improve the feasibility of practical application but also to balance both sides between engineering concerns and driver characteristics.

CHAPTER 6 DISCUSSION

This study has explored analytical models and the two-stage experiment for the uncertainties of PRS and RT which are necessary factors in car-following behavior. Based on this research the following discussions were offered.

6.1 The reliability of the PRS measurement

This study wrote a sub-program in the driving simulation program to record the nine scenarios throughout the driving simulation of each participant. Then each participant could replay the result of each scenario on the screen in the driving simulator room or the computer, measure the relative speeds, and complete the questionnaire. So the measurement of PRS is considerable reliant.

The measurement of PRS in this study was taken according to the literature of Hoffmann and Mortimer (1996). So, there is considerable credible.

According the measurement of uncertainty, we increased the number of tests to five times.

6.2 Two different experiments are needed

The two-stage experiments aim to serve two purposes as follows.

(1) The purpose of first-stage experiment was to investigate the psychological energy-time uncertainty, $\Delta \mathbf{K} \times \Delta RT \geq h'$, that the joint uncertainty in the psychophysical energy ($\mathbf{K}$) and the deviation of RT is greater and equal to an action constant (h') for a single lead vehicle and the follow vehicle under perception uncertainties. The $\mathbf{K}$ consists of the factors of PRS and W. The reaction time (RT) is affected by the speed perception and optical information produced by driving on a straight open road. If the psychological energy-time uncertainty exits, then the action constant (h') and the driving mental workload W can be found and determined.

(2) The purpose of the second stage experiment is to identify the revised trade-off relationship between the $\ln(\Delta T_{j_D \to i}(t))$ and the $\ln(\Delta V_{j_D \to i}(t))$ under driver perception uncertainties.

There are two reasons for measuring two same variables in the first stage and the second stage experiments as follows.

(1) According to definition of psychophysical energy defined by Baker (1999), the

PRS is a key factor to affect psychophysical energy. The purposes of the first stage and the second stage experiments are relative to psychophysical energy. So the PRSs were measured in two experiments.

(2) According to the derivation of the time-dependent Schrödinger equation (TDSE) by the work of Briggs and Rost (2001), we further postulate that the uncertainty in PPE has the trade-off relationship with the uncertainty in driver RT. The RT plays an important role in the uncertainty in PPE and the uncertainty in driver RT. The purposes of the first stage and the second stage experiments are relative to the uncertainty in driver RT. So the RTs were measured in two experiments.

In additional, driving work-loads were measured and an action constant was found in the first-stage experiment. To decrease the propagation of uncertainty, we assumed that the uncertainty of workload is zero. Then the simplified relationship between the uncertainty of PRS and the uncertainty of RT was tested in the second stage experiment.

6.3 Trade-off between Uncertainties of psychological energy and RT

This study investigated the trade-off relationship between psychological energy and RT in a plain area. The first hypothesis that explained the trade-off association between standard deviations (SDs) of psychological energy and SDs of RT in car following under driver perception uncertainties might exist and appear acceptable. The first-stage experimental results in Figure 4-9 and Figure 4-10 revealed some important findings as follows. First, on a straight highway segment and in fixed spacing scenarios, the vehicle driver, when perceiving that the uncertainty of psychological energy increased as the speed increased while the leading vehicle was braking, spent less RT and the uncertainty of RT decreased. The likely reason is that facing the leading vehicle braking in the higher speed the driver might feel more workload, shift attention from dissociation to association (Tenenbaum and Connolly, 2008) on reaction to avoid a vehicle collision and pay less dissociation attention on perceiving the psychological energy, so the driver could spend less RT and perceive the uncertainty, larger deviation, of psychological energy. Second, in unchanging vehicle speed scenarios, the vehicle driver, when feeling that the uncertainty of psychological energy increased as the spacing decreased while the leading vehicle was braking, spent less RT and the uncertainty of RT decreased. The likely reason is similar to the reason mentioned above, except that due to the less spacing the driver

paid less dissociation attention on perceiving the psychological energy. Third, consistent with the literature in car following and RT, the average of RT decreased as the spacing decreased and the speed increased. Fourth, on an aspect of psychology it was worthy to emphasize that the average of the psychological energy increased as the spacing decreased and the speed of vehicle increased. Fifth, the preliminary test results suggest that the trade-off association between the SDs of psychological energy and the SDs of RT in car following under driver perception uncertainties might exist. As the SD of psychological energy increases, the SD of RT decreases and as the SD of psychological energy decreases, the SD of RT increases.

6.4 Trade-off between Uncertainties of PRS and RT

Due to the each average of the driving mental workload in the nine scenarios and the action constant were determined in the first stage experiment, the trade-off relationship between PRS and RT in a plain area was explored further and the proposed hypothesis two showed suitable. The second-stage experimental results in Figure 4-12 and Figure 4-13 exposed some important findings as follows. First, on a straight highway segment and in fixed spacing scenarios, the vehicle driver, when recognizing that the uncertainty of PRS became bigger as the speed of vehicle was up and the leading vehicle was braking, spent less RT and the uncertainty of RT was down. The likely reason is similar to the reason mentioned in discussion 6.1. Second, in unchanging speed scenarios, the vehicle driver, when perceiving that the uncertainty of PRS was up as the spacing was down while the leading vehicle was braking, spent less RT and the uncertainty of RT was down. The likely reason is similar to the reason mentioned in subsection 6.1. Third, it seemed reasonable that the average of the PRS was up as the spacing was down and the speed of vehicle was up while the average of mental work was up. Fourth, consistent with the literature in speed perception and vision angle, the average of PRS was up and depended on the spacing and vision angles. Fifth, as the SD of PRS increases, the SD of RT decreases. As the SD of PRS decreases, the SD of RT increases. This R-squared ,0.705, of ln(△V) and ln(△T) in the second-stage experiment results is sufficiently large to be statistically useful in linking the trade-off relationship of uncertainties of △V and△T, although each scenario driving mental workload was considered as a different constant. The implication is that the trade-off between △V and△T was not easy found to be directly and statistically significant but the trade-off between ln(△V) and ln(△T) was statistically significant by transforming with the Curve Fitting analysis. It may be important to note the two extreme different scenarios including the high speed

with short-spacing one (*e.g.*, 90 kph with 20 m) seen in response to high driving mental workload and the low speed with long space one (*e.g.*, 30 kph with 60 m) seen in response to low driving mental workload

6.5 Psycho-physical aspect and quantum optical flow perspective

This study seems to confirm some previous researchers' observation with Psycho-physical models (Weidmann, 1974; Leutzbach, 1988) that the increased alertness of drivers at small headways and the lack of car following behavior at large headways.

The definition of the RT in this study different from the previous literature review (Mehmood and Easa, 2009) is adopted for two reasons. First, the time of t_1 and t_2 are obvious and easy to be recorded in the driving simulation. Second, the RT does not include machine time due to reduce the uncertain effect to the RT. As the results show that the definition is fit for the experiment in quantum optical flow-based car-following mode.

The definition of the perceived psychological energy in this study is applied and redefined for two reasons. First, the perceived psychological energy during the RT could exist and be measured by the subjective questionnaire. Second, this perceived psychological energy seems to confirm some previous researchers' observation in quantum optical flow (Baker, 1999; Gibson, 1966; Lee, 1980).

According with the results of the experiments in this research, the parameters, such as the deviation of the RT, can be conducted in quantum optical flow-based car-following model created by Sheu (2011). The simulation capability of the quantum mechanics-based car-following model in traffic uncertain environment will be improved. Besides, traffic phenomena are complex and rely on the interactions of many vehicles. Owing to the individual reactions of human drivers, vehicles do not interrelate simply adhering to the laws of mechanics, but rather display phenomena of cluster formation and shock wave propagation. For example, congestion upstream from a traffic bottleneck or shockwave could vary in propagation length, depending upon the upstream traffic flow, density. Due to the perceived information is uncertain, the stationary traffic does not exist and is an ideal scenario.

The findings presented in this paper also suggest the need for further research. The experiment for certificating the Heisenberg Uncertainty Principle (HUP) by using IOT Driving Simulation must be regarded as preliminary because of the limitations of

our data of participants used for the hypothesis test. In fact, some effort is already underway in this area. There are cheering signs that our experiment is starting to yield some useful results and we plan to continue with them in the future. Finally, the results are expected to help to characterize car following phenomena under driver perception uncertainties to facilitate road safety improvement and stimulate new ideas for traffic theory development.

6.6 Safety perspective and application

The findings from the experiment indicates that as the deviation of perceived psychological energy increases, the deviation of RT decreases inferring that there is a trade-off relationship between the uncertainties of driver's perceived psychological energy and RT. The results may help to characterize car following phenomena under driver perception uncertainties to facilitate road safety improvement and stimulate new ideas for traffic theory development.

Besides, by comparing with the safety distance, the decreased averages of RT presented in Table 4-4 as the speed increases and the spacing decreases while the spacing is smaller than the safety distance, imply that on the safety aspect, the risk is higher than those spacing is bigger than the safety distance.

By carrying out a small pretest without a rear brake light, we can detect the stimuli of the front vehicle and the reactions of the participants. The results showed that the averages and the SDs of the RT without a rear brake light were both larger than the average and the SDs of the RT with a rear brake light. On application aspect, this implies that a rear brake light can reduces the averages and the SDs of the RT.

6.7 Uncertainties of PRS and RT in foggy and braking conditions

The results of the first-stage experiment revealed the following important findings. First, in a foggy condition the LV taking the emergency brake, the trade-off relationship between the uncertainties of the FV driver's PPE uncertainty and the RT uncertainty may be similar to the Heisenberg principle of uncertainty. The trade-off relationship in foggy is also similar to the trade-off relationship in a clear weather condition (Sheu and Wu, 2015). Second, on the view point of PPE, the minimum value of the mean value of the PPE of the nine scenarios in foggy occurs at a distance of 60 m and a vehicle speed of 30 kph, with the maximum occurring at a distance of 20 m and a speed of 90 kph. In analogy to the concept that objects tend to move at

low energy levels, the driver of the vehicle may tend to have a lower PPE context, ie, increasing spacing and slowing down the vehicle in foggy, consistent with the findings of literature (Hoogendoorn *et al.*,2011; Pretto *et al.*,2012). In addition, the average driving mental workloads in the nine foggy scenarios were greater than ones in clear weather. The results indicate that the driver in the same situation on the LV braking in foggy has a larger average of the driving mental workload and transfers attention to the LV to avoid vehicle collision, similar to the movement of research (Matthews, 2001). In addition, there is no significant difference between the two action constants (h'_f, h'_c) in foggy and clear weather conditions. It is further deduced that if the uncertainty of PPE in foggy is less than that in clear weather then the reaction time in foggy is more uncertain. The above findings provide some directions on how to improve the safe and comfortable driving environment from the point of view of psychology.

The interesting findings were obtained from the results in the second-stage experiment. First, in foggy and LV taking an emergency brake, the trade-off relationships between the FV driver's PRS uncertainty and RT uncertainty may be similar to Heisenberg Uncertainty Principle. The trade-off relationship in foggy is similar to the trade-off relationship in the clear weather condition (Sheu and Wu, 2015). The possible reason is that the LV taking brake at a high speed, the FV driver increases the driving mental workload to make a rapid brake response to avoid a collision and feels a greater sense of sudden changes of the relative speed between the LV and FV. Secondly, the averages of PRS in the nine foggy scenarios are smaller than averages of the clear weather. It shows that the PRS is affected by a fog in the same visual situation and causes a relatively small relative speed perception. If the PRS in foggy is less than one in clear condition then the FV driver may mistakenly believe that there is a little decreasing PRS error comparing to PRS in a clear weather. The FV driver tends to negligence and increase speed. Finally, on the view of reaction time, the means of RT in the nine scenarios in foggy were greater than those in a clear condition, indicating that the driver's RTs in the nine situations were significantly affected by fog. If there is no significant difference in standard deviation of RT in foggy or clear condition, then the RT in foggy is longer, indicating a longer safety braking distance, which means that the risk of collisions with the LV is relatively high.

CHAPTER 7 CONCLUSION AND RECOMMENDATION

Based on the results mentioned above in this study, the conclusions regarding the contributions of the novel model provided above are summarized in subsection 7.1. Finally, recommendations to future research related to this issue were presented in subsection 7.2.

7.1 Conclusion

(1) This study developed the perception uncertainty theory that can be applied in some car following models mentioned above. There are three contributions: (a) the results of perception uncertainty can be regarded the foundations of car following models; (b) we provided a new method considering the psychological factors to support the development of car following models; and (c) the range of applications for perception uncertainty is larger than traditional car following due to the spacing of perception uncertainty in our study is longer than the traditional safety spacing.

(2) This study has identified the trade-off between uncertainties of driver's PRS and RT using a quantum optical flow perspective to characterize driver perception uncertainty in car-following behavior. Considering the possible effects of drivers' psychological factors on the aforementioned stimulus-response driving behavior, a quantum optical flow methodology has been developed by integrating several psychological factors, including the external stimuli arising from different scenarios of optical flows, workload, and internal stimuli into the proposed two-stage experimental framework. According to experimental results, those key psychophysical factors investigated and their relationships under driver perception uncertainty have been identified and discussed such that the characterization of driver psychology and behavior using quantum optical flow-based models in uncertain traffic environments can be improved.

(3) Nevertheless, great potential remains for future research considering the limitations of experimental tools used in this work. According to RT results, driver demands for software in auxiliary warning systems while cruising and car following, such as alarm timing (early alarms, late alarms, and no alarms) in a forward collision warning system, driver strategy of braking to avoid a collision with the LV, and performance when braking under different scenarios, can be developed. Different RT combinations applied in simulation programs and quantum optical-flow based car-following models (*e.g.*, Sheu, 2008, 2013) may

help us to accurately project driver car-following behavior under perception uncertainty. Additionally, numerous enhancements are possible. For example, findings obtained by this study suggest that further research is needed. The experiment to validate the proposed Car-Following Behavioral Uncertainty Principle using an IOT Driving Simulator must be regarded as preliminary because of data limitations. In fact, efforts are underway to overcome these limitations. There are positive signs indicating that our driving simulator experiments, despite their limitations, have already yielded useful results. Finally, experimental results may help characterize car-following phenomena under driver-perceived uncertainties, thereby facilitating road safety improvements and stimulating new ideas for traffic theory.

(4) Uncertainties of PRS and RT were analyzed in foggy and clear weather conditions when the LV was braking due to an emergency braking situation. Moreover, the experimental results in foggy weather were compared with those in clear weather. The statistical significant no-difference between the two action constants imitating Heisenberg Uncertainty Principle in foggy and clear weather conditions was confirmed by a Wilcoxon signed-rank test. Considering the possible effects of drivers' psychological factors on the aforementioned stimulus-response driving behavior in foggy and clear weather conditions, a quantum optical flow perspective methodology is planned by integrating several psychological factors, including the stimulus arising from the different scenarios of optical flows, PRS, and workload into the two-stage experiment. The parameters, such as the standard deviations of RTs ($\Delta T^{f}{}_{j_D \to i}(t)$ and $\Delta T^{c}{}_{j_D \to i}(t)$), can be conducted in a quantum optical flow-based car-following model created by Sheu (2008, 2013). The results may help to characterize foggy and clear weather conditions phenomena and explain the driver perception uncertainties to facilitate road safety improvement and stimulate new ideas for traffic theory development. Then, the simulation capability of the quantum optical flow-based car-following model in traffic uncertain environment (*e.g.*, foggy weather conditions) might be improved.

(5) The results of the first-stage experiment in foggy revealed the following important findings. First, in a foggy condition the LV taking the emergency brake, the trade-off relationship between the uncertainties of the FV driver's PPE uncertainty and the RT uncertainty may be similar to the Heisenberg principle of uncertainty. The trade-off relationship in foggy is also similar to the trade-off relationship in a clear weather condition (Sheu and Wu, 2015). Second, on the

view point of PPE, the minimum value of the mean value of the PPE of the nine scenarios in foggy occurs at a distance of 60 m and a vehicle speed of 30 kph, with the maximum occurring at a distance of 20 m and a speed of 90 kph. In analogy to the concept that objects tend to move at low energy levels, the driver of the vehicle may tend to have a lower PPE context, *e.g.*, increasing spacing and slowing down the vehicle in foggy, consistent with the findings of literature (Hoogendoorn *et al.*,2011; Pretto *et al.*, 2012). In addition, the average driving mental workloads in the nine foggy scenarios were greater than ones in clear weather. The results indicate that the driver in the same situation on the LV braking in foggy has a larger average of the driving mental workload and transfers attention to the LV to avoid vehicle collision, similar to the movement of research (Matthews, 2001). In addition, there is no significant difference between the two action constants (h'_f , h'_c) in foggy and clear weather conditions. It is further deduced that if the uncertainty of PPE in foggy is less than that in clear weather then the reaction time in foggy is more uncertain. The above findings provide some directions on how to improve the safe and comfortable driving environment from the point of view of psychology.

(6) The interesting findings were obtained from the results in the second-stage experiment in foggy. First, in foggy and LV taking an emergency brake, the trade-off relationships between the FV driver's PRS uncertainty and RT uncertainty may be similar to Heisenberg Uncertainty Principle. The trade-off relationship in foggy is similar to the trade-off relationship in the clear weather condition (Sheu and Wu, 2015). The possible reason is that the LV taking brake at a high speed, the FV driver increases the driving mental workload to make a rapid brake response to avoid a collision and feels a greater sense of sudden changes of the relative speed between the LV and FV. Secondly, the averages of PRS in the nine foggy scenarios are smaller than averages of the clear weather. It shows that the PRS is affected by a fog in the same visual situation and causes a relatively small relative speed perception. If the PRS in foggy is less than one in clear condition then the FV driver may mistakenly believe that there is a little decreasing PRS error comparing to PRS in a clear weather. The FV driver tends to negligence and increase speed. Finally, on the view of reaction time, the means of RT in the nine scenarios in foggy were greater than those in a clear condition, indicating that the driver's RTs in the nine situations were significantly affected by fog. If there is no significant difference in standard deviation of RT in foggy or clear condition, then the RT in foggy is longer, indicating a longer safety braking distance, which means that the risk of collisions with the LV is

relatively high.

7.2 Recommendations

The recommendations for future studies were addressed in this section.

(1) After all, traffic phenomena are complex and rely on interactions among vehicles. Because reactions are individual, vehicles do not interrelate simply adhering to the laws of mechanics, but rather display cluster formation and shock wave propagation phenomena. Because perceived information of drivers is uncertain, stationary traffic, in practice, does not exist and is merely an unrealistic scenario. Thus, we do hope that this study is a preliminary step to stimulate more researchers moving ahead to develop stochastic and dynamic driver behavior and traffic flow models fit for characterizing the reality of diverse traffic phenomena under uncertainty.

(2) Analyze the action constant (h'_n) at night.

(3) According with the experimental design in this research, the characteristic of participants, such as age and gender, can be analyzed by a repeated-measure ANOVA. The difference with different groups, male or female, can be considered in the quantum mechanics-based car-following model.

(4) Use the Quantile Regression to analyze the trade-off relationship.

APPENDIX A. PROOF OF COROLLARY 1.

As $m_{j_D \to i}(t)$ is defined as the light mass of vehicle j_D perceived by the driver of FV vehicle i at time t in the text, the magnitude of $m_{j_D \to i}(t)$ varies with PRS (*i.e.*, $V_{j_D \to i}(t)$) within the driver's quantum optical field $D[\Delta x(t), \Delta y(t)]$, as illustrated in Figure A-1. Let $m_{j_D \to i}(t)$ be a function of $V_{j_D \to i}(t)$ and $X_{j_D \to i}(t)$. Based on Figure A-1, we have

$$\dot{m}_{j_D \to i}(t) \equiv \frac{\partial m_{j_D \to i}(t)}{\partial t} = \begin{cases} \dfrac{m^{(1)}_{j_D \to i} - m^{(0)}_{j_D \to i}}{\partial t} & when\ V_{j_D \to i}(t) < 0 \\ 0 & when\ V_{j_D \to i}(t) = 0 \\ \dfrac{m^{(2)}_{j_D \to i} - m^{(0)}_{j_D \to i}}{\partial t} & when\ V_{j_D \to i}(t) > 0 \end{cases}$$

$$= \left[\frac{2X_{j_D \to i}(t) \cdot V_{j_D \to i}(t) + \left(V_{j_D \to i}(t)\right)^2 \partial t}{\left(X_{j_D \to i}(t)\right)^2} \right] \cdot m_{j_D \to i}(t) \qquad (\forall i, t; \forall j_D \in J_D) \text{(A1)}$$

Let $m'_{j_D \to i}(t)$ be defined as the first-order differentiation of $m_{j_D \to i}(t)$ with respect to $V_{j_D \to i}(t)$ (*i.e.*, $m'_{j_D \to i}(t) \equiv \frac{\partial m_{j_D \to i}(t)}{\partial V_{j_D \to i}(t)}$). Using Eq. (A1), we have

$$m'_{j_D \to i}(t) \equiv \frac{\partial m_{j_D \to i}(t)}{\partial V_{j_D \to i}(t)} = \dot{m}_{j_D \to i}(t) \cdot \frac{\partial t}{\partial V_{j_D \to i}(t)}$$

$$= \left[\frac{2X_{j_D \to i}(t) \cdot V_{j_D \to i}(t) \cdot \partial t + \left(V_{j_D \to i}(t) \cdot \partial t\right)^2}{\left(X_{j_D \to i}(t)\right)^2} \right] \cdot \frac{m_{j_D \to i}(t)}{\partial V_{j_D \to i}(t)} \qquad (\forall i, t; \forall j_D \in J_D) \text{ (A.2)}$$

Using Eq.s (2), and (3) (in the text) and (A2), we further have $\mathrm{K}'_{j_D \to i}(t)$ ($\mathrm{K}'_{j_D \to i}(t) \equiv \frac{\partial \mathrm{K}_{j_D \to i}(t)}{\partial V_{j_D \to i}(t)}$) given by

$$\mathrm{K}'_{j_D\to i}(t)\equiv\frac{\partial \mathrm{K}_{j_D\to i}(t)}{\partial V_{j_D\to i}(t)}=\frac{m'_{j_D\to i}(t)\cdot\left[V_{j_D\to i}(t)\right]^2\cdot W_i(t)}{2}+m_{j_D\to i}(t)\cdot V_{j_D\to i}(t)\cdot W_i(t)$$
$$=\left[\frac{2X_{j_D\to i}(t)\cdot V_{j_D\to i}(t)\cdot\partial t+\left(V_{j_D\to i}(t)\cdot\partial t\right)^2}{\left(X_{j_D\to i}(t)\right)^2\partial V_{j_D\to i}(t)}\right]\cdot\mathrm{K}_{j_D\to i}(t)+\mathrm{P}_{j_D\to i}(t)$$
$$=\left[\frac{2X_{j_D\to i}(t)\cdot\partial X_{j_D\to i}(t)+\left(\partial X_{j_D\to i}(t)\right)^2}{\left(X_{j_D\to i}(t)\right)^2\partial V_{j_D\to i}(t)}\right]\cdot\mathrm{K}_{j_D\to i}(t)+\mathrm{P}_{j_D\to i}(t)\qquad(\forall i,t\,;\forall j_D\in J_D)\ (\text{A.3})$$

Thus, Corollary 1 is proved.

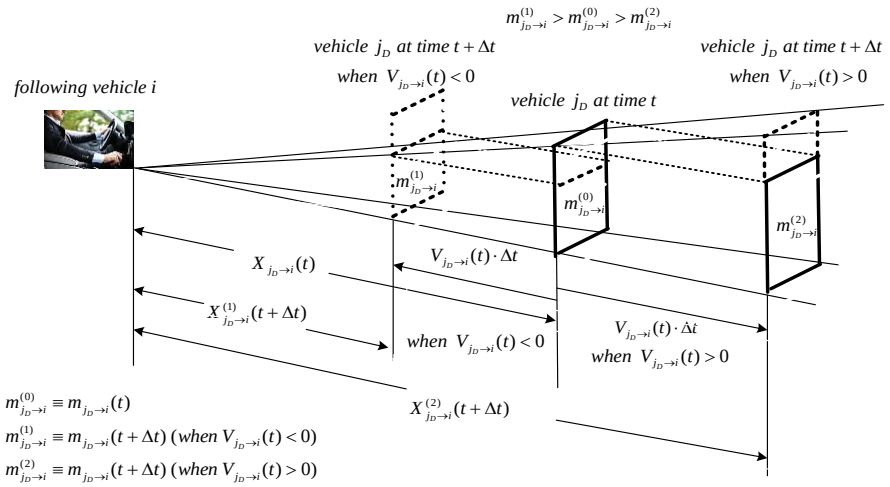

Figure A-1 Relationship between $m_{j_D\to i}(t)$ and $V_{j_D\to i}(t)$

APPENDIX B EXPERIMENTAL DESIGN

一、實驗設計

實驗 1

1.目的:實驗以平原地區高速公路為環境,使駕駛者於 3 個車道的中間車道行駛，於行駛過程中所行經路段將設置 9 種不同的目標車行車速度(90 kph、60 kph、30 kph)，以及與前車跟車距離(60 m、40 m、20 m)，配合前車踩煞車事件發生的基底情境,一共 9 組實驗隨機分配於路段中於駕駛模擬器進行實驗。蒐集單一駕駛者在不同行車速度下，對於前車踩煞車時煞車燈(含第 3 煞車燈)亮的反應時間(前車踩煞車時煞車燈(第 3 煞車燈)亮之 t_1，後車駕駛者腳踩煞車踏板 t_2，$RT=t_2-t_1$)。

2.道路場景：直線 3 車道(如 Figure B-1)

實驗環境選擇 3 車道的快速公路,其道路、分隔線寬度等規格皆與台灣相符，其車道寬度 3.75 公尺，實驗要求受測者保持於中間車道行駛，交通車流部份有前車保持行駛於受測者前方 D 公尺處。

3. 9 個情境：(2 個控制變數：速度變數為 V kph (90 kph、60 kph、30 kph 等 3 種)與距離變數為 D 公尺(60 m、40 m、20 m 等 3 種)組合成 9 個情境)

(1)控制前車與目標車保持固定距離(60 m、40 m、20 m)，駕駛人接受語音或螢幕提示車速(V KM/HR)控制車速(例如 90 kph、60 kph、30 kph)，。

(2)前車煞車時間為隨機變化並搭配煞車燈亮燈，減速度為 2 m/s^2 ，減速作用時間為 2 秒。

表 B-1 9 個情境：(控制變數：速限為 V kph 與 D 公尺)

	V kph	D 公尺
1	90	60
2	60	60

3	30	60
4	90	40
5	60	40
6	30	40
7	90	20
8	60	20
9	30	20

(3)駕駛者於直線道路上依系統提示之3種速度行駛，30 kph, 60 kph與90 kph，並依規定行駛於中間車道上並不變換車道，而與前車的距離模擬系統將分別控制在 20 m, 40 m, 與 60 m。實驗路段為 4,500 m，並分為 9 段，每段長500 m，每段的前車將定速行駛(速度由模擬器隨機指定為30 kph, 60 kph, 90 kph)。

4.周邊環境：平原區

5.天候：晴天

6.車輛：1 部前車與 1 部後車

(1)前車(事件車)：可以顯示前車踩煞車踏板時，煞車燈(第 3 煞車燈)亮

(2)後車(目標車或實驗車)：受測者駕駛之車輛看到前車煞車燈(第 3 煞車燈)亮時踩煞車踏板

Figure B-1 簡易示意圖

7.記錄實驗影像可輸出，並可擷取影像檔(avi)，再搭配JPG檔時間兩者相互結合。

8.舉例

(1)初始設定

(A)前車(事件車)：位置(x, y, z)= (60 m,15 m,0.6 m)

(B)後車(目標車或實驗車)：位置(x, y, z)= (0 m,15 m,0.6 m)

(C)前車與後車隨 X 軸移動

(D)共計 9 個區段(i= 1…9)，每個區段 500 公尺，全長共 4, 500 公尺。

(2)開始(i=1)

(A)隨機選擇 9 種情境之 1(未曾實驗之情境)並輸入其設定值與相關檔(例如第 1 種情境：速度 V = 90 kph,距離 D= 60 公尺，語音提示速度檔”時速保持 90 公里”)，前車(事件車)：位置(x, y, z)= (500(i-1)+60 m,15 m,0.6 m) ，未啟動(trigger) 前車與後車連動。

(B)語音提示速度檔播放(例如”時速保持 90 公里”)

(C)在第 i 個區段中，後車在 500*(i-1)公尺至 500*(i-1)+200 公尺內加速至語音提示速度(例如時速 90 公里)

- 判斷 1: 前車與後車 X 軸座標距離小於 D 公尺時，不啟動前車與後車連動(保持車間距 D 公尺)； 等於 D 公尺或大於時，則啟動(trigger) 前車與後車連動(保持車間距 D 公尺)。

(D)在第 i 個區段中，後車 X 軸座標在 500*(i-1)+200 至 500*(i-1)+500 公尺內保持語音提示速度(例如保持時速 90 公里)

- 判斷 2:後車 X 軸座標距離大於 500*(i-1)+200 且等於 500*(i-1)+200+random(0~250)公尺時，解除前車與後車連動且同時前車搭配煞車燈亮燈，減速度為 2 m/s^2 ，減速作用時間為 2 秒後再啟動(trigger) 前車與後車連動。

(E)在第 i 個區段中，判斷後車 X 軸座等於 500*(i-1)+500 公尺時則結束前車與後車連動，並結束此第 i 個區段中情境實驗並記錄此區段內之時

間軸內前車與後車之相關數據(例如前車煞車燈亮燈時間，後車煞車起始時間)。

(F)i=i+1

- 判斷 3: 若 i<9 並進入(2)重新開始下一個區段，若 i=9 時結束。

實驗 2

場景與實驗 1 相同，僅前車由減速改變為加速，即前車加速時間為隨機變化並搭配煞車燈熄滅，加速度為 2 m/s^2，加速作用時間為 2 秒。記錄後車駕駛人踩加速，或煞車踏板，或離開加速踏板。

實驗 3

場景與實驗 1 相同，僅前車由減速改變為加速為 0，即前車加速時間為隨機變化並搭配煞車燈閃亮即滅 0.1 秒，加速度為 0 m/s^2，作用時間為 2 秒。記錄後車駕駛人踩加速或煞車踏板，或離開加速踏板。

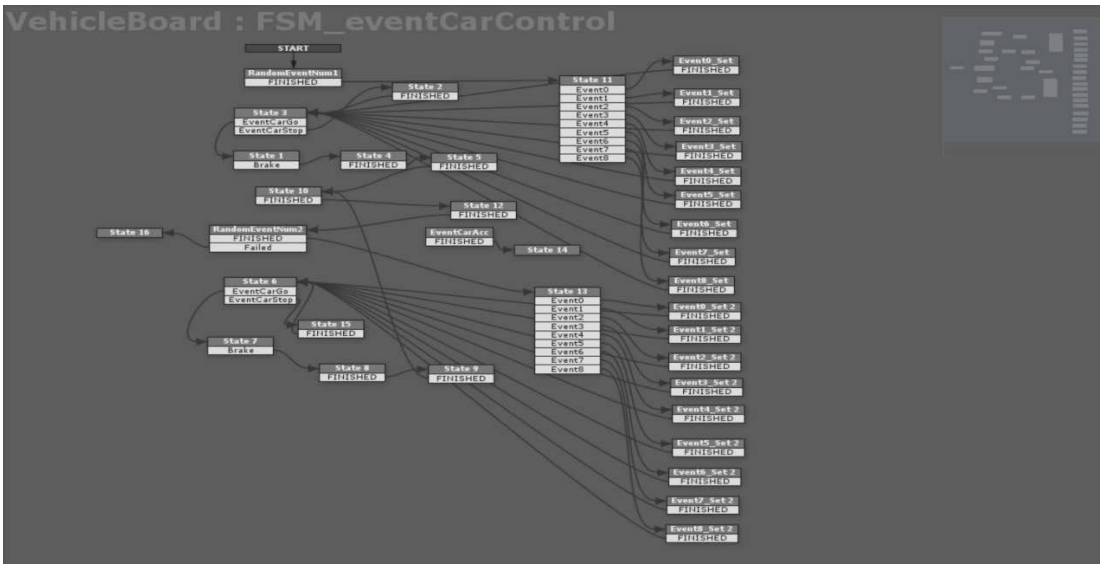

Figure B-2 Programs relations

```
//program 1
// the purpose of the program is to show the leading vehicle Activates or deactivates
// for recursive event trigger
using UnityEngine;

namespace    HutongGames.PlayMaker.Actions
{
    [ActionCategory(ActionCategory.GameObject)]
    [Tooltip("Activates/deactivates a Game Object. Use this to hide/show areas, or enable/disable many Behaviours at once.")]
    public class ActivateGameObject : FsmStateAction    // Finite State Machine
    {
        [RequiredField]
        [Tooltip("The GameObject to activate/deactivate.")]
        public FsmOwnerDefault gameObject;

        [RequiredField]
        [Tooltip("Check to activate, uncheck to deactivate Game Object.")]
        public FsmBool activate;

        [Tooltip("Recursively activate/deactivate all children.")]
        public FsmBool recursive;

        [Tooltip("Reset the game objects when exiting this state. Useful if you want an object to be active only while this state is active.\nNote: Only applies to the last Game Object activated/deactivated (won't work if Game Object changes).")]
        public bool resetOnExit;

        [Tooltip("Repeat this action every frame. Useful if Activate changes over time.")]
        public bool everyFrame;

        // store the game object that we activated on enter
        // so we can de-activate it on exit.
        GameObject activatedGameObject;

        public override void Reset()
        {
```

```
        gameObject = null;
        activate = true;
        recursive = true;
        resetOnExit = false;
        everyFrame = false;
    }

    public override void OnEnter()
    {
        DoActivateGameObject();

        if (!everyFrame)
        {
            Finish();
        }
    }

    public override void OnUpdate()
    {
        DoActivateGameObject();
    }

    public override void OnExit()
    {
        // the stored game object might be invalid now
        if (activatedGameObject == null)
        {
            return;
        }

        if (resetOnExit)
        {
            if (recursive.Value)
            {
#if UNITY_3_5 || UNITY_3_4      //different versions are compactable
                activatedGameObject.SetActiveRecursively(!activate.Value);
#else
                SetActiveRecursively(activatedGameObject, !activate.Value);
```

```
                #endif
            }
            else
            {
                #if UNITY_3_5 || UNITY_3_4
                    activatedGameObject.active = !activate.Value;
                #else
                    activatedGameObject.SetActive(!activate.Value);
                #endif
            }
        }
    }

    void DoActivateGameObject()
    {
        var go = Fsm.GetOwnerDefaultTarget(gameObject);

        if (go == null)
        {
            return;
        }

        if (recursive.Value)
        {
#if UNITY_3_5 || UNITY_3_4
            go.SetActiveRecursively(activate.Value);
#else
            SetActiveRecursively(go, activate.Value);
#endif
        }
        else
        {
#if UNITY_3_5 || UNITY_3_4
            go.active = activate.Value;
#else
            go.SetActive(activate.Value);
#endif
        }
```

```
            activatedGameObject = go;
        }

#if !(UNITY_3_5 || UNITY_3_4)
        public void SetActiveRecursively(GameObject go, bool state)
        {
            go.SetActive(state);
            foreach (Transform child in go.transform)
            {
                SetActiveRecursively(child.gameObject, state);
            }
        }
#endif

#if UNITY_EDITOR
        public override string AutoName()
        {
            return (activate.Value ? "Activate " : "Deactivate ") +
ActionHelpers.GetValueLabel(Fsm, gameObject);
        }
#endif
    }
}
```

```
//program 2
// the purpose of this program is to save data in file.csv
//
import System.Array;
import System.Collections;
import System.Text;
import System.IO;
import HutongGames.PlayMaker;
import UnityEngine;
private var iot:IOTLog = new IOTLog();

// declaim items of saving

private var LabItem_Table =
["LogTime","Speed","Car_X","Car_Y","Car_Z","Car_Angle","Car_Pedal","Car_Bra
ke","Car_Steer","EventCar_X","EventCar_Y","EventCar_Z","EventCar_Collission","
EventNum"];

private var Data : Array = new Array();

private var CollisionMsg :String;

public var subjectID : String = "00";
//public var other:DataManager;

public var player:GameObject;
public var eventCar : GameObject;
public var PlayerData1:GameObject;
public var PlayerData2:GameObject;
public var PlayerData3:GameObject;

public var speedPlayer : float;
public var log : String;

private var Timing :float;
private var nodeID:int=0;

//public var light =new Boolean(false);
```

```
//public var theFsm:PlayMakerFSM;
var SiteName:String;
function Start ()
{


}

function Update ()
{

	Data[IndexOf(LabItem_Table,"LogTime")] = Timing.ToString();
	Data[IndexOf(LabItem_Table,"Speed")] = String.Format("{0:0.0000}" ,
PlayerData1.transform.position.x);
	Data[IndexOf(LabItem_Table,"Car_X")] = String.Format("{0:0.0000}" ,
Mcar.position.x);
	Data[IndexOf(LabItem_Table,"Car_Y")] = String.Format("{0:0.0000}" ,
Mcar.position.y);
	Data[IndexOf(LabItem_Table,"Car_Z")] = String.Format("{0:0.0000}" ,
Mcar.position.z);
	Data[IndexOf(LabItem_Table,"Car_Angle")] = String.Format("{0:0.0000}" ,
Mcar.eulerAngles.y);
	Data[IndexOf(LabItem_Table,"Car_Pedal")] = String.Format("{0:0.0000}" ,
PlayerData2.transform.position.x);
	Data[IndexOf(LabItem_Table,"Car_Brake")] = String.Format("{0:0.0000}" ,
PlayerData2.transform.position.y);
	Data[IndexOf(LabItem_Table,"Car_Steer")] = String.Format("{0:0.0000}" ,
PlayerData2.transform.position.z);
	Data[IndexOf(LabItem_Table,"EventCar_X")] = String.Format("{0:0.0000}" ,
eventCar.transform.position.x);
	Data[IndexOf(LabItem_Table,"EventCar_Y")] = String.Format("{0:0.0000}" ,
eventCar.transform.position.y);
	Data[IndexOf(LabItem_Table,"EventCar_Z")] = String.Format("{0:0.0000}" ,
eventCar.transform.position.z);
	//Data[IndexOf(LabItem_Table,"EventCarSpeed")] =
String.Format("{0:0.0000}" , PlayerData3.transform.position.x);
	Data[IndexOf(LabItem_Table,"EventCar_Collission")] =
String.Format("{0:0.0000}" , PlayerData1.transform.position.y);
```

```
	Data[IndexOf(LabItem_Table,"EventNum")] = String.Format("{0:0.0000}" ,
PlayerData1.transform.position.z);

	iot.WriteLog = Data;

	CollisionMsg = "";
}

public function GetCollisionLog (msg:String)
{
	CollisionMsg = msg;
}

private	class IOTLog
{
	 private static var log_src : String;


	 static function set Subject_ID(value : String)
	 {
		var myTime : System.DateTime	=	System.DateTime.Now;

		//MSDN Code:System.Text.RegularExpressions.Regex.Replace
		//http://msdn.microsoft.com/zh-tw/library/e7f5w83z(v=vs.110).aspx

		var StartLabTime : String = myTime.ToString("u");
		StartLabTime = Regex.Replace(StartLabTime,"-","");
		StartLabTime = Regex.Replace(StartLabTime,":","");
		StartLabTime = Regex.Replace(StartLabTime,"Z","");
		StartLabTime = Regex.Replace(StartLabTime," ","");

		//MSDN Code:System.IO.Directory.GetParent

	//http://msdn.microsoft.com/zh-tw/library/system.io.directory.getparent(v=vs.110
).aspx

		var LogSrc : String;
	//	LogSrc =
```

```
System.IO.Directory.GetParent(Application.dataPath.ToString()).ToString();
      // 需在 D:中新增 UnitySave 資料夾~This is the File name
            LogSrc = "D:/UnitySave/Wu/"+"IOT_實驗者 ID_"+value+"_開始時間
_"+StartLabTime+".csv";
//          LogSrc = "D:/UnitySave/99.csv";
            log_src = LogSrc ;

        }

        static function set WriteLog(value : String)
        {
            if(log_src == null)
            {
                Debug.Log("警告-IOTLog.Subject_ID 未設置實驗者 ID");

                return;
            }

            if(value == null)
            {
                Debug.Log("警告-IOTLog.WriteLog 未設置實驗數據");

                return;
            }

            var    send = value + System.Environment.NewLine;


      //System.IO.File.AppendAllText(log_src,send,System.Text.Encoding.GetEncodi
ng(950));//System.Text.Encoding.GetEncoding(950) //System.Text.Encoding.UTF8
            System.IO.File.AppendAllText(log_src, send);
        }
}
```

REFERENCES

Abbasi-Kesbi, R., Memarzadeh-Tehran, H., and Deen, M. J., 2017. Technique to estimate human reaction time based on visual perception. Healthcare Technology Letters, 4(2), 73-77.

Anwar, M. I., and Khosla, A., 2015. Vision Enhancement in Bad Weather. Handbook of Research on Emerging Perspectives in Intelligent Pattern Recognition, Analysis, and Image Processing, 65.

Baker, R.G.V., 1999. On the quantum mechanics of optic flow and its application to driving in uncertain environments. Transportation Research Part F (2), 27–53.

Baldock, M. R. J and McLean, A J, 2005. Older Drivers: Crash Involvement Rates and Causes. University of Adelaide, Australia.

Bar-Anan, Y., Wilson T.D., and Gilbert, D.T., 2009. The feeling of uncertainty intensifies affective reactions. Emotion 9(1), 123–127.

Bartmann, D., Spijkers, W., and Hess, M., 1991. Street environment, driving speed and field of vision. In: Gale, A.G., Brown, I.D., Haslegrave, C.M., Moorhead I., Taylor S. P., Vision in vehicles III . Amsterdam: Elsevier.

Blanco, M.,2002. Relationship between driver characteristics, nighttime driving risk perception, and visual performance under adverse and clear weather conditions and different vision enhancement systems (Doctoral dissertation, Virginia Polytechnic Institute and State University).

Brackstone, M., and McDonald, M., 1999. Car-following: a historical review, Transportation Research Part F: Traffic Psychology and Behaviour 2(4), pp.181-196.

Briggs J.S., and Rost J.M., 2001. On the derivation of the time-dependent equation of Schrödinger. Foundations of Physics 31(4), 693–712.

Born, M., Heisenberg, W., and Jordan, P., 1926. On quantum mechanics II. Z. Phys, 35(8-9), 557-615.

Bose, A., and Ioannou, P., 2000. Shock Waves in Mixed Traffic Flow. 9th IFAC Symposium on Control in Transportation Systems.

Brookhuisa, K.A., and de Waard, D., 2010. Monitoring drivers' mental workload in driving simulators using physiological measures. Accident Analysis and Prevention 42 (3), 898–903.

Cavallo, V., 2002. Perceptual distortions when driving in fog. In Proc., 2nd International Conference on Traffic and Transportation Studies.

Cavallo, V. and Laurent, M., 1988. Visual information and skill level in

time-to-collision estimation. Perception 17, 623-632.

Chandler, R. E., Herman, R., and Montroll, E. W., 1958. Traffic dynamics: studies in car following, Operations Research, 6, 165-184.

Chen, D., Ahn, S., Laval, J., and Zheng, Z., 2014. On the periodicity of traffic oscillations and capacity drop: The role of driver characteristics. Transportation Research Part B: Methodological, 59, 117–136.

Chiu, Y.-C., Zhou, L., and Song, H., 2010. Development and calibration of the Anisotropic Mesoscopic Simulation model for uninterrupted flow facilities. Transportation Research Part B: Methodological, 44(1), 152–174.

Conte1 E., Khrennikov A.Y., Todarello O., Federici1 A., Mendolicchio L., and Zbilut J.P., 2009. Mental States Follow Quantum Mechanics During Perception and Cognition of Ambiguous Figures. Open Systems & Information Dynamics Vol. 16, No. 1,1-17.

Davis G. A., and Swenson T.,2006. Collective responsibility for freeway rear-ending accidents? An application of probabilistic causal models. Accident Analysis and Prevention 38 (2006) 728–736.

Davis L.C.,2003 Modifications of the optimal velocity traffic model to include delay due to driver. Physica A 319 (2003) 557-567.

De Lucia, P. R., and Tharanathan, A.,2005. Effects of optic flow and discrete warnings on deceleration detection during car-following. In Proceedings of the Human Factors and Ergonomics Society 49th Annual Meeting (pp. 1673-1676). Santa Monica, CA: Human Factors and Ergonomics Society.

De Waard D., Van den Bold T. G.M.P.R., and Lewis-Evans B., 2010. Driver Hand Position on The Steering Wheel While Merging Into Motorway Traffic. Transportation Research Part F, 13, 129-140

Dijksterhuis, C., Brookhuis, K. A., and De Waard, D., 2011. Effects of steering demand on lane keeping behaviour, self-reports, and physiology. A simulator study. Accident Analysis & Prevention, 43(3), 1074-1081.

Dingus, T.A., Klauer, S.G., Neale, V.L., Peterson, A., Lee, S.E., Sudweeks, J., Perez, M.A., Hankey, J., Ramsey, D., Gupta, S., Bucher, C., Doerzaph, Z.R., Jarmeland, J., Knipling, R.R. , 2006. The 100-Car naturalistic driving study, Phase II – Results of the 100-Car field experiment. National Highway Traffic Safety Administration, Washington, DC., USA.

Dirac, P. A., 1927. The physical interpretation of the quantum dynamics. Proceedings of the Royal Society of London. Series A, Containing Papers of a Mathematical and Physical Character, 621-641.

Doğan, S., Temiz, M.S., and Külür, S., 2010. Real time speed estimation of moving vehicles from side view images from an uncalibrated video camera. Sensors

10, 4805–4824.

Dumont, E., Paulmier, G., Lecocq, P., and Kemeny, A., 2004. Computational and experimental assessment of real-time front-lighting simulation in night-time fog. In Proceedings of the Europe Driving Simulation Conference.

Durrani, U., Lee, C., and Maoh, H., 2016. Calibrating the Wiedemann's vehicle-following model using mixed vehicle-pair interactions. Transportation Research Part C: Emerging Technologies, 67, 227-242.

Ferson, S., Kreinovich, V., Hajagos, J., Oberkampf, W., Ginzburg, L., 2007. Experimental uncertainty estimation and statistics for data having interval uncertainty. Applied Biomathematics, New York.

Fitts, P.M., and Posner, M.I., 1967. Human Perfomance. Belmont, CA: Brooks/Cole; 1967.

Forbes, T. W., Zagorski, M. J. Holshouser, E. L. and Deterline, W. A., 1959. Measurement of Driver Reaction to Tunnel Conditions, Proceedings of the Highway Research Board, Vol. XXXVII, 345-357.

Fukushima, K.,2008. Extraction of visual motion and optic flow. Neural Networks 21, 774–785.

Gazis, D. C., Herman, R., and Rothery, R. W, 1961. Nonlinear follow the leader models of traffic flow, Operations Research, Vol. 9, 545-567.

Geldard, F., 1972. The human senses. New York: Wiley.

Gibson, J.J., and Crooks, L.E., 1938. A theoretical filed analysis of automobile driving. Journal of Psychology, 51, 453-471.

Gibson, J.J., 1950. The Ecological Approach to Visual Perception. Boston: Houghton Mifflin.

Gibson, J.J., 1966. The Senses Considered as a Perceptual System. Boston: Houghton Mifflin.

Hanaura, H., Nagatani, T., Tanaka, K., 2007. Jam formation in traffic flow on a highway with some slowdown sections. Physica A: Statistical Mechanics and Its Applications 374 (1), 419–430.

Hart, S.G., 2006. Nasa-Task Load Index (Nasa-TLX); 20 years later. Human Factors and Ergonomics Society Annual Meeting Proceedings 50, 904-908.

Harris, W., and Levey, J., 1975. The new Columbia encyclopedia. New York: Columbia University Press.

Hoffmann, E.R., and Mortimer R.G., 1996. Scaling of relative velocity vehicles. Accident and Analysis and Prevention 28 (4), 415–421.

Houtenbos, M., de Winter, J. C. F., Hale, A. R., Wieringa, P. A., and Hagenzieker, M. P., 2017. Concurrent audio-visual feedback for supporting drivers at intersections: A study using two linked driving simulators. Applied

Ergonomics, 60, 30-42.

Huang, S. N., Chan, S. C., and Ren, W., 1999. Mixture of automatically-and manually-controlled vehicles in intelligent transport systems, Journal of Intelligent and Robotic Systems, 24(2), 175-205.

Iida, S., Yukawa, M., Yonezawa, H., Yamamoto, N., and Furusawa, A., 2012. Experimental demonstration of coherent feedback control on optical field squeezing. IEEE Transactions on Automatic Control, 57(8), 2045–2050.

Jacoby, J., 2002. Stimulus-organism-response reconsidered: an evolutionary step in modeling (consumer) behavior. Journal of Consumer Psychology, 12 (1), 51–57.

Jiang, R., Wu, Q.-S., and Zhu, Z.-J., 2002. A new continuum model for traffic flow and numerical tests. Transportation Research Part B: Methodological, 36(5), 405–419.

Jiang, R., Hu, M. B., Zhang, H. M., Gao, Z. Y., Jia, B., Wu, Q. S., Wu, B. W., and Yang, M., 2014. Traffic experiment reveals the nature of car-following. PloS one, 9(4), e94351.

Kilpeläinen M., and Summala H., 2007. Effects of Weather and Weather Forecasts on Driver Behaviour. Transportation Research Part F 10 (2007) 288-299.

Kirkup L. And Frenkel R. B., 2006. An Introduction to Uncertainty In Measurement Using The Gum (Guide To The Expression Of Uncertainty In Measurement). Cambridge University Press, 35-52.

Knipling, R.R., Wang, J.S., and Yin, H.M., 1993. Rear-end crashes: problem size assessment and statistical description. Technical Report. National Highway Traffic Safety Administration, Washington, DC., USA.

Koutsopoulos, H.N., and Farah, H., 2012. Latent class model for car following behavior. Transportation Research Part B: Methodological, 46(5), 563–578.

Laval, J. A., Toth, C. S., and Zhou, Y., 2014. A parsimonious model for the formation of oscillations in car-following models. Transportation Research Part B: Methodological, 70, 228-238.

Lee, D.N., 1976. A theory of visual control of braking based on information about time-to-collision. Perception, 5(4), 437-459.

Lee, D.N., 1980. The optic flow field: the foundation of vision. Philosophical Transactions of the Royal Society 290, 169–179.

Leutzbach, W., 1988. Introduction to the theory of traffic flow. Springer-Verlag, Berlin.

Lewis-Evans B., De Waard D., and Brookhuis K. A., 2010. That's Close Enough-A Threshold Effect of Time Headway on The Experience of Risk, Task Difficulty, Effort, and Comfort. Accident Analysis and Prevention 42 (2010)

1926-1933.

Li, Z., and Milgram, P., 2008. An empirical investigation of a dynamic brake light concept for reduction of rear-end collisions through manipulation of optical looming. International journal of human-computer studies, 66(3), 158-172.

Liu, T.C., 2010. The Dual-Task Interference and Information-Processing Model Research. Dissertation of doctoral degree of the National Central University.

Lunenfeld, H. and Alexander, G.J., 1990. A user's guide to positive guidance, 3rd Edition, FHWA-SA-90-017, Federal Highway Administration, Washington, DC.

MacLeod, R. W. and Ross, H. E., 1983. Optic flow and cognitive factors in time-to-collision estimates. Perception 12, 417-423.

Malhotra, N.K., 2005. Attitude and affect: new frontiers of research in the 21st century. Journal of Business Research, 58, 477-482.

Markkula, G., Engström, J., Lodin, J., Bärgman, J., and Victor, T., 2016. A farewell to brake reaction times? Kinematics-dependent brake response in naturalistic rear-end emergencies. Accident Analysis & Prevention, 95, 209-226.

Marsh, B., Lautner, B., Fournier, L., Klang, J., Anelli, P., Kang, W. E., Brumec, U., Cota, K., 2017. The Role of Road Engineering in Combatting Driver Distraction and Fatigue Road Safety Risks.

Matthews, G., 2001. A transactional model of driver stress. In P. A. Hancock & P. A. Desmond (Eds.), Stress, workload and fatigue (pp. 133–166). New Jersey: Lawrence Erlbaum Association.

Mehmood, A., Easa, S.M., 2009. Modeling reaction time in car-following behaviour based on human factors. International Journal of Engineering and Applied Sciences 5(2), 93–101.

Miller J. C.,1988. Integrated human factors test and evaluation methods. Presented at the American Institute of Aeronautics and Astronautics Conference, San Diego, CA.

Mitra, S., and Mukhopadhyay, S., 2013. An analytical investigation on the interactions between a squeezed and a coherent optical signal. Optik 124, 4586-4589.

Miura, T., 1987. Behavior oriented vision: functional field of view and processing resources. Eye movements: from physiology to cognition, 563-572.

Morrison, M.A., 1990. Understanding Quantum Physics: A User Manual. New Jersey: Printice-Hall.

Nagai, R., Hanaura, H., Tanaka, K. and Nagatani, T., 2006. Discontinuity at edge of traffic jam induced by slowdown. Physica A: Statistical Mechanics and Its Applications 364 (5), 464–472.

Naseri, H., Nahvi, A., and Karan, F. S. N., 2015. A new psychological methodology

for modeling real-time car following maneuvers. Travel Behaviour and Society, 2(2), 124-130.

Ni, R., Bian, Z., Guindon, A., and Andersen, G. J., 2012. Aging and the detection of imminent collisions under simulated fog conditions. Accident Analysis & Prevention, 49, 525-531.

Ngoduy, D., and Jia, D., 2017. Multi anticipative bidirectional macroscopic traffic model considering cooperative driving strategy. Transportmetrica B: Transport Dynamics, 5(1), 100-114.

Ohtsuka, H. and , and Vlacic, L., 2002. Stop & Go Vehicle Longitudinal Model, Proceeding of IEEE 5th International Conference on Intelligent Transportation Systems, 206-209.

Oron-Gilad, T., Ronen, A., and Shinar, D., 2008. Alertness maintaining tasks (AMTs) while driving. Accident Analysis and Prevention 40(3), 851-860.

Öz, B., Özkan, T., and Lajunen, T., 2010. Professional and non-professional drivers' stress reactions and risky driving. Transportation research part F: traffic psychology and behaviour, 13(1), 32-40.

Pande, A., and Wolshon, B., 2016. The Institute of Transportation Engineers, Traffic Engineering Handbook, Seventh Edition. John Wiley and Sons, Inc.

Papageorgiou, G., Maimaris, A., 2012. Modelling, Simulation Methods for Intelligent Transportation Systems, Intelligent Transportation Systems, Dr. Ahmed Abdel-Rahim (Ed.), ISBN: 978-953-51- 0347-9, InTech, Available from: http://www.intechopen.com/books/intelligent-transportation-systems/modellingsimulation-methods-for-intelligent-transportation-systems.

Parush, A., Gauthier, M. S., Arseneau, L., and Tang, D., 2011. The Human Factors of Night Vision Goggles Perceptual, Cognitive, and Physical Factors. Reviews of human factors and ergonomics, 7(1), 238-279.

Pasetto, M., and Manganaro, A., 2009. Nighttime speed negotiation on rural road s-shaped curves: Discussion of an experimental case-study. In Proceedings of the international driving symposium on human factors in driver assessment, training and vehicle design, Vol. 5, pp. 475-481. University of Iowa Public Policy Center.

Pašagić, S., Pašagić, J., and Lovretić, M., 2012. Increased Visual Perception in Night-Time Driving Conditions and/or Reduced Optical Visibility. PROMET-Traffic&Transportation, 13(5), 293-297.

Paz, A., Peeta, S., 2009. Information-based network control strategies consistent with estimated driver behavior. Transportation Research Part B: Methodological, 43(1), 73–96.

Pegg, D. T., Barnett, S. M., Zambrini, R., Franke-Arnold, S., and Padgett, M., 2005.

Minimum uncertainty states of angular momentum and angular position. New Journal of Physics, 7(1), 62.

Pipes, L. A., 1953. An Operational Analysis of Traffic Dynamics, Journal of Applied Physics, 24, 271-281.

Pretto, P., Bresciani, J.-P., Rainer, G., and Bülthoff, H. H., 2012. Foggy perception slows us down. eLife, 1, e00031. doi:10.7554/eLife.00031.

Purves D. and Lotto R. B., 2003. Why we see what we do: an empirical theory of vision. Sinaeur Associates, http://www.purveslab.net/research/.

Qian, Z. S., Li, J., Li, X., Zhang, M., Wang, H., 2017. Modeling heterogeneous traffic flow: A pragmatic approach. Transportation Research Part B: Methodological, 99, 183-204.

Robinson, G.H., Erickson, D.J., Thurston, G.L., and Clark, R.L., 1972. Visual search by automobile drivers. Human Factors 14 (4), 315–323.

Recarte, M. A. and Nunes, L., 2002. Mental load and loss of control over speed in real driving. Towards a theory of attentional speed control. Transportation Research Part F 5 (3), 111–122.

Roeckelein J. E., 1998. Dictionary of Theories, Laws and Concepts in Psychology. Greenwood Press, Westport, CT.

Rolke B. And Hofmann P., 2007. Temporal uncertainty degrades perceptual processing. Psychonomic Bulletin & Review, 14 (3), 522-526.

Rothengatter T., 2002. Drivers' Illusions-No More Risk. Transportation Research Part F 5 (2002) 249-258.

Rößing, C., 2016. Intuitive Motion and Depth Visualization for Rear-View Camera Applications. In Handbook of Camera Monitor Systems (pp. 485-510). Springer International Publishing.

Salvia, E., Guillot, A., Collet, C., 2012. Autonomic nervous system correlates to readiness state and negative outcome during visual discrimination tasks. International Journal of Psychophysiology, 84 (2), 211–218.

Schrödinger, E.,1926. An undulatory theory of the mechanics of atoms and molecules. Physical Review, 28(6), 1049-1070.

Shapiro, J. H., Yen, B. J., Guha, S., and Erkmen, B. I., 2005. Classical communication in the presence of quantum Gaussian noise. International Society for Optics and Photonics. In SPIE Third International Symposium on Fluctuations and Noise, 63-73.

Sheu, .J.-B., Chou, Y.-H., and Shen, L.-J., 2001a. A stochastic estimation approach to real-time prediction of incident effects on freeway traffic congestion. Transportation Research-Part B, 35B(6), 575-592.

Sheu, J.-B. and Ritchie, S. G., 2001b. Stochastic modeling and real-time prediction

of vehicular lane-changing behavior. Transportation Research-Part B 35B(7), pp. 695-716.

Sheu, J.-B., 2003. A stochastic modeling approach to real-time prediction of queue overflows, Transportation Science 37(a), 97-119.

Sheu, J. B., 2007. Microscopic modeling and control logic for incident-responsive automatic vehicle movements in single-automated-lane highway systems, European journal of operational research, 182(2), 640-662.

Sheu, J.-B., 2008. A quantum mechanics-based approach to model incident-induced dynamic driver behavior. Physica D 237, 1800–1814.

Sheu, J.-B., 2013. Characterization of driver behavior during car following using quantum optical flow theory. Transportmetrica Part A, 9(3), 269-298.

Sheu, J.-B., Wu, H.-J., 2011. Uncertainties of perceived relative speed and reaction time in car following: a quantum optical flow perspective. The 16th International Conference of Hong Kong Society Transportation Studies (HKSTS), 17-20 December, Hong Kong, 11–18.

Sheu, J. B., and Wu, H. J., 2015. Driver perception uncertainty in perceived relative speed and reaction time in car following–A quantum optical flow perspective, Transportation Research Part B: Methodological, 80, 257-274.

Shiomi, Y., Yoshii, T. Kitamura, R., 2011. Platoon-based traffic flow model for estimating breakdown probability at single-lane expressway bottlenecks. Transportation Research Part B: Methodological, 45(9), 1314–1330.

Stevens S.S., 1957. On the psychophysical law. Psychol. Rev. 64:153-181.

Summala H., 2005. Traffic Psychology Theories: towards Understanding Driving Behaviour and Safety Efforts. Traffic and Transport Psychology: Theory and Application, Underwood G. (Editor), Elsevier Ltd., 383-394.

Summala H., Lamble D., and Laakso M.,1998. Driving Experience And Perception Of The Lead Car'S Braking When Looking At In-Car Targets. Accident Analysis and Prevention, 30, 401–407.

Talebpour, A., and Mahmassani, H. S., 2016. Influence of connected and autonomous vehicles on traffic flow stability and throughput. Transportation Research Part C: Emerging Technologies, 71, 143-163.

Tan, A., Brewer, P., Liesch, P.W., 2007. Before the first export decision: internationalisation readiness in the pre-export phase. International Business Review, 16 (3), 294–309.

Tanaka, K., Nagai, R., Nagatani, T., 2006. Traffic jam and discontinuity induced by slowdown in two-stage optimal-velocity model. Physica A: Statistical Mechanics and Its Applications 370(2), 756–768.

Tenenbaum, G., Connolly, C.T., 2008. Attention allocation under varied workload and

effort perception in rowers. Psychology of Sport and Exercise 9(5), 704–717.

Tian, J., Treiber, M., Ma, S., Jia B., Zhang W., 2015. Microscopic driving theory with oscillatory congested states:Model and empirical verification. Transportation Research Part B 71, 138-157

Toledo, T., 2003. Integrated driving behavior modeling. Dissertation of doctoral degree of the Massachusetts Institute of Technology.

Tordeux A., Lassarre S., Roussignol M.,2010. An adaptive time gap car-following model. Transportation Research Part B 44, 1115-1131.

Treiber M., Kesting A., Helbing D.,2006. Delays, inaccuracies and anticipation in microscopic traffic models. Physica A 360, 71-88.

Tseng Y.Y., 2005. Simulation and development of the bus car-following stimulus-response model. Dissertation of Master degree of Chung Hwan University.

Verma, A., Chakrabarty, N., Velmurugan, S., Bhat, P. B., Kumar, D. H., and Nishanthi, B., 2016. Assessment of driver vision functions in relation to their crash involvement in India. CURRENT SCIENCE, 110(6), 1063-1072.

Vision, https://www.skybrary.aero/index.php/Vision_(OGHFA_BN)

Wagner, P., 2012. Analyzing fluctuations in car-following. Transportation Research Part B: Methodological, 46(10), 1384–1392.

Wang, S.H., 2004. Analysis of Reaction Time in Car Following by Driving Simulator. (in Chinese edition). Dissertation of Master degree of Central University.

Wang, W.H., Zhang W., Guo H.W., Bubb H., Ikeuchi K., 2011. A Safety-Based Behavioural Approaching Model with Various Driving Characteristics. Transportation Research Part C-Emerging Technologies, 19(6), 1202-1021.

Wiedemann, R., 1974. Simulation des verkehrsflusses. Schriftenreihe des Instituts für Verkehrswesen, Heft 8, Universität Karlsruhe.

Wiedemann, R., 1991. Modeling of RTI-Elements on multi-lane roads. In: Advanced Telematics in Road Transport edited by the Commission of the European Community, DG XIII, Brussels.

Wiedemann, R., Reiter, U., 1992. Microscopic traffic simulation: the simulation system MISSION, background and actual state. Project ICARUS (V1052) Final Report. Brussels, CEC, vol. 2.

Wikipedia, 2013. http://en.wikipedia.org/wiki/Empirical_theories_of_perception.

World Road Association, 2003. Road Safety Menal. PIARC Technical Committee on Road Safety(C13),Version 1.00, Appendix 6-1,180-190.

Xiang, W., Yan, X., Weng, J., and Li, X., 2016. Effect of auditory in-vehicle warning information on drivers' brake response time to red-light running vehicles during collision avoidance. Transportation research part F: traffic psychology

and behaviour, 40, 56-67.

Yan, X., Li, X., Liu, Y., and Zhao, J., 2014. Effects of foggy conditions on drivers' speed control behaviors at different risk levels. Safety Science, 68, 275–287.

Young M. S. and Stanton N. A., 2002. Malleable Attentional Resources Theory: A New Explanation for the Effects of Mental Underload on Performance. Human Factors: The Journal of the Human Factors and Ergonomics Society 2002 44: 365.

Chinese

許添本、鄭雅文，「具備預測機制的追撞事件偵測新演算模式之研發」，運輸計劃季刊，第 30 卷，第 3 期，民國 90 年，頁 539-576。

許智詠，「因應事故發生自動控制車隊變換車道邏輯之構建—以單一自動車道為例」，交通大學交通運輸研究所碩士論文，民國 93 年。

董晉曄，「單一車道自動公路系統發生意外事故下自動車輛行為模擬」，交通大學交通運輸研究所碩士論文，民國 95 年。

蔡孟釗，「單一車道自動公路系統發生意外事故下自動車輛跟車邏輯」，交通大學交通運輸研究所碩士論文，民國 94 年。

張開國、葉祖宏、吳熙仁、許鉅秉、黃臣鴻、廖晟傑，「應用駕駛模擬器與光流理論於道路駕駛者對前車相對速度感知之標準差與反應時間標準差關聯性之初探」，交通部運輸研究所運輸研究專輯，民國 102 年 9 月。

陳穆臻、吳熙仁，「濃霧中前車緊急煞車時道路駕駛人對前車相對速度感知與反應時間不確性之關聯—以海森堡不確定性原理觀點」，運輸計劃季刊，第 46 卷，第 2 期，民國 106 年，頁 117-136。

CURRICULUM VITAE

Hsi-Jen Wu

❖ Education

Ph.D.	Department of Transportation & Logistics Management National Chiao Tung University Taipei, Taiwan, Republic of China (2017) Advisor: Prof. Jiuh-Biing Sheu and Prof. Mu-Chen Chen Dissertation: Experiments and Analysis on Joint Uncertainties in Psycho-Physical Factors of Car-Following Drivers - Quantum Optical Flow Perspective
BS	Department of Graduate Department of Law Fu Jen Catholic University Taipei, Taiwan, Republic of China (2006)
MS	Institute of Traffic and Transportation National Chiao Tung University Taipei, Taiwan, Republic of China (1993) Advisor: Prof. Wu-Cheng Chen Thesis: Study for Systems of Tourism Information Query and Tour Management – an example along Western Expressway
BS	Department of Transportation Eng. and Management National Chiao Tung University Hsinchu, Taiwan, Republic of China (1989)

❖ Certification

(1)83 年交通技術系交通工程科高考一級及格(現為二級)
(2)82 年交通工程技師高考及格
(3)81 年交通行政系運輸管理科高考及格

❖ Research Interest

Railway safety, Roadway safety, Driving behavior, Human factor, Simulation

❖ Publication

Journal Papers (2010~2017)

陳穆臻、吳熙仁 (2017)，「濃霧中前車緊急煞車時道路駕駛人對前車相對速度感知與反應時間不確性之關聯—以海森堡不確定性原理觀點」，運輸計劃季刊，第 46 卷第 2 期。**(TSCI)**

許鉅秉、吳熙仁、蔡孟釗 (2016)，「自動公路系統發生事件下自動駕駛車輛於鄰近混合車道跟車邏輯之研究」，運輸計劃季刊，第 45 卷第 2 期。**(TSCI)**

Sheu, J. B., and Wu, H. J., (2015), " Driver perception uncertainty in perceived relative speed and reaction time in car following–A quantum optical flow perspective", *Transportation Research Part B: Methodological*, Vol.80, 2015, pp. 257-274. **(SCI)**

林杜寰、孫千山、鍾志成、李治綱、張開國、吳熙仁 (2014)，「臺鐵平交道風險處理－以裝設障礙物偵測器為例」，運輸計劃季刊，第 43 卷第 1 期，頁 63-88。**(TSCI)**

孫千山、鍾志成、張開國、吳熙仁 (2014)，「臺鐵旅客遭受攻擊的風險管理」，臺鐵資料季刊，第 351 期，頁 45-61。

孫千山、林杜寰、李治綱、張開國、吳熙仁 (2013)，「國內外鐵路系統風險處理案例」，中興工程季刊，第 118 期，第 75-85 頁。

鍾志成、孫千山、李治綱、陳一昌、吳熙仁 (2011)，「國外鐵路系統風險管理實務」，中興工程季刊，第 110 期，頁 13-25。

Conference Papers (2010~2017)

孫千山、張恩輔、韓念祖、施佑林、李治綱、張開國、吳熙仁 (2015)，「增進鐵路安全風險管理工具及輔助蒐集資料穿戴科技設備之評估」，第 30 屆中華民國運輸學會論文集。

孫千山、施佑林、鍾志成、李治綱、張開國、吳熙仁 (2015)，「軌道安全與風險評估之研究_風險式與自主式鐵路安全管理制度之推動策略研究」，臺灣軌道運輸發展研討會。

孫千山、施佑林、鍾志成、李治綱、張開國、吳熙仁 (2014)，「風險式與自主式鐵路安全管理制度之回顧與案例分析」，中華民國運輸學會 103 年年會暨學術論文研討會論文集，第 1313-1336 頁。

林杜寰、孫千山、鍾志成、李治綱、張開國、吳熙仁 (2012)，「臺鐵平交道風險處理-以裝設障礙物偵測器為例」，第 27 屆中華民國運輸學會論文集。

Sheu, J.-B., Wu, H.-J., (2011), “Uncertainties of perceived relative speed and reaction time in car following: a quantum optical flow perspective”, Proceedings of The 16th International Conference of Hong Kong Society Transportation Studies (HKSTS), December, Hong Kong, pp.11–18.

孫千山、鍾志成、林杜寰、李治綱、張開國、吳熙仁 (2011)，「應用FaultTree+軟體於平交道防護設備失效之初探」，2011 電子計算機於土木水利工程應用研討會論文集。

孫千山、鍾志成、林杜寰、李治綱、張開國、吳熙仁 (2011)，「鐵路安全風險分析方法之回顧與案例分析」，第 26 屆中華民國運輸學會論文集，12 月。

J. C. Jong, T. H. Lin, C. S. Suen, C. K. Lee, I. C. Chen, H. J. Wu (2011), “Using Fault Tree Analysis to Identify the Failures of Level Crossing Protection Devices”, Proceedings of the 7th International Conference on Urban Regeneration and Sustainability, Belgium.

孫千山、鍾志成、李治綱、陳一昌、吳熙仁 (2010)，「鐵路系統風險辨識方法之回顧」，第 25 屆中華民國運輸學會論文集。

Reports (2009~2017)

風險式與自主式鐵路安全管理制度之實務調查與分析 (2014)，交通部運輸研究所。

風險管理應用於鐵路運輸安全之初探—以臺鐵風險處理、管理監督、管理改善為例 (2013)，交通部運輸研究所。

風險管理應用於鐵路運輸安全之初探—以臺鐵風險分析與評量為例 (2012)，交通部運輸研究所。

風險管理應用於鐵路運輸安全之初探—以臺鐵風險辨識為例 (2011)，交通部運輸研究所。

建立臺鐵安全績效指標之研究 (2009)，交通部運輸研究所。

運輸安全風險管理初探-職業駕駛人身心健康與駕駛危險分析 (2009)，交通部運輸研究所。